Brno University of Technology

Faculty of Mechanical Engineering

Institute of Machine and Industrial Design

DIAGNOSIS OF PNEUMATIC CYLINDERS USING ACOUSTIC EMISSION METHODS

Author: **Ing. Houssam Mahmoud**

Supervisor: Assoc. Prof. Pavel Mazal, CSc.

Dissertation thesis

Brno 2018

STATEMENT

I hereby declare and confirm that I have written the PhD thesis "***Diagnosis of Pneumatic Cylinders Using Acoustic Emission Methods"*** on my own based on the advices of my supervisor **Assoc. Prof. Pavel Mazal.** The sources listed in the references.

Brno 30. 08. 2018

Houssam Mahmoud

BIBLIOGRAPHICAL REFERENCE

MAHMOUD, H. *Diagnosis of Pneumatic Cylinders Using Acoustic Emission Methods.* Brno, 2018, 74 pages. PhD thesis. Brno University of Technology, Faculty of Mechanical Engineering, Institute of Machine and Industrial Design. Supervisor: Assoc. Prof. Pavel Mazal.

ACKNOWLEDGEMENT

Foremost, I would like to express my sincere gratitude to my supervisor Assoc. Prof. Pavel Mazal, CSc. for the continuous support of my Ph.D., and his guidance helped me in all the time in research and writing this thesis.

Besides my supervisor, I would like to thank all people in the Institute of Machine and Industrial Design.

My sincere thanks also go to Dr. František Vlašic for the support and many thanks to my colleagues in my office, Poličské strojírny a.s. and DAKEL Company.

Last but not the least; I would like to thank my family and all my friends.

ABSTRACT

This work demonstrates the development of a new efficient diagnostic procedure for checking the function of pneumatic cylinders using acoustic emission. The aim of this work is to suggest and determine the diagnostic criteria that evaluate the quality of the pneumatic cylinder.

The first step is to find the typical acoustic emission signal that associated with a particular type of damage in the cylinder by the frequency spectrum. This parameter was replaced later by the parameter RMS during the monitoring of changes in the test results. The relationship between Acoustic Emission (AE) and different types of defects in pneumatic cylinders was discussed, shedding light on a new approach to determining these types of defects and distinguishing between them through Acoustic Emission.

The second step is to compare undamaged and damaged cylinders to find distinctive differences that determine whether the cylinder is damaged or undamaged. Several undamaged cylinders were tested by acoustic emission, before artificial defects were created in each one. The signals from the progress and retreat strokes were recorded and analysed into many parameters. The RMS was normalized, and the different responses between damaged and undamaged pneumatic cylinders were recognized by the time delay of the strokes. The differences were identified by the ratio of the max RMS from the sensor that fixed in the head cap of the cylinder and the max RMS from the sensor that fixed in the rear cap of the cylinder for one cycle in the retreat stroke. The damaged and undamaged cylinders were distinguished using the difference in energy values which present in the signals from the two sensors in the retreat stroke. The final evaluation of the cylinder was determined by the calculation of the total value of RMS.

In the third step in the experiment, the cylinders were loaded gradually by different weights in a vertical direction. The signals of the acoustic emission were recorded from the progress and retreat strokes and then analysed. The time delay is calculated between the digital input and the initiation of movement. The energy and root mean square of the acoustic emission compare between the different responses in damaged and undamaged pneumatic cylinders, with and without loading. The results of the test showed a linear relationship between the RMS curve and loading. The defect affects the relationship between the applied load and the recorded signal of the sensors.

KEYWORDS

Acoustic Emission (AE), Pneumatic cylinders, Detection Coefficient, Energy, Loading Root Mean Square, Defects, Leakage.

ABSTRAKT

Tato práce se zabývá vývojem nového efektivního diagnostického postupu pro kontrolu funkce pneumatických válců pomocí metody akustické emise. Cílem práce bylo navrhnout a určit diagnostická kritéria pro hodnocení kvality vybraných typů pneumatických válců.

Prvním krokem bylo nalezení typického akustického emisního signálu, který je spojen s určitým typem poškození ve válci využitím frekvenčního spektra signálu. Později byl tento parametr nahrazen parametrem RMS během sledování změn v průběhu testů. Na konkrétních válcích byl sledován vztah mezi akustickou emisí a různými typy defektů a byl představen nový přístup k určování těchto typů vad a jejich odlišením v signálu akustické emise.

Druhý krok studie že neporušené a poškozené válce byly porovnávány tak, aby se zjistily výrazné rozdíly, které určují, zda je válec poškozen nebo nepoškozen. Několik nepoškozených válců bylo testováno akustickou emisí a následně v nich byly vytvořeny umělé vady. Signály z vysouvání a zasouvání pístu byly zaznamenány a analyzovány pomocí řady parametrů. Na základě časového zpoždění a normalizace RMS byly rozpoznány odezvy mezi poškozenými a nepoškozenými pneumatickými válci. Rozdíly byly zjištěny porovnáním maximální hodnoty RMS ze snímače upevněného na předním víku válce a snímače upevněného na zadním víku válce pro jeden cyklus. Poškozené a nepoškozené válce byly rozlišeny pomocí rozdílů energetických hodnot přítomných v signálech z obou snímačů v závislosti na zdvihu pístu. Konečné vyhodnocení válce bylo určeno výpočtem celkové hodnoty RMS.

Ve třetím kroku experimentu byly válce postupně zatěžovány různými závažími ve svislém směru. Signály akustické emise byly zaznamenány z vysouvání a zasouvání pístu a poté analyzovány. Časové zpoždění se vypočítává z digitálního vstupu a začátku pohybu pístu. Energie signálu a RMS akustické emise porovnávají různé reakce v poškozených a nepoškozených pneumatických válcích s a bez zatížení. Výsledky testu ukázaly lineární vztah mezi křivkou RMS a zatížením. Defekty ovlivňují vztah mezi aplikovaným zatížením a zaznamenaným signálem snímačů.

KLÍČOVÁ SLOVA

Akustická emise (AE), Pneumatické válce, Detekční koeficient, Energie, Zatížení, Root Mean Square, defekty, Únik.

Table of Contents Page

1. Introduction

This study tried effectively to apply real-time diagnostics to detect any malfunctions in automatic production lines and in the transport field, and looking for new ways to inspect and predict any defects. One option is the condition monitoring by acoustic emission method.
Non-destructive testing (NDT) is defined as the technical method to examine materials or components in ways that do not impair future usefulness and serviceability. NDT can be used to detect, locate, measure, and evaluate flaws; to assess integrity, properties, and composition. Each NDT technique has both advantages and disadvantages with regard to cost, speed, accuracy, and safety [1].
Acoustic emission testing is considered to be an important method of non-destructive testing (NDT) and condition monitoring. It can be conducted during operation and does not require any interruption of activity. Acoustic emission is the term given to transient elastic stress waves generated by the energy released when microstructural changes occur in a solid material or turbulence in the liquid. The main factors of the propagation velocity of the elastic stress wave are the wave type, the wave frequency, and the properties of the material. These waves are detected by sensors (transducers) attached to a specific place on the surface; the sensors convert the mechanical disturbance into voltage. Acoustic emission is usually divided into three categories: pressure testing, diagnostics condition monitoring, and leak detection. Leak detection includes detecting, locating and assessing leaks, and determining when the fluid flow becomes turbulent. Fundamental principles of AE leak detectors rely on the fact that escaping gas or liquid through a small breach creates a high-frequency sound wave that travels through the enveloping system via an acoustic leak path [2].
Pneumatic actuators convert fluid energy into straight line motion (linear actuators). During normal operation of a pneumatic actuator, a variety of defects can occur, which could lead to a catastrophic failure if left undetected. Therefore, it is crucial to detect even the minor problems and their sources as quickly and accurately as possible to ensure an uninterrupted safe operation. Defects may affect the function of the pneumatic cylinders and cause malfunctions [3].
The existence of the detection coefficient “D” facilitates the evaluation of defects, taking values that range from 1 to 10, with 10 being highly difficult to detect. The detection coefficient was taken from the method FMEA (Failure Mode and Effects Analysis) and was developed and classified using AE. The Coefficient "S" expresses the severity of a particular defect [4].
A number of undamaged pneumatic cylinders were tested with AE before artificial defects were made on the same cylinders and the results were compared. And undamaged and damaged cylinders were analysed using a frequency spectrum within a specified time and the results were compared. A set of defects was identified through this comparison, but the frequency spectrum, counts and events were not sufficient to identify all defects. The frequency spectrum was replaced later by the RMS, the average energy of acoustic emission signal RMS gives a clear picture of the different responses between damaged and undamaged pneumatic cylinders [5].
The cylinders were loaded gradually by different weights in a vertical direction. The effect of the defect occurs when the cylinder is loaded at the retreat and progress strokes. This defect affects the relationship between the applied load and the recorded signal of the sensors. The relationship between the RMS curve and loading is linear [6].
The main goal is to investigate the possibilities of implementing AE system for pneumatic cylinder leakages detection. The AE laboratory at the “*Institute of Machine and Industrial Design of Brno University of Technology*” has long focused on the use of AE for diagnostics of damage development in cyclically loaded materials and machine parts (standard fatigue, contact fatigue, bearings etc.). In addition to these relatively traditional applications, theses laboratory specialists implement other non-traditional possibilities of using acoustic emission method. This is possible by using a prototype of the newly developed diagnostic equipment.

2. State of The Art and Previous Studies

Non-destructive testing (NDT) is defined as the technical method to examine materials or components in ways that do not impair future usefulness and serviceability. NDT can be used to detect, locate, measure, and evaluate flaws; to assess integrity, properties, and composition; and to measure geometric characteristics. The NDT technologies include radiographic methods, dynamic methods, X-rays, ultrasonic methods, acoustic emission (AE) techniques, and acoustic-ultrasonic (AU) techniques etc.

The first documented observations of AE appear to have been made in the 8th century by Arabian alchemist Jabir ibn Hayyan. Hayyan wrote that Jupiter (tin) gives off a 'harsh sound' when worked, while Mars (iron) 'sounds much' during forging.

The 19th century brought further verification with the work of Robert Anderson (tensile testing of an aluminium alloy beyond its yield point), Erich Scheil (linked the formation of martensite in steel to audible noise), and Friedrich Forster, who with Scheil related an audible noise to the formation of martensite in high-nickel steel. Experimentation continued throughout the mid-1900's, culminating in the PhD thesis written by Joseph Kaiser entitled "Results and Conclusions from Measurements of Sound in Metallic Materials under Tensile Stress." Soon after becoming aware of Kaiser's efforts, Bradford Schofield initiated the first research program in the United States to look at the materials engineering applications of AE. However, Kaiser's research is generally recognized as the beginning of modern day acoustic emission testing.

Acoustic emission is a non-destructive structural integrity monitoring method, and to characterize the behaviour of materials when they undergo deformation or fracture. Unlike ultrasonic or radiographic techniques, AE does not require external energy; it is released from the test object itself. Acoustic emission techniques have been used for monitoring components and systems during manufacturing, detecting and locating leaks, mechanical property testing, and testing pressurized vessels. AE technique relies on the fact that escaping gas or liquid through a small breach creates a high frequency sound wave that travels through the enveloping system [7].

Fluid power system, which is used in pneumatic control, requires an adequate knowledge of pneumatic components and their function to ensure their integration into an efficient working system. The compound air compressor was first patented in 1829, and it was seen for the first time in 1872. The 1900s saw further evolution for pneumatics as components were used for the first time in jet engines in the form of centrifugal and axial-flow compressors. Further developments took place throughout the century with advancements in labor-saving devices in the form of machinery that would assist or even reduce the need for manpower as well as automatic machinery, tools and control systems. Towards the end of the 1960s, the first digitally controlled pneumatic components began to enter the market, once again revolutionizing the way in which this highly effective equipment played a part in our everyday lives. Modern pneumatic cylinders offer fast, accurate power for low-pressure applications, giving a variety of industries, from packaging to amusement park rides and medical devices to automation control, simple, safe and powerful controls [8].

2.1.Relationship between AE and leakage 2.1

Fundamental principles of acoustic emission leak detectors are sensitive to airborne sound and inaudible sound waves due to escaping gas. Acoustic emission techniques, on the other hand, detect high frequency sounds that travel within the envelope itself. The acoustic emission technique relies on the fact that escaping gas or liquid through a small breach creates a high frequency sound wave that travels through the enveloping system via acoustic leak path. It is the capture and recording of these waves that make up the acoustic emission technique. Applicability, sensitivity and characteristics of the acoustic emission technique is best used where there is a direct sound path between the suspected leak location and the location of the sensor. Acoustic emission sensors are small piezoelectric transducers, similar in construction to those used in ultrasonic testing. The received signal is highly amplified and transmitted to the monitor where the number of events, the event rate and changes in the event rate are observed. Acoustic emission tests are susceptible to background noise (false positives) due to equipment rotation, friction, or other operating sources. On the other hand, using several transducers and by triangulation, it is possible to very accurately pinpoint the location of source of the emission, i.e. the leak. Acoustic emission testing is considered to be considerably more sensitive than airborne acoustic testing but does require access to the surface of the pressure envelope [9].

Researchers have found that the AE signals are able to monitor the process of fluid leakage such as the valve leakage. The high frequency stress wave caused by the turbulence, which is the result of the random flow when the fluid goes through the leaks orifices of the valve. The frequency amplitude values vary from 100 kHz to 1 MHz, and it can be easily identified by environmental noise from the factory. El-Shorbagy found the methods to measure the flow rate by the automatic online control using monitoring the sound level of valve noise [10]. *Sharif and Grosvenor* analyzed the frequency spectrum of the AE signal on the leakage of compressed air through an industrial control valve. The results demonstrated the relationship between the frequency and leakage and could be clearly picked up from AE signal with background noise [11]. *Lee et al.* studied the AE characteristics monitoring the leakage in two valves (the steam ball valve and water ball valve) on different leakage modes, and it was concluded that the leakage rate of valves is directly proportional to the AE amplitude. Recently, the rate of gas leakage of a valve was estimated by the theoretical relationship between the features of AE signals and internal leakage rate of valves [12].Thus, it is feasible that AE technique can be applied in the inner leakage detection of valves.

2.1.1. Parameters of Acoustic emission

The parameters analysis of AE signals in valves is a dominant method in the signal processing field. Compared with the full waveform analysis method, the parameters analysis has many advances, for example, fast recording and rapid processing. Many parameters, such as the rise time, ring down counts, amplitude, peak, duration and root mean square (RMS) value, and kurtosis, were analysed using this method. *Dickey et al.* found that the peak amplitude of AE signal in frequency domain was tightly related to transducer response or valve geometry [13]. The characteristic of AE signal in frequency domain and a relationship between the AE signal and the leakage rate were studied in a ball valve. *Jiang et al.* explored the function between the Reynolds number (Re) and the sound pressure level of gas leakage with AE technique. The mass of gas leakage in the flow field was calculated, which is the foundation for the detection of the valve leak [14]. *Gao et al.* presented the quantitative relationship between the valve leakage rate of coal-fired power plants and the AE_{rms}. Its precision was verified by the practice results. The experiment system which consists of the leakage system and the AE measurement

system. For leakage system, valves are chosen to be the test subjects, which mainly are ball and globe balls because of their wide applications [15].

The correlation between the AE parameters and leakage rate are able to monitor the operating condition of critical valves. Some researchers tried made improvements of portable devices for leakage detection of valves based on the previous studies. The principle of measurement is that using a sensor to detect the leakage of valves this sensor converting the elastic wave to voltage by micro processing to the parameter of the AE signal. Simplifying the system and reducing the cost are depending on the accuracy. The devices are particularly inadequate for detecting the leakage of valves applied in engineering fields, because the devices that detect the leakage of valves with the AE technology are usually huge and inconvenient to move. [16].

Yang et al. applied the AE technique to identify the internal leaky modes of globe valve, which could be classified as the untight closing and crack. It was tested in the valves and the results showed it worked effectively [17]. *Wang et al.* proposed a method for detecting the actual working condition of a valve using the AE signal and the simulated valve motion. This method can easily distinguish the normal valve, valve flutter, and valve delayed closing conditions [18].

Pollock et al studied the characteristic of acoustic leak signals owing to the gas leakage through a ball valve in frequency domain. As a consequence, the correlation between the AE and the leakage rate was presented [19]. *Dickey et al* found that the peak amplitude of AE signal in frequency domain is independent of leak part or leakage rate but dependent on transducer response and valve geometry. However, they did not describe the relationship between AE parameters and valve leakage rate which is the primary basis for predicting leakage rate by AE method [13]. *Watit Kaewwaewnoi, Asa Prateepasen and Pakorn Kaewtrakulpong* presented the relationship between AE parameters and the leakage rate of valve at various valve sizes and inlet pressures. The equation utilized to find out the leakage rate at different valve sizes and inlet pressures was also established. The degree of turbulence is predicted by the Reynolds number (Re) defined as:

$$Re = \frac{\rho r v}{\eta} \qquad 2.1$$

Where ρ is the density of the liquid, ν the flow velocity, r the radius of flow path and η the viscosity [32]. The basic mechanism generating AE signals at the orifice is the turbulence resulting from the high pressure and high velocity of fluid flow [19]. The Reynolds number Re can be written as:

$$Re = \frac{Ud}{v} \qquad 2.2$$

Where U is Mean fluid velocity through orifice, d is Mean orifice diameter, v is viscosity of fluid. It has been found that the turbulence occurs when the Reynolds number is between 1,000 and 10,000 giving leakage produce an acoustic emission. The actual detection of the leakage depends on the flow rate as this factor decides the energy contents of the leak signal [19]. The AE signal of leaking valve is more obviously identified on the downstream side of a valve. This is due to the turbulence created when the gas flows from the high pressure side, through the leakage area to the low pressure side. Hence, AE sensors should be located at the downstream side of the valves. For continuous AE signal from both time and frequency domains, the most frequently used AE parameters are the average energy (AE_{rms}).

2.1.2. Apparatus of Acoustic emission

Jomdecha et al. developed a system that consists of a field programmable gate array-PC (FPGA-PC) and three AE sensors with 150 kHz resonant frequency, he was locating the AE source from the corrosion in austenitic stainless steel. Furthermore, a system based on FPGA-PC and LOCAN 320 AE analyser was developed. The system is able to analyse the amplitude, counts, hits, and time of AE signals from corrosion for different types of corrosion. [20]. *David Taylor Naval Ship RID Center* developed (DTNSRDC)The acoustic valve leak detector (AVLD) which is currently used for trouble shooting, overhaul planning, and a systematic preventive maintenance program for seawater valves [21]. *Noipitak et al.* made a foundation for the application of AE technique in valves and reduced the recalibration time and the cost by presenting a relative calibration method for an internal valve leakage rate measurement system based on the microcontroller and AE methods. *Prateepasen et al.* developed a smart portable device for detection of internal air leakage of a valve using AE signals. The measurement was made by an embedded system, the relation between AE_{rms} and the leakage rate, and the micro controller. The valve was turning off and the sensor was assembled before the instrument works. Which helps maintenance technicians to identify the leaking valves quickly and easily [22]. The applications of AE technique in detecting failure of valves focused on the leakage of valves, identification of failure modes, and valve degradation. *Nakamura and Terada* used an AE sensor to monitor the minor leak of pressurized valves based on the opposite properties of AE signals and background noise [23]. *Seong et al.* proposed a method in which the AE sensors were used for detecting the failures of check valves and developed a diagnostic algorithm to identify the type and the size of the failure of valve. The results showed that this method worked well in identification of failure and estimation of the relationship between the size and failure type [24].

2.1.3. Leakage and RMS of acoustic emission

Gao et al. presented the relationship between the AE parameters and the fluid filed and valves. It was found that the ring-down counts, energy, amplitude, or AE_{rms} signals induced by leakage was directly proportional to the inlet pressure. However, the AE signal induced by the valve leakage is continuous. Two parameters are used to describe the leakage [25]. *Kaewwaewnoi et al.* found that a good correlation existed between the leakage rate and the ASL (average signal level). An equation related to the valve leakage rate was achieved. Many literatures presented the average energy of AE signal (AE_{rms}) as a more sensitive parameter of valve. Chen et al in italic. evaluated the various parameters of AE signals in terms of their capability of estimating the internal leakage rate of a water hydraulic cylinder. They have shown AE_{rms} value was more suitable to interpret AE signals generated by internal leakage [26]. *Kaewwaewnoi et al.* also found the relationship between the AE_{rms} and the parameters such as inlet pressure levels, valve sizes, and valve types. The AE_{rms} could be used to predict the actual leakage rate qualitatively [27].

Sim et al. employed AE signal to detect valve failure in reciprocating compressor. Any abnormalities of the valve motion could be detected effectively by analysing the RMS value. In their further study, the detection of other types of valve and the initiation of materials deformation in valves could be achieved [28]. *Yan, Jin, Y. Heng-Hu, Y. Hong, Z. Feng, L. Zhen, W. Ping and Y. Yan* studied the relation between valve and acoustic emission. A review of the applications of AE techniques for detecting the condition and faults of valves was presented. The popular parameters analysis methods were discussed. The parameter of AE_{rms} is proved to have a strong relationship with the fluid parameters and the valve parameters, such as the valve types and valve size, the leakage rate, the inlet pressure, and the types of fluid. The detection of leakage, condition monitoring of faults, cavitation detection of valves, and portable measurement device were proposed in this review [29].

Bezn and Joon-Hyun Lee et al suggested that AE_{rms} (V_{rms} in the figure) could be used to determinate the open and close positions of valves, such as relief and safety valves, and also to indicate aging and degradation of check valves in nuclear power plants. The RMS values of AE signal in different failure modes are shown in figure 2.1 [30].

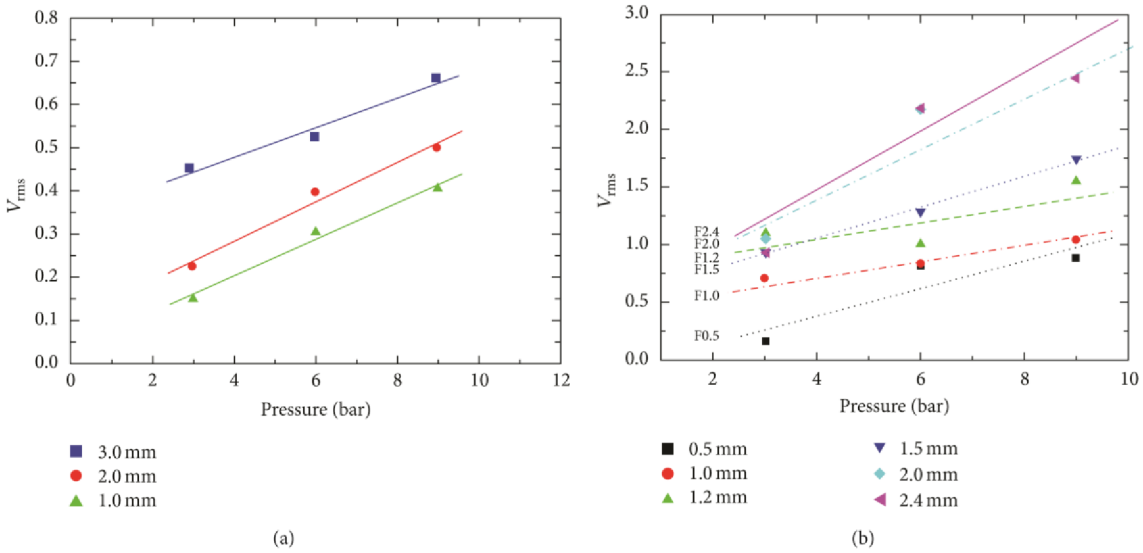

Figure 2.1 RMS values of the acoustic signals: (a) disk wear and (b) foreign objects [30].

Typical AE system comprises of several AE electronic modules such as AE sensors, preamplifiers, filters, amplifiers, and a data acquisition system. In order to eliminate background noise, a band-pass filter operated in the range of 100 kHz to 400 kHz [3] is normally used. For continuous AE signal, the most frequently used AE parameters are (AE_{rms}) and (ASL). The AE_{rms} is the root mean square value of the AE signal. Since Acoustic Emission activity is attributed to rapid releases of energy in the material, the energy content of the acoustic emission signal is related to this energy release. AE_{rms} can be defined as:

$$AE_{rms} = \sqrt{\frac{1}{T}\int_{t_0}^{t_0+T} v^2(t)dt} = \sqrt{\frac{1}{N}\sum_{n=1}^{N} v^2(n)} \qquad 2.3$$

Where v is the voltage signal from an AE sensor, t0 the initial time, T the integration time of the signal and N the number of discrete AE data within the interval T. Another AE parameter, which is often used, is the Average Signal Level (ASL) defined as:

$$ASL_v = \frac{1}{T}\int_{t_0}^{t_0+T} |v(t)dt| = \frac{1}{N}\sum_{n=1}^{N} |v(n)| \qquad 2.4$$

$$ASL_{dB} = 20log\frac{ASL_v}{1\ (\mu)} \qquad 2.5$$

Where ASL_v is an average signal level in volts and ASL_{dB} an average signal level in decibel (dB) [31]. The leakage rate can be calculated from differential pressure of the chamber from the equation.

$$Q = V \times \frac{(\Delta P/P_1)}{\Delta T} \qquad 2.6$$

Where Q is the leakage rate (ml/sec), V the volume of the chamber, ΔT the time span of the testing, ΔP the pressure increased over the time ΔT, and P1 the system pressure.

W. Kaewwaewnoi, A. Prateepasen and A. Kaewtrakulpong presented a novel method to find the relation between AE_{rms} of AE and valve leakage rate detection [32]. This method aims at transferring the information between AE inspection systems using different types of sensors by relationship called a transfer function. The results demonstrated a very good similarity transfer function in various conditions.

The experiment had been conducted using three sizes of ball valve of diameter 1, 2 and 3 inches and inlet pressure between 1-5 bars. The result was investigated.

$$log(Q) = 1{,}782log(AE_{rms}) - 0{,}543log(P) + 0{,}320log(S) - 3{,}55 \qquad 2.7$$

Where Q is the leakage rate in ml/sec, *P* the inlet pressure in bars and *S* the valve size in inches.

The figure 2.2 shows the relationship between AE_{rms} and the leakage rate at 5 bars of different valve sizes. AE signals from different sensors were studied to establish the correlation in form of frequency response ratio of RMS.

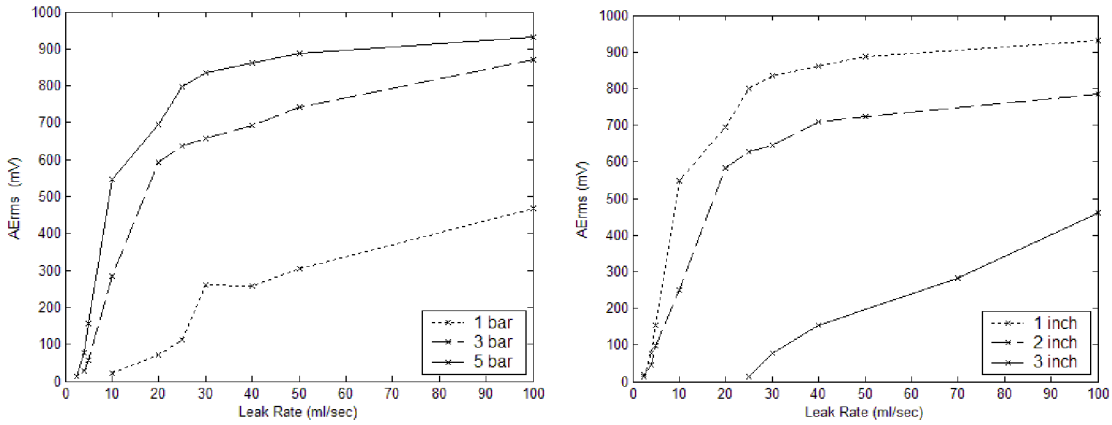

Figure 2.2 Relationship between AE_{rms} and leakage rates of 1inch ball valve at different pressures and leakage rates of different valve sizes at P = 5 bar [32].

2.2.Location of leakage

2.2

Several researchers has studied The AE since 1980s. *Kupperman et al.* demonstrated that the leak detection in reactor components with acoustic emission with the minimum leak; however, the threshold to detect the leak rate depends on pipe geometry, material, internal pressure and measurement system selected [33]. *Miller et al.* designed a reference standard pipe to evaluate the AE equipment for leak detection. The fundamental advantage of the AE method is the

capability to pinpoint the leak location in real time [34]. *Grabec* developed leak localization using cross correlation technique, which has limited success due to the influence of reflected waves and multiple wave modes. There are many studies since then to improve the location accuracy of continuous emissions [35]. *Gao et al.* also studied the effect of filtering on leak detection in plastic water pipelines [36]. *Fukuda and Mitsuoka* applied pre-whitening filter to AE waveforms to improve the leak detection and location through identifying a definite peak in the result of cross correlation of two waveforms [37]. *Wavelet* transformation is implemented to analyse complex leak signatures [38]. *Jiao et al.* used the dispersion curves of pipelines to identify the leak location with single sensor while the waveform can be influenced with reflections and multiple-sources in a realistic test. However, for any leak localization method, the dispersion (wave mode and frequency dependent velocity) and attenuation limit the minimum detectable leak rate and the maximum sensor spacing [39]. *Muggleton et al.* studied wave attenuation in plastic water pipes for frequencies less than 1 kHz. The attenuation factor depends on pipe material and geometry, surrounding medium and internal medium [40]. The leak detection and location in gas pipelines are more challenging than water pipelines because of smaller particle size of gas as compared to water that is the main source of AE through creating turbulence event at the leak location. Leak detection and location becomes more challenging for soil-buried pipelines as compared to on-ground pipelines or submerged pipelines. The reliable leak detection using the AE method requires understanding leak waveform characteristics as a function of pipe operational conditions and estimating the signal attenuation to define the discrete sensor spacing for pinpointing leak position spatially. The leak detection in gas pipelines using a continuous monitoring system can be used as an early diagnostic tool to prevent catastrophic failures [41].

The AE amplitudes for different leak conditions are presented in figure 2.3. The AE amplitude increases when the pressure increases. There is a slight difference in the responses of two sensors that reflects into the output signal. When the leak size or the orifice size increases, the AE amplitude increases as well. When the pressure increases the turbulence at the leak location increases and causes more chaotic behaviour and higher impacts, consequently, higher amplitude elastic waves, which agrees with the result of Yang et al. [42]. There is an exception for the fully buried case that the AE amplitudes of orifices 2 and 3 indicate similar trends with the pressure change.

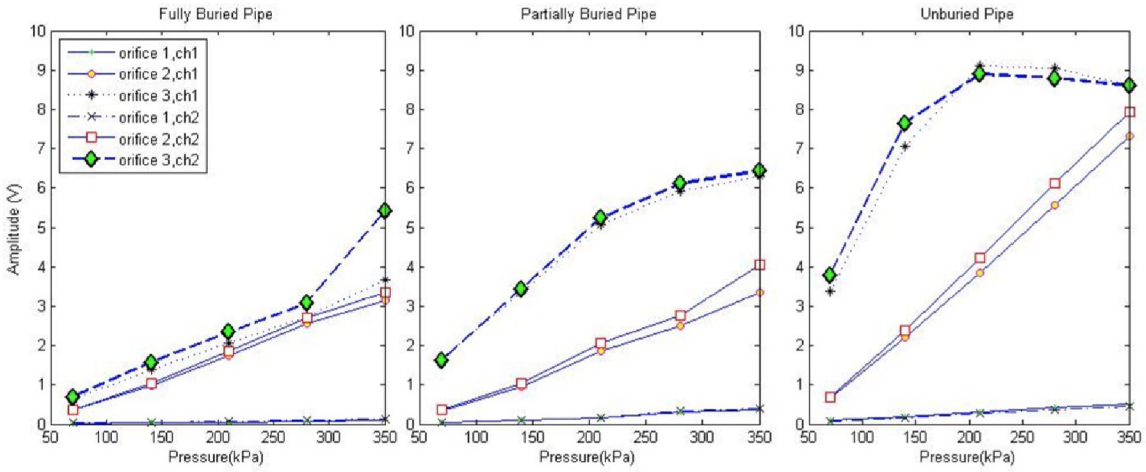

Figure 2.3 Leak waveform (time versus voltage) for unburied [42].

The leak AE amplitudes are driven for specific pipe geometry and leak simulator design. It is important to note that the amplitudes may show some variations depending on pipe thickness and geometry of leak hole.

The arrival time difference is the most critical input to the leak location algorithm as there is no well-defined arrival time of continuous emissions. The cross correlation function is typically used to determine the arrival time difference while this approach has limited success if the waveform includes reflected waves as in the case of this study as discussed in the introduction section . However, the AE method is a statistical method; therefore, an accumulation of an event cluster would be sufficient to pinpoint the leak location. The cross correlation function for discrete and finite duration signals is defined as:

$$R_{y_1y_2}(\tau) = \sum_{t=1}^{N} y_1(t)\, y_2(t+\tau) \qquad 2.8$$

Where $R_{y_1y_2}(\tau)$ is the cross correlation coefficient of two signals, y1 and y2, as a function of a time delay τ, N is the length of signal. The time delay becomes the input to the equation for linear localization as:

$$x = \frac{\tau V(f,h) + L}{2} \qquad 2.9$$

Where L is the distance between the sensors and V is the wave velocity, which depends on the frequency and the pipe thickness. The equation is valid if the source to sensor path is straight. *Ozevin and Harding* showed that the leak can be localized in multi-dimensional space using the linear localization equation and the geometric connectivity of the pipeline networks, which eliminates the limitation of source-sensor direct path need. Using the equations above, the leak location in the model pipeline is identified [43].

Z. Farova, Z. Prevorovsk , V. Kus, Serge Dos Santos studied AE localization and sources using Time reversal in nonlinearity position in the material applying TR operator to AE signal. Convolutional signal was obtained in the closest neighbourhood of acoustic source. The mathematical background was described for backside deconvolution by the Green functions. The disadvantage of this experiment is the initial source position localized beforehand because the measurements of the TR signal has to be done at the initial source position [44].

Shama et al. simulated a section of underwater oil pipeline to study the possibility of using AE technology to monitor leakage in a submarine oil pipeline. The researchers set up various defects and leaks with different flow rates in the pipelines [45]. The results show that AE can monitor and identify leakage in underwater oil pipelines. To address the inconvenience of leak measurement in long-distance buried pipelines, *Xu et al.* designed a guide rod that can be inserted into the soil. This rod extends directly to the surface of the pipeline. The AE information transmitted by the guide rod is used to locate the damaged area [46]. For pipeline leakage with high-pressure gas, *Mostafa pour et al*. deduced the radial displacement of pipeline vibration in AE wave propagation and compared the measured signal spectrum with numerical simulation calculation, proving that the AE stress wave can theoretically be used in pipeline leakage detection. To solve two problems related to leakage monitoring in buried liquid-filled pipes. This study attempts to locate the AE sensors installed inside a pipeline to collect leakage signals and to verify the effectiveness of the method used. This provides a basis for subsequent built-in self- capacitive AE sensors to monitor the damage of fluid - filled pipelines. In addition, to identifying leakage types and locations. Moreover, the time-delay estimation method is employed to accurately locate the leakage source in the pipeline [47]. *S. Davoodi and A. Mostafapour* studied pipe radial displacement caused by acoustic emission due to the leakage. [48].

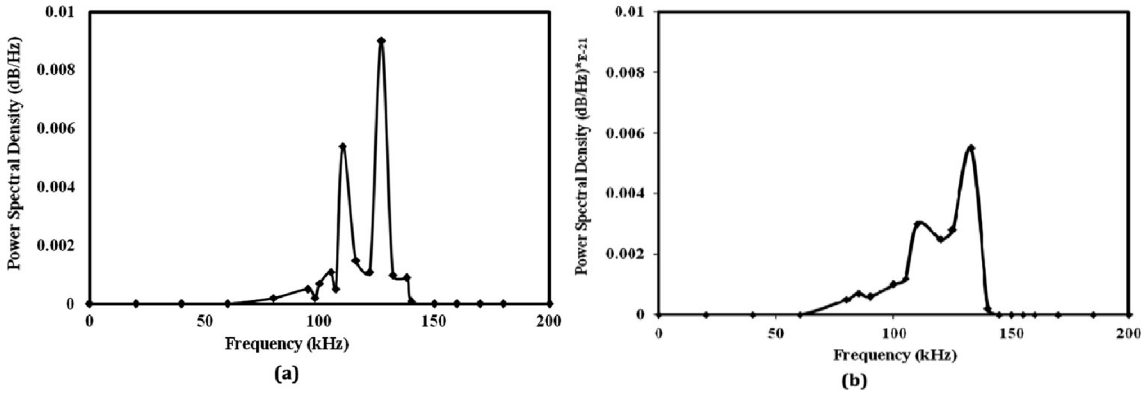

Figure 2.4 FFT results of test no. 1 for sensor S1 (a) experimental, (b) theoretical [48].

A. Anastasopoulos, D. Kourousis and K. Bollas [49] studied service buried pipelines of different sizes. It is a common understanding in all the above works that AE can be produced by the highly unstable turbulent pressure field at the orifice, and the condition of detection is that the Reynolds number. The flow is laminar when $Re < 2300$, transient when $2300 < Re < 4000$, turbulent when $Re > 4000$ at the orifice, to ensure turbulent flow. The corresponding AE signals generated are of a "continuous" nature. Additional sources that may produce AE in the occasion. Re = Reynolds number of a leak are local crack/orifice growth, cavitation due to local sub-pressure at the orifice, temporary entrapments and impacts of solid particles at the orifice, soil movements, or even external sources such as impacts etc., which are mainly "burst" type sources. The generated AE waves from such sources propagate through the fluid or through the pipeline itself.

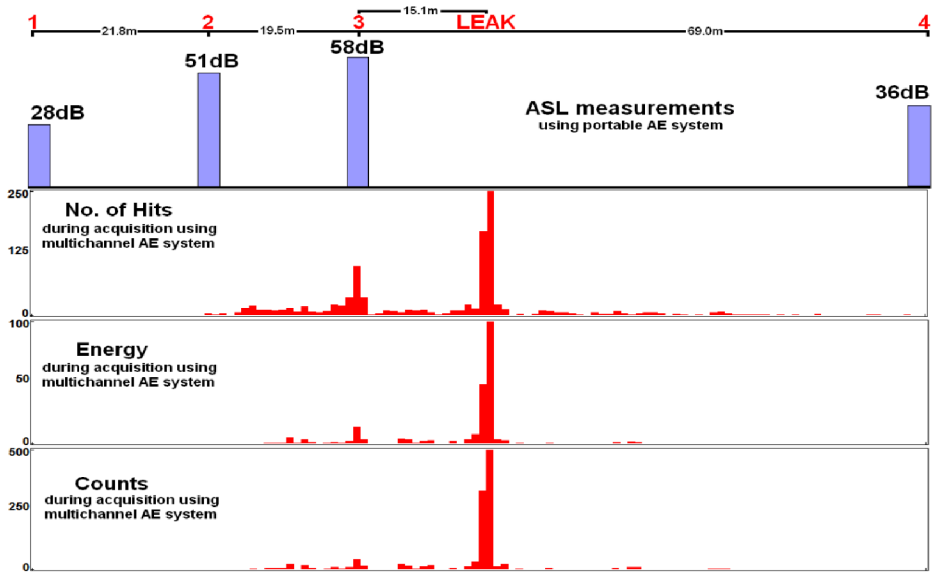

Figure 2.5 ASL vs. channel (top) and linear location indicating the leak point based on number of hits, energy and counts (bottom) of the acquired signals, after only 240 seconds of acquisition [49].

The suspect section of pipe can be isolated and pressurized to 4 to 9 bar, while the desired minimum pressure is above 10 bar. Based on experience, excavations and measurements are performed using low-frequency resonant sensors at about every 100 m.
Real-time linear location during acquisition provides most of the times a precise leak position within a few minutes, without any further analysis and the leak is confirmed immediately. *Augutis and Saunoris* studied fundamentally two types of detection method. The first one consists of a microphone that picks up airborne ultrasound, typically in the 35 to 450 kHz

frequency range. The second method detects structure-borne signals by attaching a sensor on the structure. Such a practice utilizes the technique of acoustic emission and is capable of leak location, continuous on-line monitoring hard-to-access location. Effectively applying acoustic detection methods requires full characterization of the particular leak signals, including the frequency spectrum, attenuation, and minimum leak rate detectable under given test conditions. Using results obtained through this study, an optimum detection system can be set up for either short term proof tests or long-term surveillance [50].

2.3. High frequency and pneumatic cylinders 2.3

Yan, Jin, Y. Heng-Hu, Y. Hong, Z. Feng, L. Zhen, W. Ping and Y. Yan studied Pneumatic cylinders. They are wearing down and it is an urgent problem to diagnose working conditions of pneumatic cylinders. The diagnostics of pneumatic cylinders is mostly based on pressure measurements and visual methods. The visual methods are simple and cheap, but inaccurate [51].

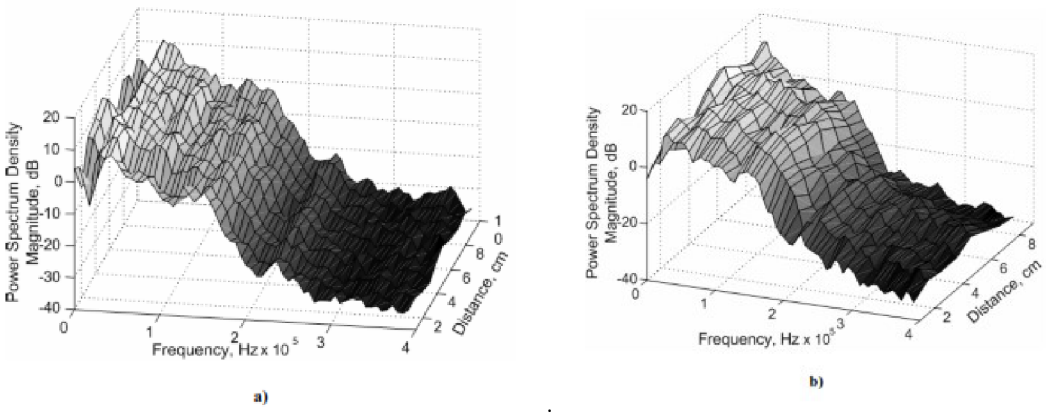

Figure 2.6 Power spectrum densities of the HFV high frequency voltage at various measurement points: a) new pneumatic cylinder; b) worn pneumatic cylinder [51].

While the pneumatic cylinder is working, the pneumatic cylinder housing is wearing down due to the piston repeated movement. This causes the leak between the piston and the pneumatic cylinder housing. It was found that the leak causes higher intensity of the. HFV. The parameters of the HFV may be used for the diagnostics of pneumatic cylinder.

The HFV are generated inside the object under investigation while the pneumatic cylinder works. The generated HFV signal is the noise type non-stationary signal. The basic characteristics of the generated HFV, which are measured, are root mean square value, the envelope of the root mean square values and the power spectrum density.

The friction between the piston and pneumatic cylinder housing is a dominating factor in the formation of the HFV in the worn pneumatic cylinder. It was found that the influence of the friction is approximately 10 times bigger than the influence of the leak between the piston and the pneumatic cylinder. In the new pneumatic cylinder, the HFV are generated just due to the friction between the piston and the pneumatic cylinder housing. The intensity of the HFV on the worn pneumatic cylinder housing is about 5 times higher than the intensity of the HFV measured inside of the pneumatic cylinder. Correlation of AE signals from two AE systems with valve leakage rate detection application was studied in various conditions including different valve leak sizes and inlet pressures. Nevertheless, the result is still practically useful with the application of AE_{rms} instead of individual frequencies of the whole spectrum.

2.4.Cylinder and loading

T. Fujita, J. Jang, T. Kagawa and M. Takeuchi [52] studied that drive a pneumatic cylinder, meter-out circuit is used in many cases, since time to move the piston is constant even if the load is changed. That is, the meter-out restriction method realized velocity control. However, this principle of velocity control has not been explained sufficiently. The purpose of this study is to clarify the velocity control mechanism. Consequently, six parameters controlling the cylinder response are obtained. As a result, by drawing the block diagram of cylinder system, it is found that the compliance of a cylinder makes the feedback loop in cylinder velocity and the flow characteristics of retread in damping compensates the constant velocity for changing a load force.

M. Doll, R. Neumann and O. Sawodny [53] studied dimensioning pneumatic cylinders for motion tasks, considered the standard pneumatic cylinders with common directional control valves and exhaust flow throttles. The dimensioning of the cylinders for point-to-point motions is regarding energy efficiency. The proposed strategy is based on the Eigen frequency and considers similarity transformations.

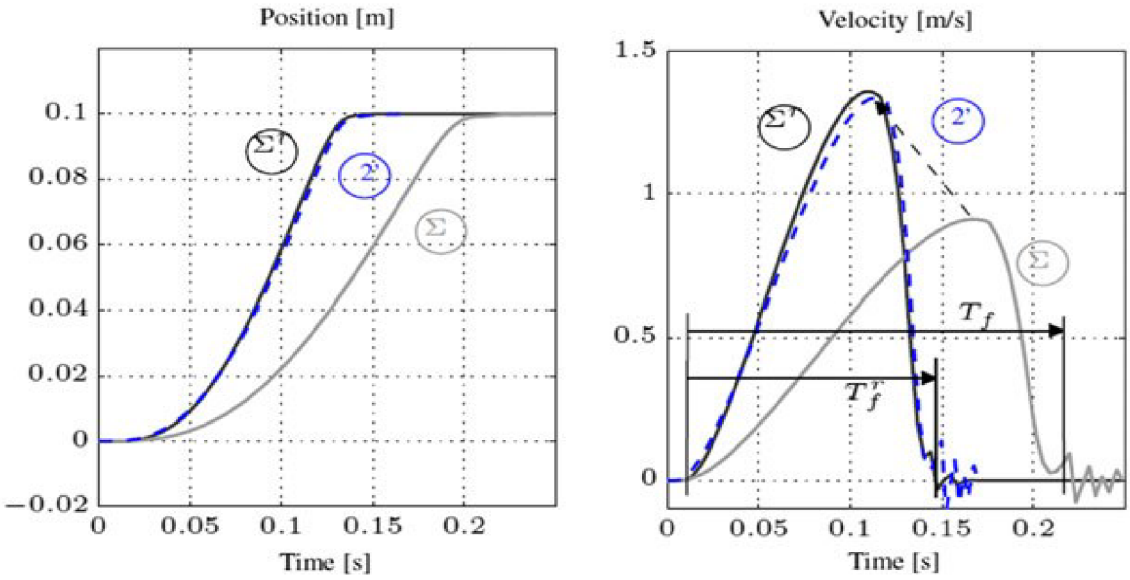

Figure 2.7 Illustration of a similar system dynamics between two systems [53].

This paper shows a new approach for sizing pneumatic cylinders. Eigen-frequency of a pneumatic cylinder is a characteristic quantity expressing the possible speed of the system. A new characteristic factor is introduced with the PFR, which expresses the ratio between the demanded speed and the possible speed. The dimensioning approach is validated by using the differential equations of the system dynamics. It is shown that the PFR approach does not compensate all the nonlinearities; especially where the friction force has an influence on residual errors. The PFR expresses that an energy efficient dimensioning is achieved, if both the Eigen-frequency and the frequency correlated to the transition time match, i.e. $\Omega = 1$. It is shown that the PFR characterises the system dynamics, for instance it can be used for classification purposes.

3. Analysis and evaluation of references 3

Effectively applying acoustic detection methods requires full characterization of the particular leak signals, including the frequency spectrum, attenuation, and minimum leak rate detectable under given test conditions. Testing methods of leaks is rarely used to test the leak in cylinders. Our test was to reduce the noise by the filters and in the [10-12] they tried to apply AE to detect leak and reduce the noises and to find the relation between the AE parameters and leak. All experiments had tried the frequency spectrum in the first [13 - 18]. Modelling an internal leak in a valve with unknown leak geometry is inherently difficult to detect and presenting relationship between AE parameters and the leakage rate. The flow is laminar when Reynolds number $Re < 2300$, transient when $2300 < Re < 4000$, turbulent when $Re > 4000$ at the orifice [19]. The power spectrum density of fresh water was greater than the compressed air because the acoustic impedance of water was closer to that of the valve material.

Mobile diagnostic tool using AE methods with greater sensitivity of detection of defects using sensors [20-24].
For continuous AE signal from both time and frequency domains, the most frequently used AE parameters are the average energy (AE_{rms}) and the Average Signal Level (ASL), The AErms increased with inlet pressure, which was similar to the relationship between the AErms and the leakage rate. The AErms was inversely proportional to the size of valve. The AErms was inversely proportional to the flow coefficient [25 - 31]. When the leak rate increases the amplitude of RMS increases with constant pressure and different valve size or in constant valve size and different pressure. All results have shown that the AE technique can work well in the field of valves [32].
Leakage may also be characterized by the effective diameter of leakage orifice. A method of indirect orifice diameter estimation using working pressure and flow rate pattern magnitude of initial cylinder operation phase was presented. Comparing with other leak detection techniques, acoustic emission methods give strong advantages in regard to leak location, continuous on-line surveillance, high sensitivity, quick response time, monitoring hard to-access locations, and potential estimation of leak rate. Typical AE is able to determine the location of defect in all last researches [33 - 50]. The obtained signal very similar to the initial AE signal by experimental deconvolution using TRA principle to localize the sources of AE [44].
All defects are undesirable. The applications of new processing methods of AE signals including fast Fourier transform (FFT), wavelet transform, Hilbert-Huang transform (HHT), neural networks, and genetic algorithm in valves are presented. AE activities increases when there is leakage when the leak rate increases the amplitude of AE increases [51].
By using only, a restriction the meter-out circuit realizes velocity control. The load change does not affect much the piston velocity. It can be used to dimension systems with approximately constant speed, and it delivers interesting relations between all the system parameters. Furthermore, it can be used to increase energy efficiency by calculating a reduced, correct pressure level for existing [52,53].

4 4. Aim of Thesis

4.1. Objectives of the research

The aim of this work is to develop a new efficient diagnostic procedure for checking the function of pneumatic cylinders using acoustic emission.
This diagnostic procedure is able to detect distinctive differences that determine whether the cylinder is damaged or undamaged by finding a typical acoustic emission signal that associated with a particular type of damage, which it happens by select the necessary parameters of AE.

Determination of the relationship between parameters of AE and defects in the cylinders, precisely the relation between RMS of AE and the leakage that elucidates the rate and the location of leakage.

The possibility to determine the type of defects in the cylinders after production in order to change the damaged parts

The possibility to determine the quality of cylinders after production, and Predict the defect during actual operation of the cylinder (online checking) and determining the level of danger. Determination of the diagnostic criteria that evaluate the quality of the pneumatic cylinder and detect the defects, these diagnostic criteria are inserted later by MATLAB to make a program that is capable of evaluate the cylinders.

The novelty of the proposed solution lies in a very new concept for mobile diagnostic tool using AE methods with greater sensitivity of detection of defects. Simplified designing process of electronic equipment for data capture development and evaluation software.

4.2.Diagnostic criteria

1. The RMS was normalized, and the different responses between damaged and undamaged pneumatic cylinders were recognized by the time delay of the strokes.
2. The differences were identified by comparing the max RMS from the sensor fixed in the head cap of the cylinder and the max RMS from the sensor fixed in the rear cap of the cylinder for one cycle in the retreat stroke.
3. The damaged and undamaged cylinders were distinguished using the difference in energy values present in the signals from the two sensors in the retreat stroke.
4. The final evaluation of the cylinder was determined by the calculation of the total value of RMS.

4.3. Hypotheses and Questions.

4.3.1. The problem that we face in the work (disadvantages)

1. The different behaviour of recorded signal in undamaged cylinders.
2. Assembly of sensors on the cylinder and the type of the cylinders.
3. The noise is in the signal.
4. The signal is mixture noise of mechanical movement and pressure air inlet and outlet.

4.3.2. Hypotheses

The changing of signal takes place when the cushion portion piston inserts to cushion seal causing the initiation of throttling or damping.
When the value of the leak usually increases the signal of AE increases.
The allowance of leakage value in the cylinder is no more than 6 pa/s.
The flow is laminar when Reynolds number Re < 2300, transient when 2300 < Re < 4000, turbulent when Re > 4000 at the orifice.

4.3.3. Scientific questions

1. What is the relationship between pressure in the pneumatic cylinder and the AE?
2. What is the relationship between the kinematic energy in the cylinder and AE?
3. What is the relationship between the friction and AE?
4. What are the effects of the mixing defects in the cylinder to the AE?
5. What are the suitable conditions of testing the cylinder using AE?

4.4. Thesis layout

1. Finding the relationship between AE and the leakage using frequency spectrum.
2. Finding the relationship between typical acoustic emission signal and particular type of damage in the cylinder using RMS.
3. To find distinctive differences that determine whether the cylinder is damaged or undamaged.
4. The relationship between AE parameters and loaded cylinders.

5 5. Experiment, Measurement and Methods

5.1.Pneumatic actuators

Pneumatic actuator is a device, which transform the energy from a compressed air supply into a linear or rotary movement. In essence, actuators are providing specific tasks such as clamping, picking and placing, filling, ejecting and tool changing. Rapid changes in market requirements and a demand for smaller but more powerful and efficient devices made a wide range of actuators.

5.1.1. Types of cylinder

Three types of cylinders were tested - PS, PB and RD (producer Polices strojirny a.s.).

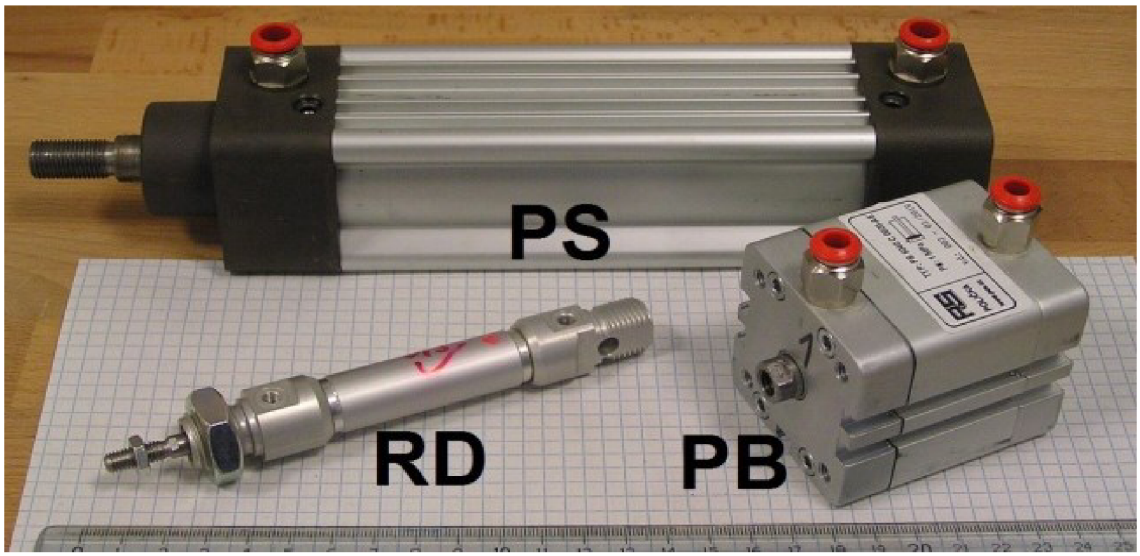

Figure 5.1 Types of tested pneumatic cylinders.

All results of this work is depending on PS pneumatic cylinders as shown in figure 5.2.

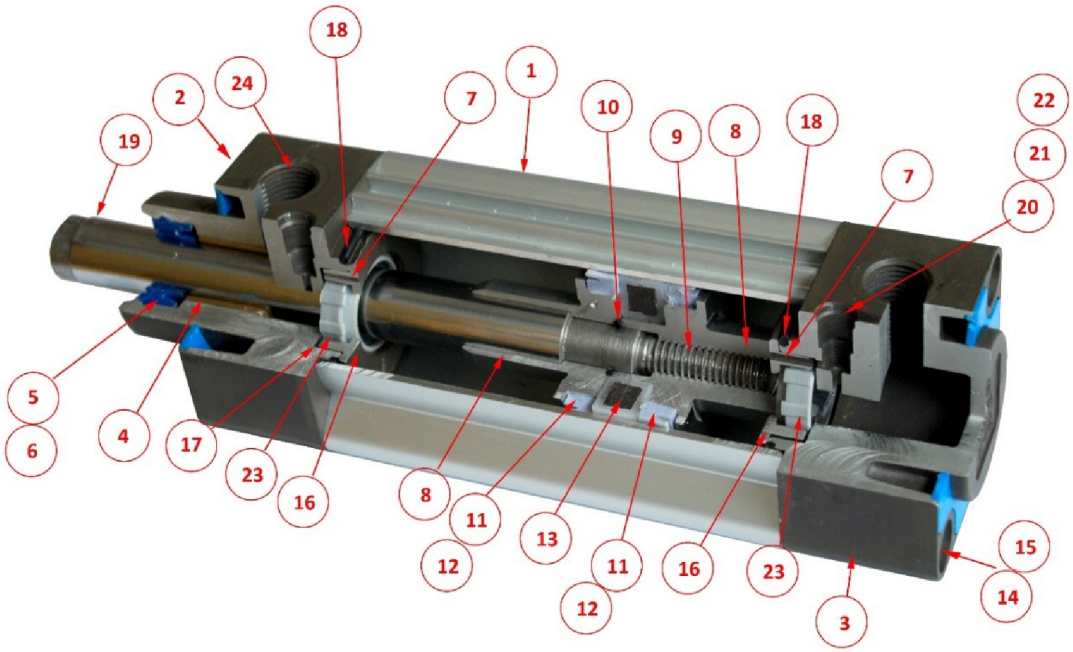

Figure 5.2 Parts of pneumatic cylinder PS.

(1) Cylinder body (barrel). (2) Head cap. (3) Rear cap. (4) Rod Bearing. (5) Rod wiper (Wiper Seal). (6) Rod Seal lip-seal. (7) Needle valve. (8) Head and rear Piston. (9) Piston fastener (Tie Rods). (10) O- ring seal piston fastener. (11) Piston seal lip-seal. (12) Piston seal bumper seal. (13) Magnetic ring. (14) Head cap fastener. (15) Rear Cap fastener. (16) Head cap cushion, rear cap cushion. (17) O- Ring seal needle valve. (18)O- Ring seal cap cushion. (19) Piston rod. (20) Throttle needle valve. (21) O- ring seal throttle needle valve. (22) Throttle knop. (23) Cushion check seal. (24) Porting.
The characterization of PS actuator: width 50mm, inside diameter 40mm, stroke 100mm, and diameter of rod 12mm port 6mm. The process of understanding of defects requires detailed knowledge of the different parts of the cylinder. The main parts are shown in figure 5.2.

5.1.2 Principle of pneumatic cylinder work

Each cycle of the cylinder is divided into two strokes: the progress and retreat strokes.

Progress stroke

The valve is opened by a digital input, and the air starts entering through port B in the rear cap to the damping area, the air passes around the cushion throttle and then through the throttle nozzle to the space between the cushion seal lip and the damping rear piston. When the minimum required pressure is reached the piston starts moving from the BDC (bottom dead centre), and the piston extends to reach the TDC (top dead centre). The cushion head piston pushes out the air to expel it through port A in the head cap. The damping phase starts when the head damping piston touches the head seal cushion at a distance of 21.7mm. In the damping phase the air is pushed through the throttle nozzle only, until the piston reaches the TDC. The end of the progress stroke is when the head cushion piston impacts the head cushion cap. The air is supplied from Port B during this stroke and the air of chamber A is vented to the atmosphere, see figure 5.3.

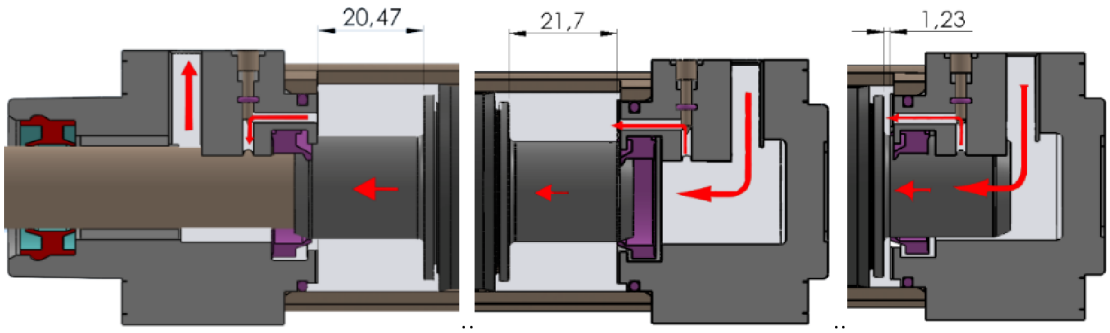

c) Initiation of damping, b) Piston leaving the damping area, a) Initiation of piston movement.

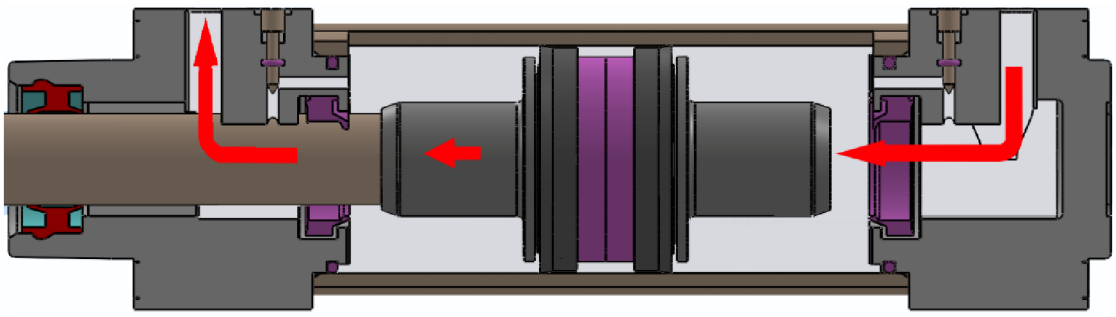

Figure 5.3 Progress stroke steps and position of piston.

Retreat stroke

The valve is opened by a digital input, and the air starts entering through port A in the head cap, to the damping area. The air passes around the cushion throttle and then through the throttle nozzle to the space between the cushion seal lip and the damping head piston. When the minimum required pressure is reached the piston starts moving from the TDC, and the piston eventually retreats to the BDC. The cushion rear piston pushes out the air to expel it through the port A. The rear damping piston is inserted into the rear seal cushion at a distance of 21.7mm before the BDC. Subsequently, the damping phase starts when the air is pushed only through the throttle nozzle and continues, until the rear cushion piston impacts the rear cushion cap, to finish the retreat stroke. The air is supplied through port A during the retreat stroke and the air of chamber B is vented to the atmosphere, see figure 5.4.

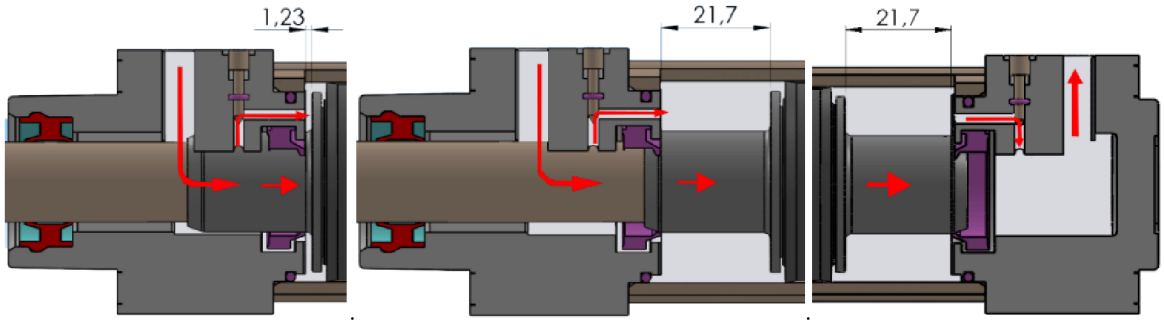

a) Initiation of piston movement, b) Piston leaving the damping area, c) Initiation of damping.

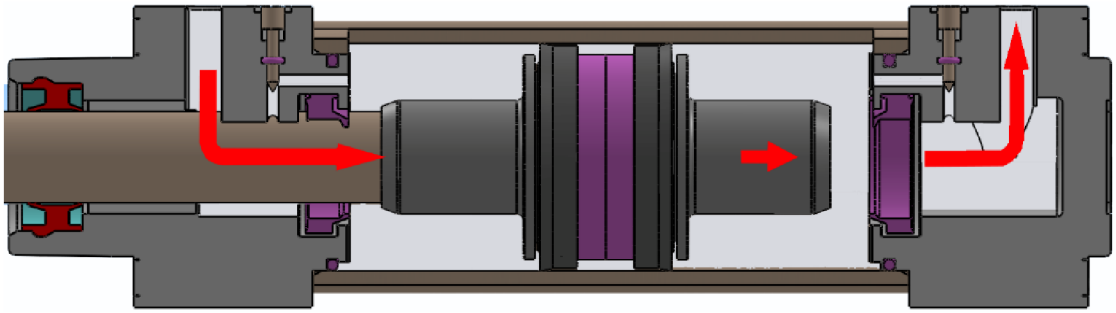

Figure 5.4 Retreat stroke steps and position of piston.

5.2. Defects

All defects are undesirable. Defects may affect the function of the product and deteriorate its parameters, possibly it causes disorder in the product which is no longer able to fulfil its function. Defects can arise in the production stage, damage by external influences, wear, fatigue, etc. AE diagnostic methods for the pneumatic elements is projected to increase the quality in the production process, the possibility to detect damage during operation and diagnostic status and to predict fatal malfunction. Possible defects of the cylinders based on their construction in condition of operation. Early detection of defects can prevent critical equipment failure. The existence of the detection coefficient facilitates the evaluation of defects, taking values that range from 1 to 10, with 10 being highly difficult to detect. The detection coefficient was taken from the method FMEA (Failure Mode and Effects Analysis) and was developed and classified using AE. These tests achieved impressive results, which demonstrated that the detection coefficient from AE produces small values compared with other non-destructive testing methods. Defects can be evaluated according to the criteria of their relevance to the customer. The Coefficient "S" expresses the severity of a particular defect, taken from the method FMEA.This parameter is given in two forms: "S1" for a single defect with no consequences, and "S2" reflecting the worst possible consequences, which may indicate a defect [54].

5.2.1. Leakage

Leakage is caused by deterioration or loss of sealing function, damage of the seals surfaces of the components or through the part. Note: This list excludes defects that are recognizable outside the control of the test, such as: fittings and bolts are tightened, there is no obvious mechanical damage of cylinder. Leaks in the end position when the pressure above the piston / retracted piston rod [54].

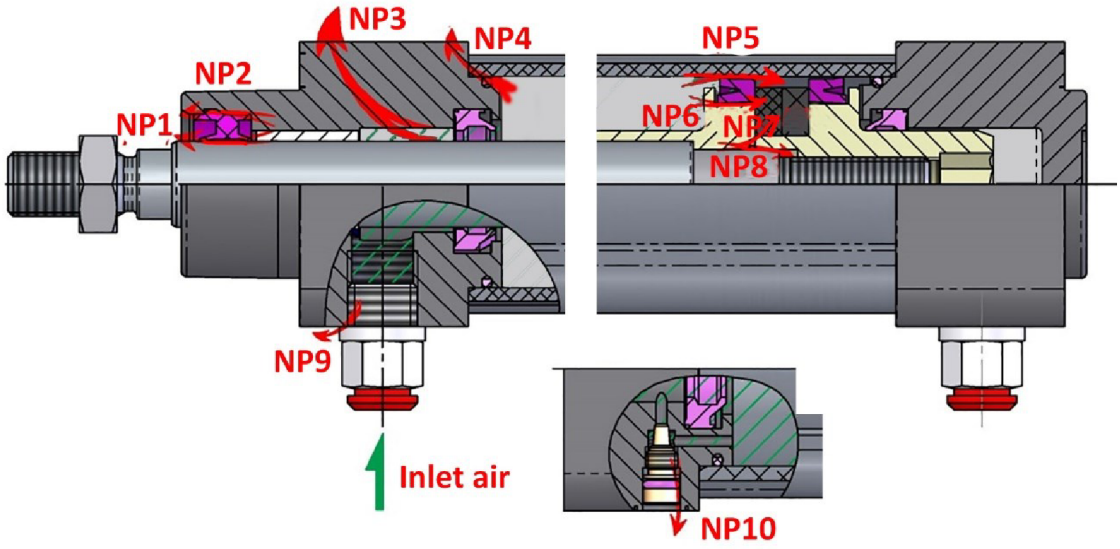

Figure 5.5 Leaks above the piston in the retreat stroke [54].

NP1. Rod wiper seal in the head cap, NP02. Rod wiper seal in the head cap, NP3. Head cap, NP4. Sealing the barrel on the head cap, NP05. Sealing the front, Piston seal bumper seal, NP6. Sealing the front Piston seal lib seal, NP07. Sealing the front and rear piston O- ring seal piston fastener, NP8. Sealing the front of the piston on the piston rod, NP9. Seal porting, NP10. Seal throttle needle.

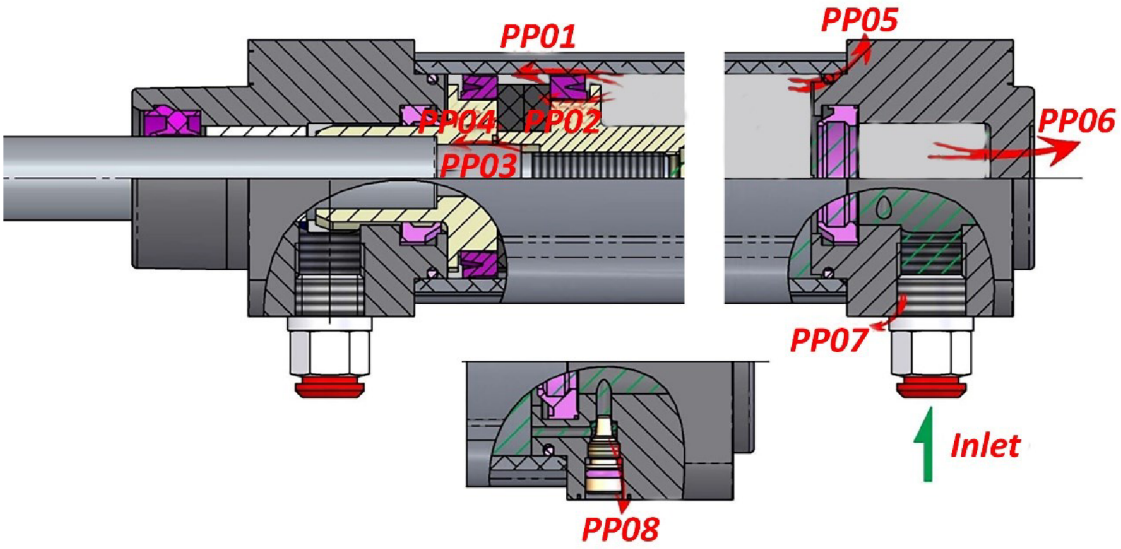

Figure 5.6 Leaks below the piston in progress stroke [54].

PP01. Sealing the rear piston in the barrel, PP02. Sealing the rear piston in the barrel, PP03. Sealing the rear piston on the piston rod, PP04. Sealing the front and rear piston O- ring seal piston fastener, PP05. Sealing the barrel in the rear cap, PP06. The rear cap, PP07. Seal porting, PP08. Seal throttle needle.

5.2.2. Leaks in motion

When the damping is on, before reaching of end position. Throttle needle was deteriorated it makes leakage, then damping is lost [54].

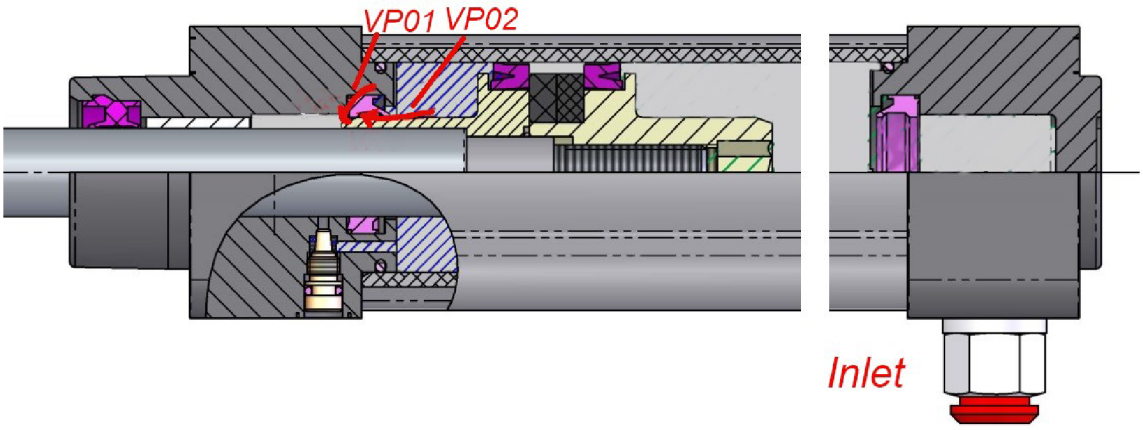

Figure 5.7 Leaks during damping in progress stroke [54].
VP01. Damping and throttling in the head cap, VP02. Damping and throttling in the head cap.

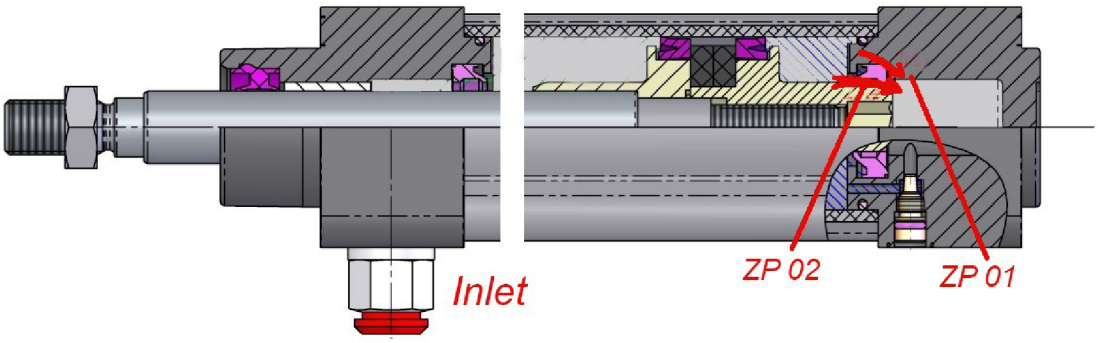

Figure 5.8 Leaks during damping in retreat stroke [54].

ZP01. Damping and throttling in the rear cap, ZP02. Damping and throttling in the rear cap.

5.2.3. Galling

During operation the sliding surfaces may cause deterioration in the friction conditions. The result is a deterioration of the cylinders, reduce the force on the piston rod during ejection and retraction, unwanted sound speeches or complete loss of function [53].

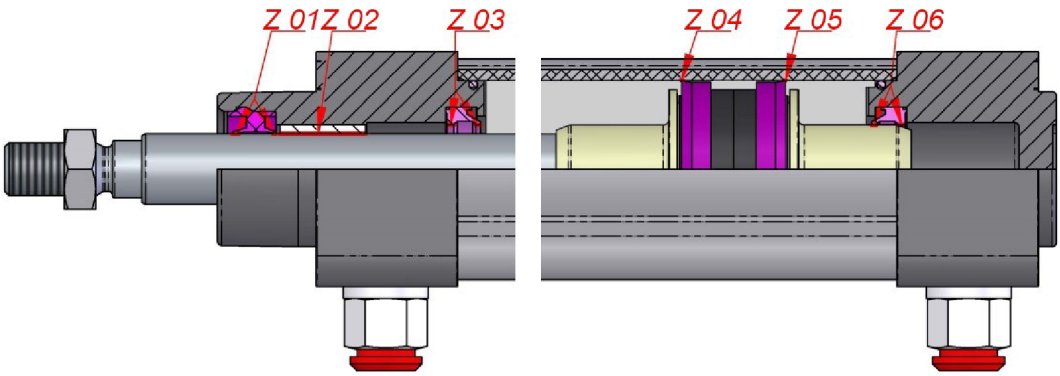

Figure 5.9 Places of galling [54].

Z01. Rod seal in the head cap, Z02. case in the head cap, Z03. Cushion check seal in the head cap, Z04. Cylinder tube (barrel), Z05 Cylinder tube (barrel)., Z06. Cushion check seal in the rear cap.

5.2.4. Mechanical defects

Many mechanical defects can include damage of parts from an external force, the loss of thread connection with their subsequent to release parts and high cycle fatigue damage. Damage from the external force, which may not be visible from outside as bending rod, which can cause irregularities in operation of certain sections of the stroke of the cylinder or even blocked. Loosening of bolted joints, damage of caps, can exhaust the cylinder with the destruction of the above-mentioned serious consequences indications such disorders at an early stage can significantly contribute to the prevention of serious accidents [54].

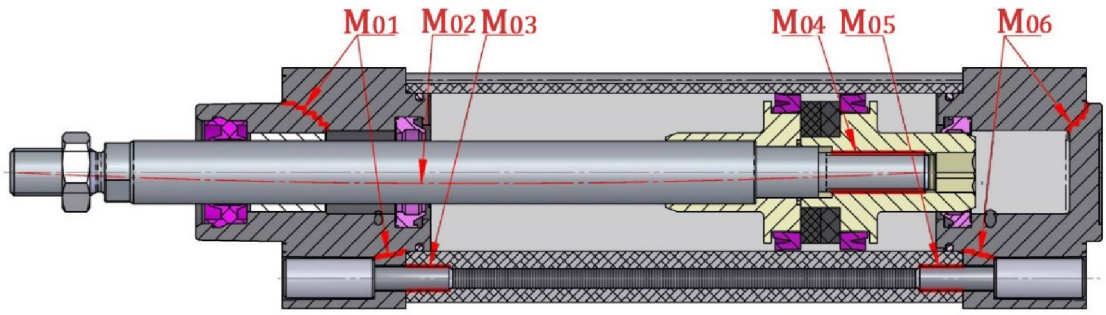

Figure 5.10 Mechanical defects [54].

M01. Damage to the head cap, M02. Deflection rod, M03. Loosening the screws of the head cap, M04. Release piston, M05. Loosening the screws of the rear cap, M06. Damage to the rear cap.

5.3. Types of specific defects

5.3

All defects are undesirable. Defects may affect the function of the product and cause malfunctions. The defects were simulated and made artificially: leakage, leaks in motion, galling and mechanical defects.
Three types of defects were chosen. All have a high value of detection coefficient

5.3.1. Mechanical defect M04

In this type of defect, the piston was loosened a quarter of a turn on the undamaged cylinders (M04) to allow some clearance for the magnetic ring (13) in figure 5.2 of about 0.3 mm, and some glue on the piston seal bumper was left. Leakage was measured using (ATEQ F 520) (a device for measuring leaks). The result was about two Pa/s, which means the leak was negligible.

5.3.2. Unsealed O-ring and notched piston thread leakage – NP08, PP03

A defect was created in undamaged cylinder No.21: an unsealed O-ring number (10) in figure 5.2 between the piston (8) and piston rod (19) produced a leak between the piston (8) and the thread (9) on the inner side. The application of soapy water demonstrated that the cylinder produced a leak around the piston rod. Measurements by ATEQ on the cylinder showed that the value of the leak at a pressure below the piston (progress stroke) is 78Pa/s, and the value of the leak at a pressure above the piston (retreat stroke) is 93Pa/s, (a suitable value for the actuator cylinder 6 Pa/sec).

5.3.3. Unsealed O-ring, leakage between front and rear Piston - NP07

A defect was created in undamaged cylinder No.32: a missing O-ring number (10) in figure 5.2, between head and rear piston (8). Application of soapy water demonstrated that the cylinder produced a leak between the front and rear piston. Measurements by ATEQ on the cylinder showed that the value of the leak at a pressure above the piston (retreat stroke) is 410 Pa/s, and there was no leakage at a pressure below the piston (progress stroke).

5.4. Equations

AE_{rms} can be defined as:

$$AErms = \sqrt{\frac{1}{T}\int_{t_0}^{t_0+T} v^2(t)dt} = \sqrt{\frac{1}{N}\sum_{n=1}^{N} v^2(n)} \qquad 5.1$$

Here, v is the voltage signal from an AE sensor, t the initial time, T the integration time of the signal, and N the number of discrete AE data within the interval T. Thus, we are attempting to highlight the parameter RMS.

Root Mean Square and Energy defined as:

$$RMS = \sqrt{(1/N)\sum_{1}^{N} u_i^2} \quad [V] \qquad 5.2$$

$$E = \sum \mathrm{u}_i^2 * \mathrm{dT} \quad [V^2 * s * ohm] \qquad 5.3$$

Where N discrete voltage values sampled over the measurement period, u is voltage, dT is the value of sampling (in our case 0.004s).

5.5. Stand of the experiment

5.5.1. Horizontal stands for pneumatic cylinder without load

At Brno University of Technology, there are in the lab the experiment platform, test devices and some equipment including damaged and undamaged cylinders. The experiment platform contains testing devices including tested cylinders PS ISO Piston diameter 40mm, piston stroke 100 mm, thread M12x1.25, air pressure supply 6 bar, pneumatic control system, linear potentiometer (working range of potentiometer is 0-200 mm, global measurement period is 156.25 Hz). Two magnetic sensors were positioned at the piston track to define the start and the end of the stroke by controlling the beginning of progress and retreat strokes. The distance between them is 100 mm and the AE monitoring system with the analyser DAKEL-ZEDO with two channels. Global measurement period of AE parameters (RMS, Energy) (sampling) is 250 Hz (0.004 s). AE piezoelectric sensors IDK-14 built-in preamplifier 34 dB frequency range [10-400 kHz]. Two sensors were installed at the cylinder and were referred to as (A) on the head cap and (B) on the rear cap. A scheme for the connection of components of experiment is shown in figures 5.11 and 5.12.

.

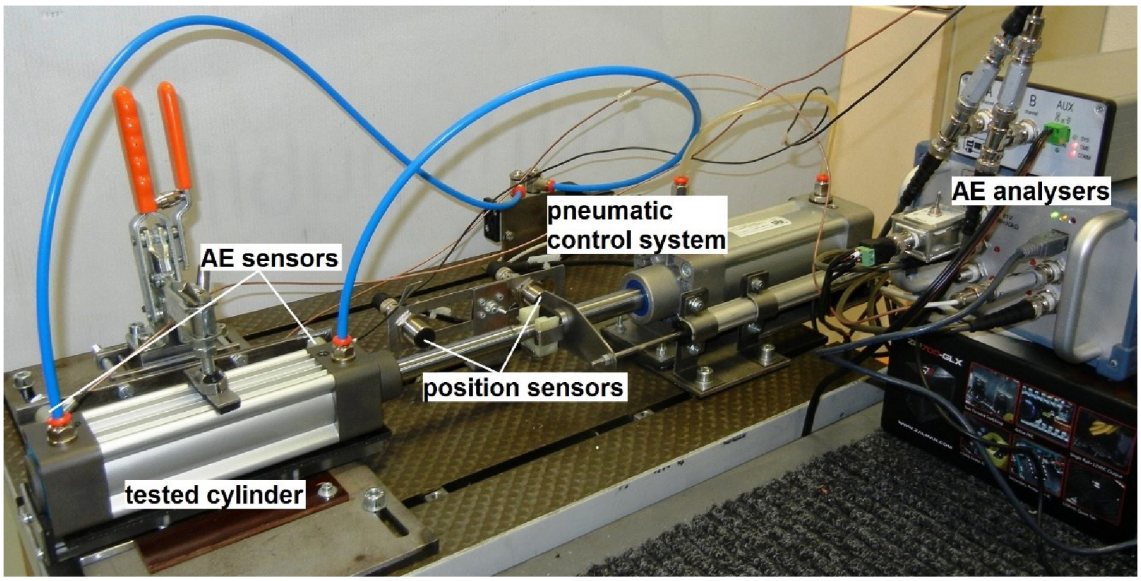

Figure 5.11 Assembly of experimental equipment.

When the progress stroke begin by the digital signal in the valve until magnetic sensor, then the retreat stroke begin. The AE signal recorded by two sensors which are installed at different positions of the cylinder. left sensor placed on the head cap (A, Red). The right sensor (B, blue).

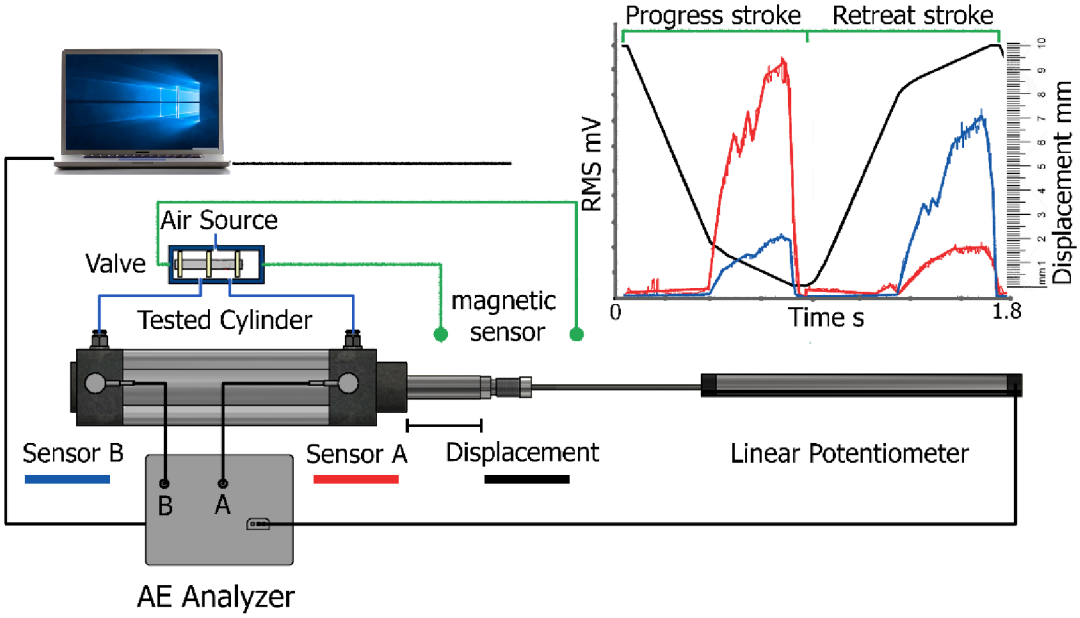

Figure 5.12 schematic drawing of the experiment.

5.5.2. Vertical stands for pneumatic cylinder with loads

The equipment used to conduct the experiment includes tested cylinders PS ISO Piston diameter 40mm, Piston stroke 100mm, Thread M12x1.25, AE sensors IDK-14 Built-in preamplifier 35 dB, air pressure supply, pneumatic control system, linear potentiometer and the AE monitoring system with the analyser DAKEL-ZEDO with two channels and different weights. The cylinder is put in the vertical position with loading and the locations of AE sensors are on head cap A and rear cap B of the cylinder body as shown in figures 5.13 and 5.14.

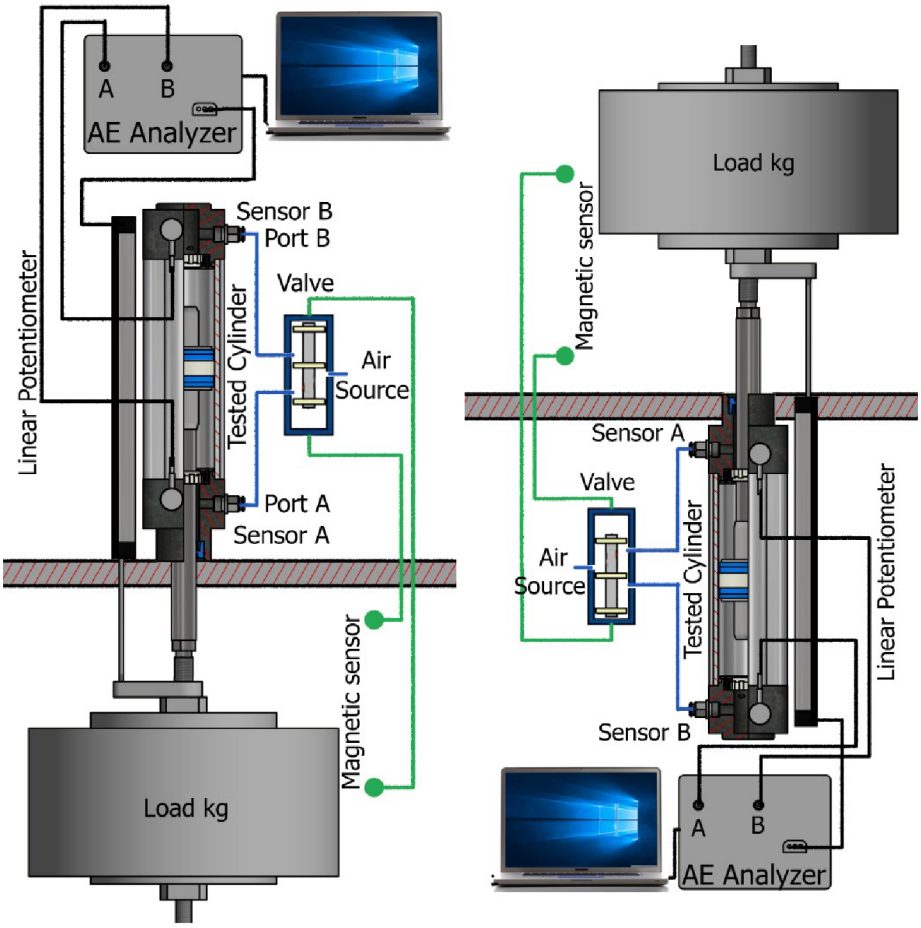

a) Loading below the rod of cylinder b) Loading above the rod of cylinder

Figure 5.13 Schematic drawing of the experiment equipment in Vertical position.

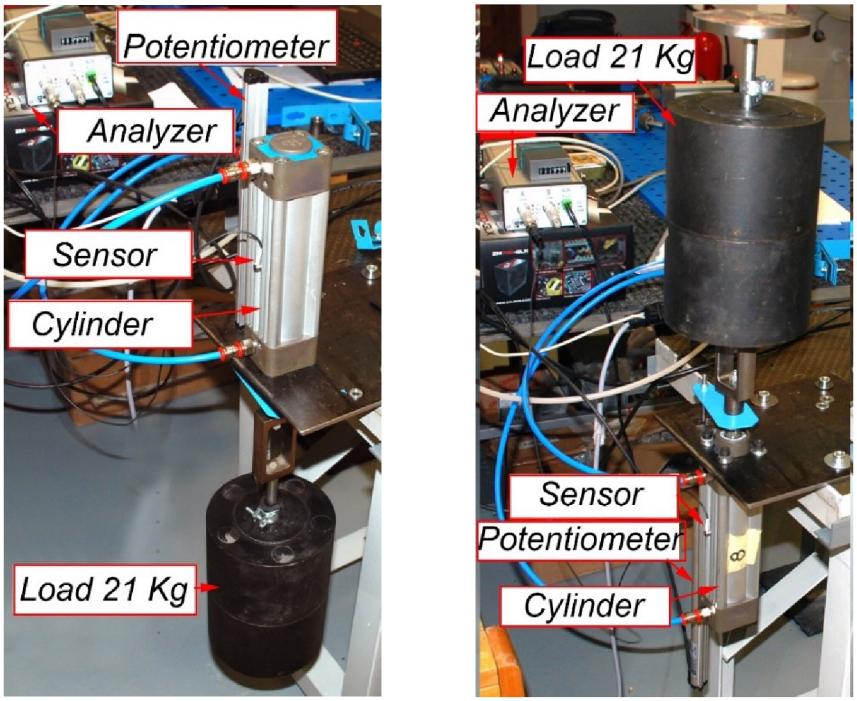

a) Loading below the rod of cylinder b) Loading above the rod of cylinder

Figure 5.14 Assembly of experimental equipment in vertical position.

5.6. Types of sensors of acoustic emission 5.6

Several types of transducers can be used for this: piezoelectric, capacitance, electromagnetic and optical. The last two are non-contact, but electromagnetic transducers are considerably less sensitive than piezoelectric transducers [55]. Piezoelectric transducers are the most popular and are of either a broadband or a resonance type. The transducers are made by using a special ceramic, usually Porous Lead Zirconated Titanite (PZT), figure 5.15 shows a schematic view of a piezoelectric transducer and how an AE is converted into an electric representation. The transducers are pressed up against the surface of the material and the vibration is transferred to the PZT inside the transducer through the wear plate. When the PZT element vibrates, it generates an electric signal. The transducer's signal is, therefore, a 1D voltage-time representation of the 3D displacement-time wave that it senses [55].

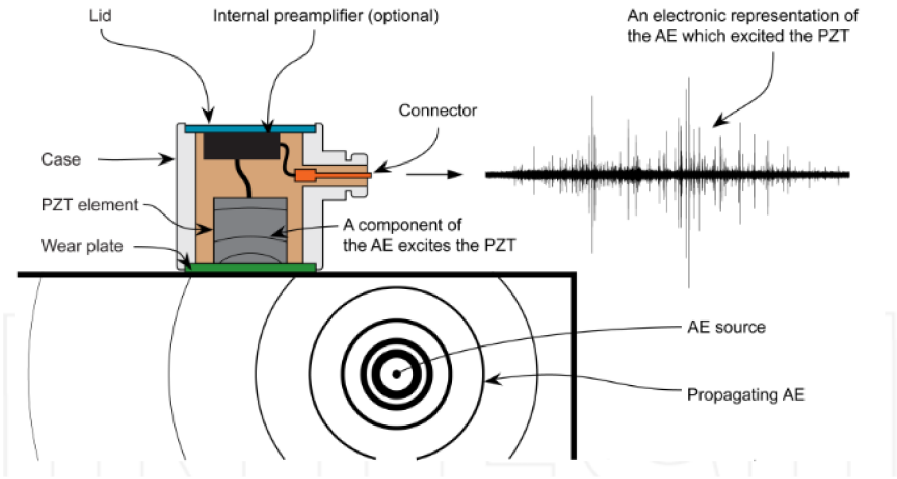

Figure 5.15 Illustration of a typical resonant piezoelectric AE transducer and how an AE is converted into an electric representation [55].

Table 5.1 Two types of sensors are used in our testing [56].

Type of sensors	**a) Model IDK-09**	**b) Model IDK-14AS**
Dimensions	Diameter 9mm, height 9mm	Diameter 14 mm, height 6 mm
Case material	Stainless steel	Stainless steel
Face material	Ceramic Contact area D 6mm	Ceramic Contact area diameter 11mm
Output	Coaxial cable D 1.7mm with BNC connector	Coaxial cable D 1.7mm with BNC connector
Piezoceramic martial	PZT class 200	PZT class 200
Operation temperature	-20C to +95 C	IDK 14AS: -20C to +65 C IDK 14: -20C to +95 C
Recommended applications	Laboratory and industrial using on small objects	Laboratory and industrial using on small objects
Preamplifier	None	None
Mounting methods	magnetic or mechanical holder	magnetic or mechanical holder
Bandwidth	25-525 KHz	50-450 KHz

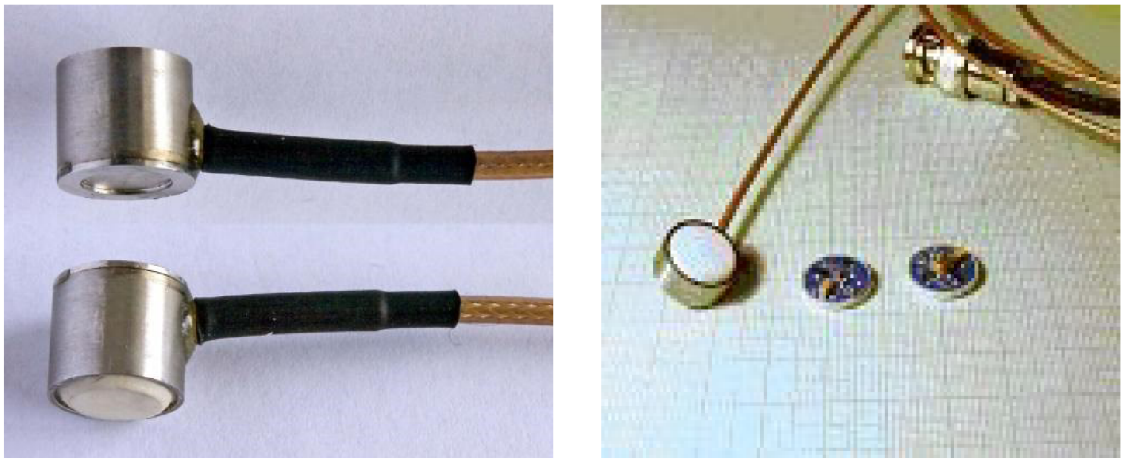

a) Model IDK-09 b) Model IDK-14AS

Figure 5.16 Type of sensors [56].

5.7. Software and apparatus 5.7

5.7.1. Main application window ZDAEMON

The main application window consists of the following customizable parts:

1. Menu and Toolbars area.
2. System Map view – with hierarchic list of items representing all system functions: data acquisition units, system alarms, localization groups, attenuation curves, recorded data readers, importers, etc. Description of the individual System Map items will follow in the next sections.
3. Data Source List view – showing a list of data sources provided by currently selected System Map item. Each such data source can be added to graph views for visualization.
4. Properties view – showing a list of properties of item or items currently selected in the System Map or in any other view within the application window. ZEDO system configuration is achieved by editing properties of various system items.

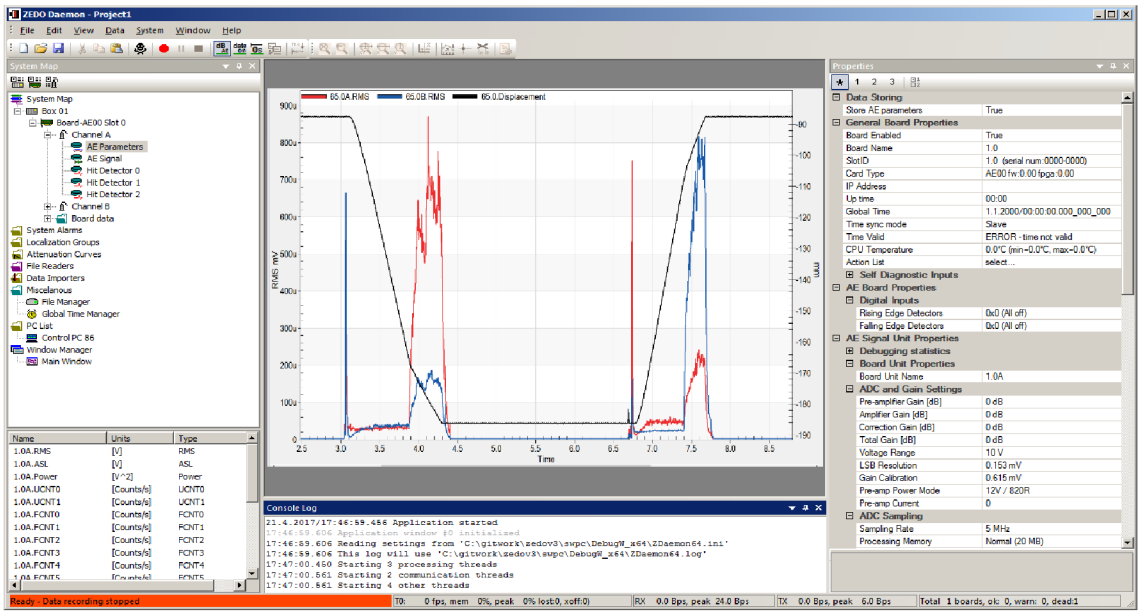

Figure 5.17 ZDAEMON application window.

5. Window area – used to position graph windows and other views, which are important for the system operation.
6. Console Log view – text area containing important system messages and user notes. It displays errors (red), warnings (orange), status messages (black) and other information (grey). User is able to add comments by pressing the F9 key any time during operation. The user messages are displayed in green colour.
7. Status line – shows key information about immediate communication throughput, data recording state and provides hints to menu and toolbar items based on the mouse position.

5.7.2. MATLAB program

It is very important to use MS EXCEL and MATLAB to analyse the data because of the large amount of data recorded from our measuring.
This program is able to open text and excel files that are exported from ZDAEMON and calculate the RMS, Energy and differences. In addition, determine whether the cylinder damaged or undamaged and this criterion is used in ZDAEMON and PNEU-ZEDO.

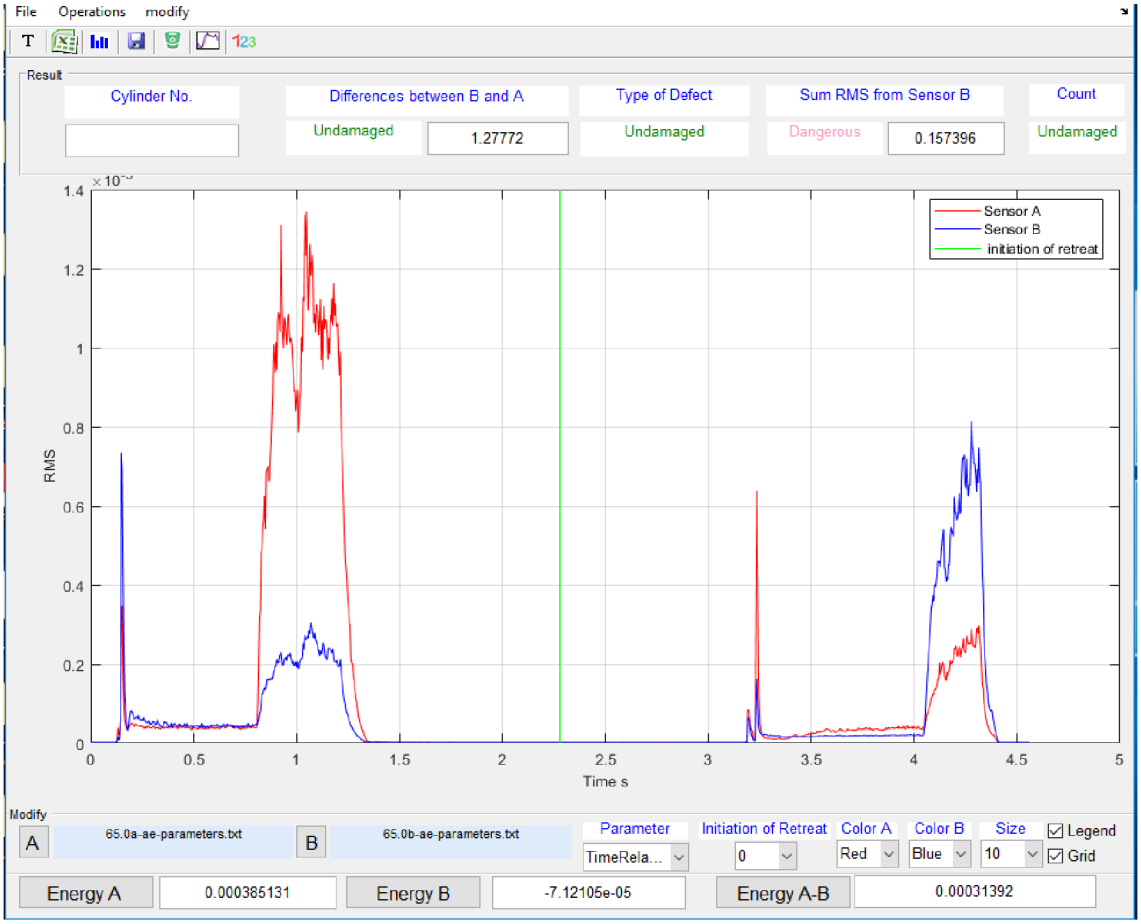

Figure 5.18 Interface for MATLAB program for pneumatic cylinder by acoustic emission.

The code of parameters calculation of this interface figure 5.18 in MATLAB programme is written in the appendix of this work.

6. Results and Discussion

6.1. Frequency spectrum of acoustic emission applied on pneumatic actuator

The main aim of this part is to find a typical acoustic emission signal associated with a particular type of damage in the cylinder. The acoustic emission signals that are obtained from the undamaged cylinders are processed and analysed, after that different types of artificial defects are made in the same cylinders. A new parameter "DAE", which is developed, evaluates and classifies the level of damage detection on the basis of the recorded differences between undamaged and damaged cylinders [57].

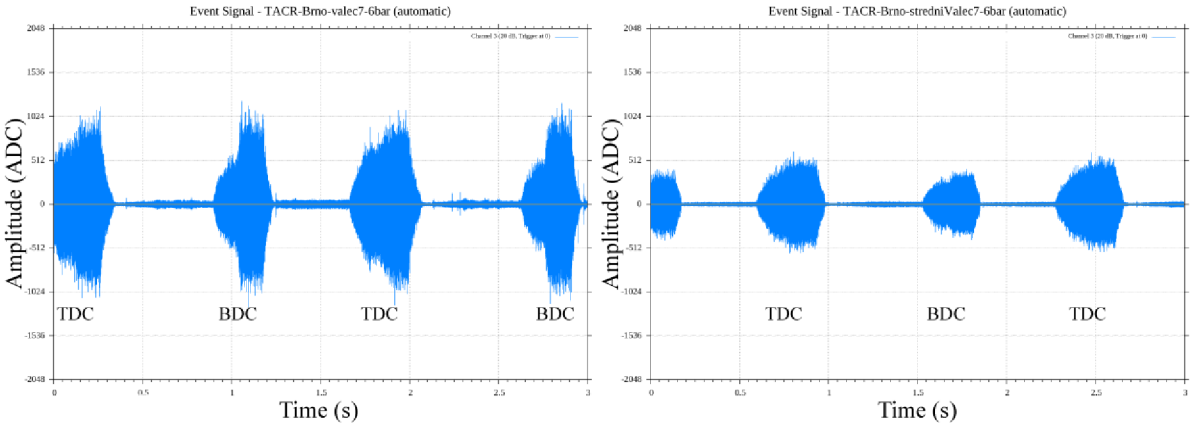

a) Undamaged cylinder. b) Damaged cylinder.

Figure 6.1 Waveforms for the undamaged and damaged cylinder.

Firstly, AE signal are obtained from cylinders without damage. After that, different types of artificial defects are made in the same cylinders. The range of measuring frequencies of the signal is approximately from 50 kHz to 400 kHz depending on AE sensors. The figures 6.1 and 6.2 show the record of one AE sensor placed in middle of the body of the undamaged cylinder. The graph shows that AE sensor detects signal only from damping area. The frequency spectrum changes over time depending on the type of damage and the number of completed cycles. The figure 6.2 shows the signal envelope of initial run of cylinder No. 14; figure 6.3 shows the artificial mechanical damaged cylinder "Loosening 4 screws under the piston". All figures were compared; the shapes of signals envelope are different.

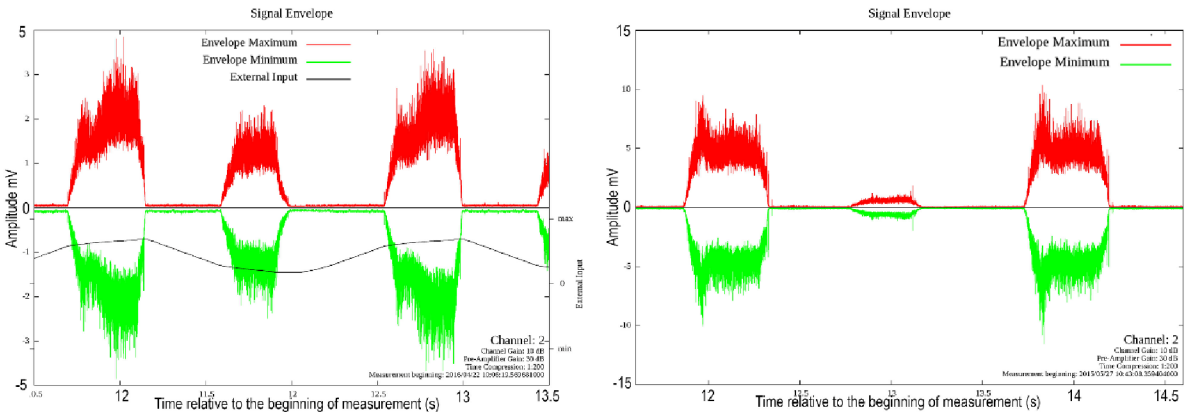

a) Undamaged cylinder. b) Damaged cylinder.

Figure 6.2 Signal envelope of undamaged and damaged cylinder No. 14.

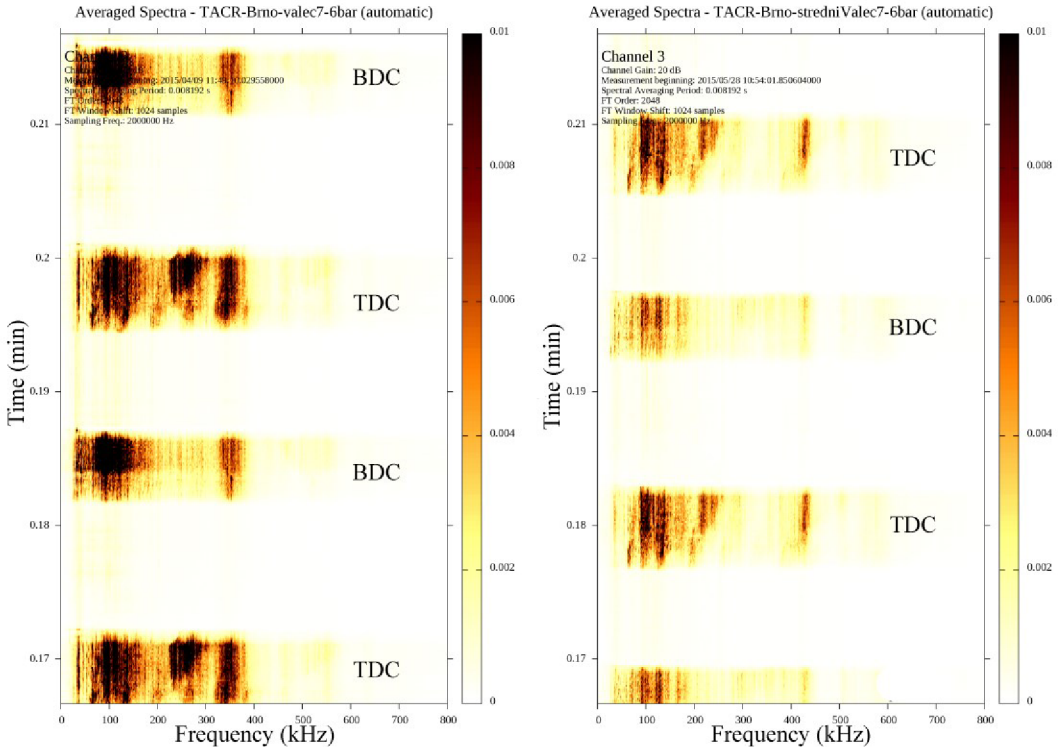

a) Undamaged cylinder. b) Damaged cylinder.

Figure 6.3 Differences between damaged and undamaged cylinder by frequency spectrum.

The figures 6.4 and 6.5 show the frequency spectrum of undamaged and damaged cylinder No. 12 and 4. The amplitude spectrum and bandwidth of both cylinders in (b) is bigger than (a) during determined time.

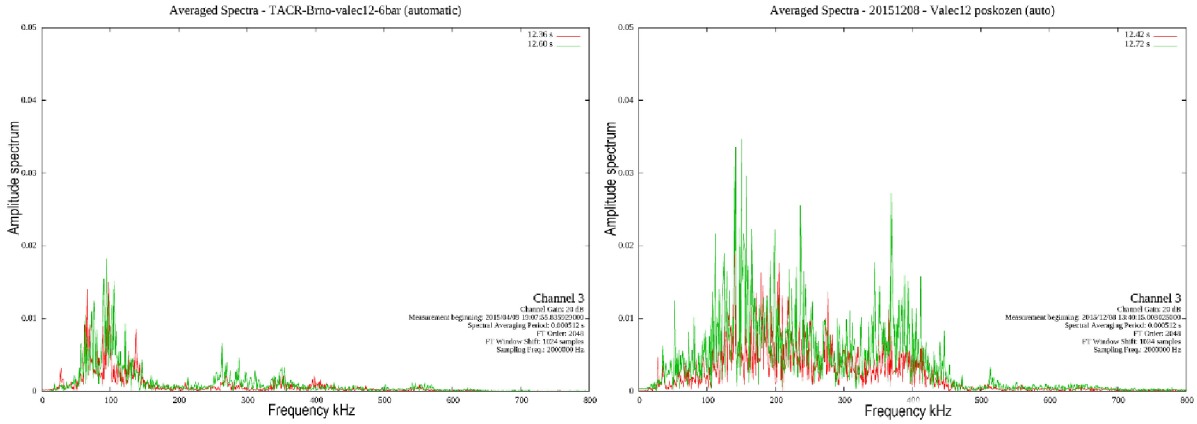

a) Undamaged cylinder. b) Damaged cylinder.

Figure 6.4 Frequency spectrum of undamaged and damaged cylinder No. 12.

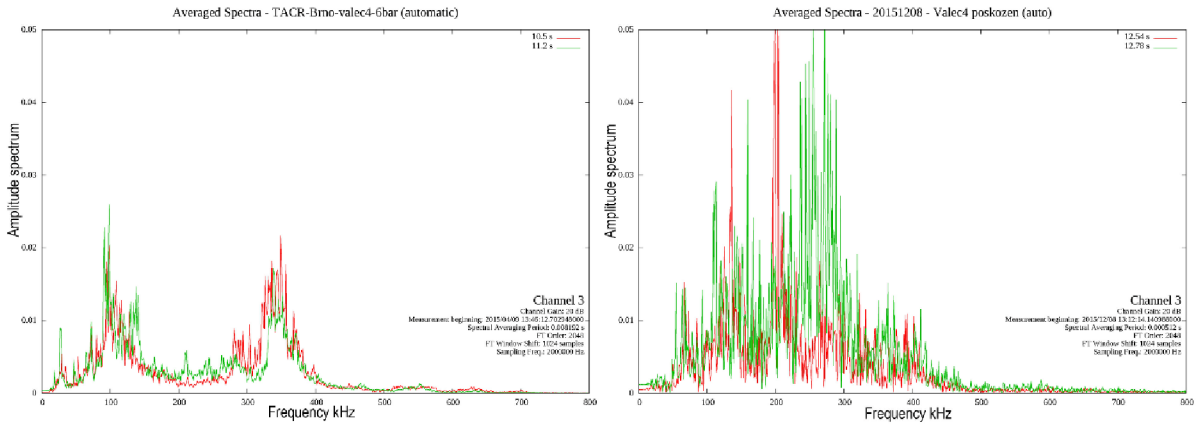

a) Undamaged cylinder. b) Damaged cylinder.

Figure 6.5 Frequency spectrum of undamaged and damaged cylinder No. 4.

There are always three basic characteristics specified bandwidth - BW1 (A1max to 100 kHz), BW2 (A2max to 280 kHz) and BW3 (A3max to 360 kHz) and sizes amplitude spectrum. Bandwidth for all test undamaged cylinders ranged from 50 to 120 kHz (BW1), 270 to 310 kHz (BW2) and 340 to 370 kHz (BW3). The figure 6.6 shows that changes in the parameters BW, A and the coefficient of detection "DAE" to the cylinders.

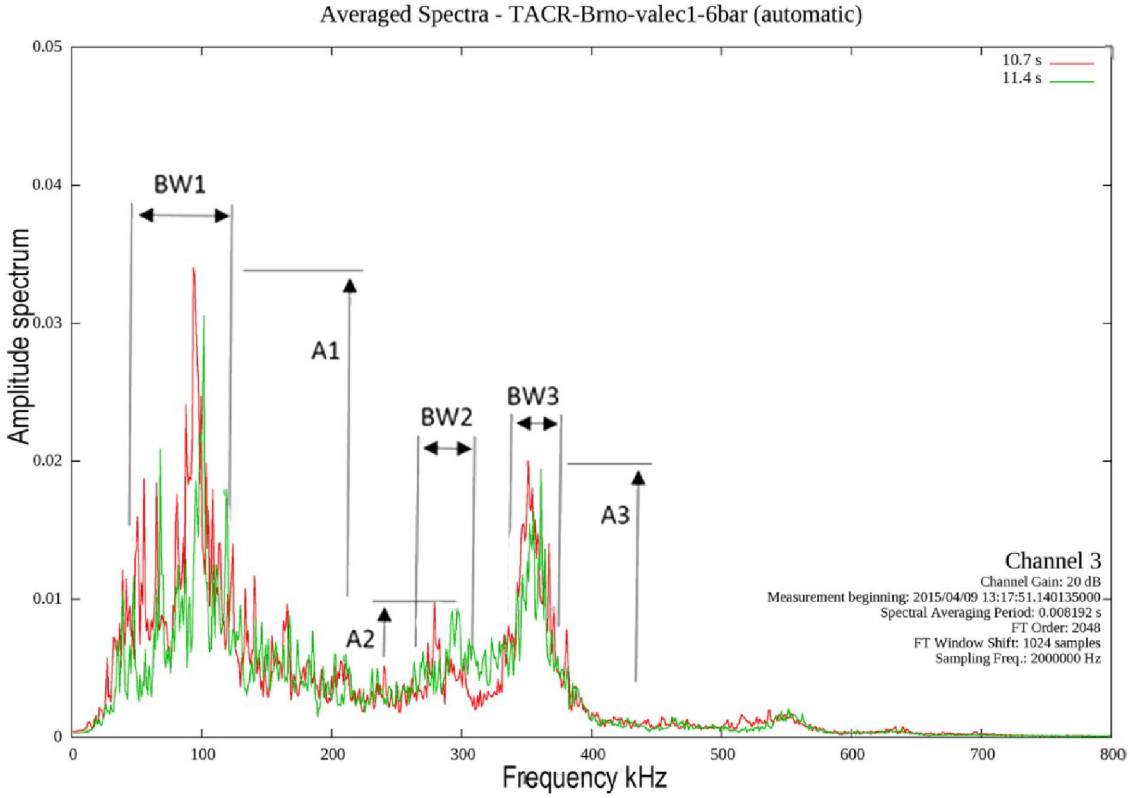

Figure 6.6 Sample determination bandwidth max. Amplitude at cylinders undamaged PS.

$$Avg = \frac{BW_1 + BW_2 + BW_3}{3} + 1000 * \frac{A_1 + A_2 + A_3}{3} \quad 6.1$$

$$D_{AE} = \frac{100 - 2 * Avg}{10} \quad 6.2$$

Where $maxAvg = 50$, $minAvg = 0$, BW is bandwidth, A is amplitude.

The basic criterion of the analysed signal is bandwidth "BW", the amplitude spectrum "A" and the frequency spectrum. We have developed a new parameter "DAE", which evaluates and classifies the level of detection (damage) based on the identified differences between undamaged and damaged cylinder. The existence of the detection coefficient (D)facilitates the evaluation of defects, taking values that range from 1 to 10, with 10 being highly difficult to detect. The detection coefficient was taken from the method FMEA, was developed, and classified using AE. These tests achieved impressive results, which demonstrated that the detection coefficient from AE produces small values compared with other non-destructive testing methods. The Coefficient "S" expresses the severity of a particular defect. This parameter is given in two forms: "S1" for a single defect with no consequences and "S2" reflecting the worst possible consequences, which may indicate a defect.
Table 6.1 provides some types of artificial defects of cylinders and assessment of changes in the monitored parameters of cylinders and constitutes a significant factor D_{AE}. The changes (percentage) were registered in cylinders No. 4, 12 and 14, of which were most pronounced.

Table 6.1 Coefficient of revelation "DAE" for cylinders.

No	Type of defect	the defect	BW (%)	A (%)	Avg (%)	S1	S2	D	DAE
1	NP 02	2x in the undercut groove	11.7	10	21.7	3	5	3	5.7
	PP 05a	Damaged surface of the body				4	6	4	
2	NP 01	Incised seals	5.3	17.3	22.6	3	5	3	5.5
	PP 08	Incised O-ring throttle needle				3	5	3	
3	NP 04a	Damage to the cylinder body	16.3	13	29.3	4	6	4	4.1
	Z 06	Incised cushion seal				3	6	8	
4	PP 03	Missing O-ring on the piston rod	28	12.3	40.3	3	10	9	1.9
	PP 04					3	10	9	
5	M 04	Released piston	19.7	3	22.7	2	10	9	5.5
6	NP 06	Two notches on seal	14.3	8.3	22.6	3	5	8	5.5
7	PP 01	Two notches on seal	25.3	8.8	34.1	3	5	8	3.2
8	NP 05	Two notches on seal	16.7	8.7	25.4	3	5	8	4.9
9	PP 02	Two notches on seal	13.3	6.7	20	3	5	8	6
10	NP 09	Missing O-ring	11	12.7	23.7	3	5	3	5.3
	PP 07	Cutting the O-ring				3	5	3	
11	NP 10	Cutting the O-ring on throttling	20.3	15	35.3	3	5	3	2.9
12	NP 07	Cutting the O-ring on the piston rod	27.7	5.2	32.9	3	10	9	3.4
	NP 08					3	10	9	
13	M 03	Loosening 4 screws under the piston	20.3	5	25.3	3	10	7	4.9
14	M 03	Loosening 4 screws under the piston	9.3	6.7	16	3	10	7	6.8
15	M 02	Curved rod	14.7	5	19.7	3	8	6	6.1
16	PP 06	Opening the rear cap	11	5.7	16.7	3	10	7	6.7

Figure 6.7 Rate changes caused by that damage coefficient (D) and Defection (DAE).

The frequency spectrum was replaced later by the parameter RMS during the monitoring of changes in the test results. This is possible by using a prototype of the newly developed diagnostic equipment.

6.2. Leakage analysis of pneumatic cylinders

This chapter discusses the relationship between AE and different types of defects in pneumatic cylinders, shedding light on a new approach to determining these types of defects and distinguishing between them through Acoustic Emission. Difficulties that face the defects detection process are related to the types of the defects, and the available methods for detection. A detection coefficient has been assigned to each cylinder by applying different methods of non-destructive testing, where a set of cylinders, which have defects that are difficult to detect, were determined. Two of those defects in the cylinders are artificially made, and it is difficult to discover the differences between undamaged and damaged cylinders in this set using current methods. Therefore, the necessary parameters for comparison have been selected after analysing the signals that were obtained from the tests. The average energy of Acoustic Emission signal RMS gives a clear picture of the different responses between damaged and undamaged pneumatic cylinders [58].

6.2.1. Kinematic scheme of intact cylinder

The signals which are recorded in each measurement of the intact cylinders have similar parameters as other cylinders. This kinematic scheme of an intact cylinder shows the progress and retreat stroke, and the response of AE_{rms} to this movement.

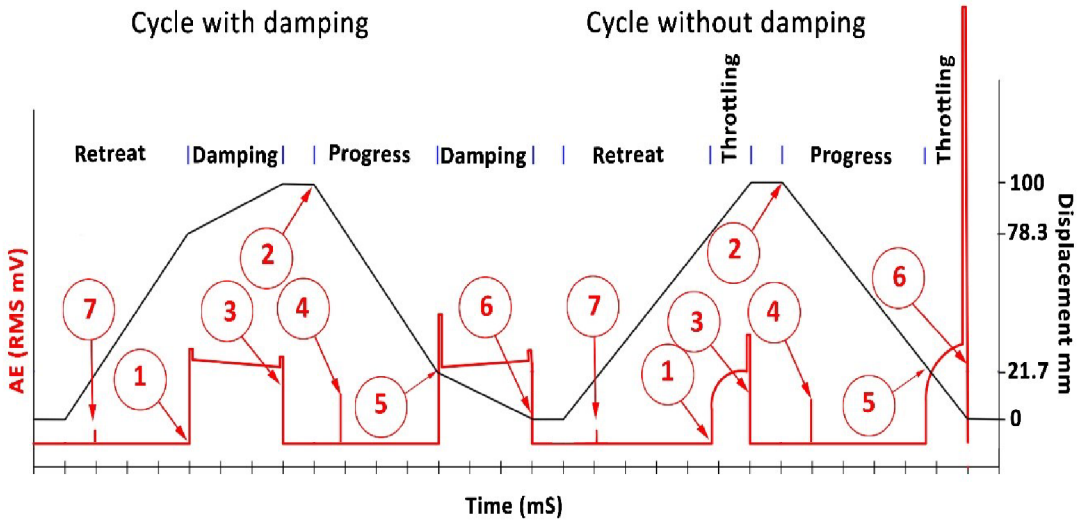

Figure 6.8 Kinematic scheme of intact cylinder.

(1). Initiation of throttling (damping) in retreat stroke, (2). Stop time and return to progress stroke, (3). End of retreat stroke, (4). End of throttling in progress stroke, (5). Initiation of throttling (damping) in progress stroke, (6). End of progress stroke, (7). End of throttling in retreat stroke.

On the progress stroke, significant signal fluctuations are not exhibited throughout the movement of the piston from the initiation of the progress stroke until the piston cushion portion contacts the cushion seal. From that moment, there is an increase in the amplitude of the signal until it stops (piston impacts the head cap cushion), ending with significant hit. A similar situation occurs during the retreat stoke, where the signal behaves similarly when the piston impacts the rear cap cushion. The sensors located on different sides of the pneumatic cylinder. The contact between the piston cushion portion and cushion seal emits a distinctive hit in the signal by the left sensor placed on the head cap (A, Red). The right sensor (B, blue) behaves similarly and it is placed on the rear cap.

6.2.2. Undamaged Cylinders

Undamaged Cylinder No.2 after 101500 cycles without damping

Piston progress: the signal behaves smoothly from the initiation of throttling until the end of the progress stroke, where the piston then impacts the head cap cushion with a large amplitude of a hit in the signal. Piston retreat: the signal behaves smoothly from the initiation of throttling until the end of retreat stroke, where the piston then impacts the rear cap cushion with a small amplitude of a hit in the signal. As shown in figure 6.9.

Undamaged Cylinder No.2 after 101500 cycles with damping

Piston progress: the signal behaves from the initiation of damping with a large hit then it remains at a constant level until the end of the progress stroke, where piston then impacts the head cap cushion with a small amplitude of a hit in the signal. Piston retreat: the signal behaves from the initiation of damping with a constant level until the end of the retreat stroke, where the piston then impacts rear cap cushion with a small amplitude of a hit in the signal. As shown in figure 6.10.

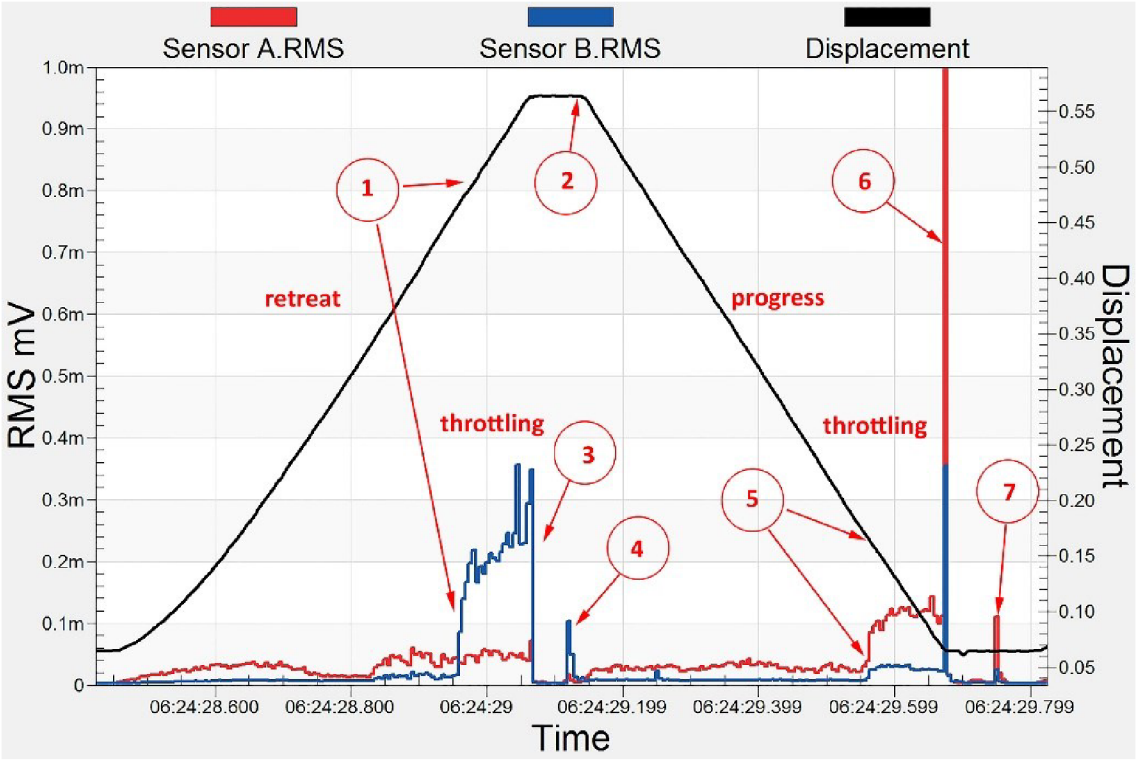

Figure 6.9 Undamaged cylinder No.2 after 101500 cycles without damping.

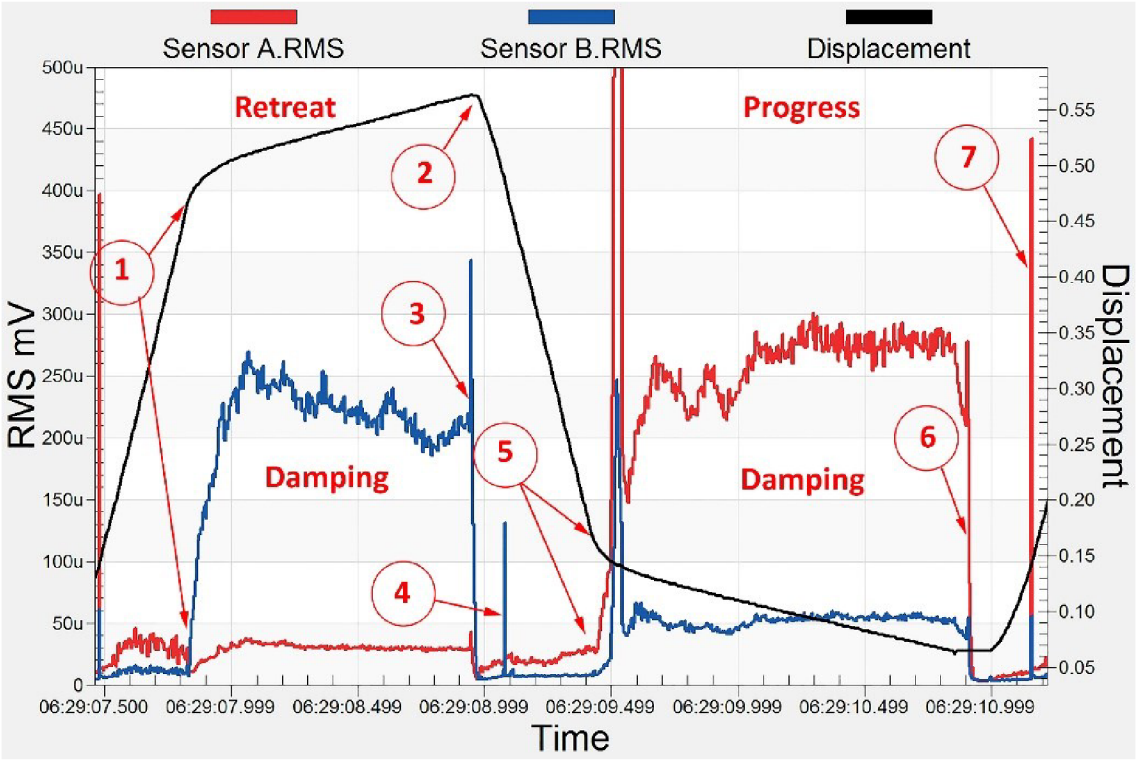

Figure 6.10 Undamaged cylinder No.2 after 101500 cycles with damping.

6.2.3. Damaged Cylinders

Damage type "unsealed piston and O-ring seal" was created in cylinder no. 8. The comparison between damaged cylinders without damping shows a significantly higher signal level in the area of the throttling process, including a higher hit at the start of the retreat stroke. In this case, it recorded leaks.

Damaged Cylinder No.8 after 51100 cycles without damping

Piston progress: the signal behaves differently from the initiation of throttling which increases and vibrates until the end of the progress stroke, and it ends when the piston impacts the head cap cushion. The black dotted circles determine the relation between the changes in the signal and possible leakage (PP03). Piston retreat: the signal behaves differently from the initiation of throttling which increases to maximum value then decreases, vibrates and ends when the piston impacts the rear cap cushion. The black dotted circles determine the relation between the changes in the signal and possible leakage (NP08). As shown in figure 6.11.

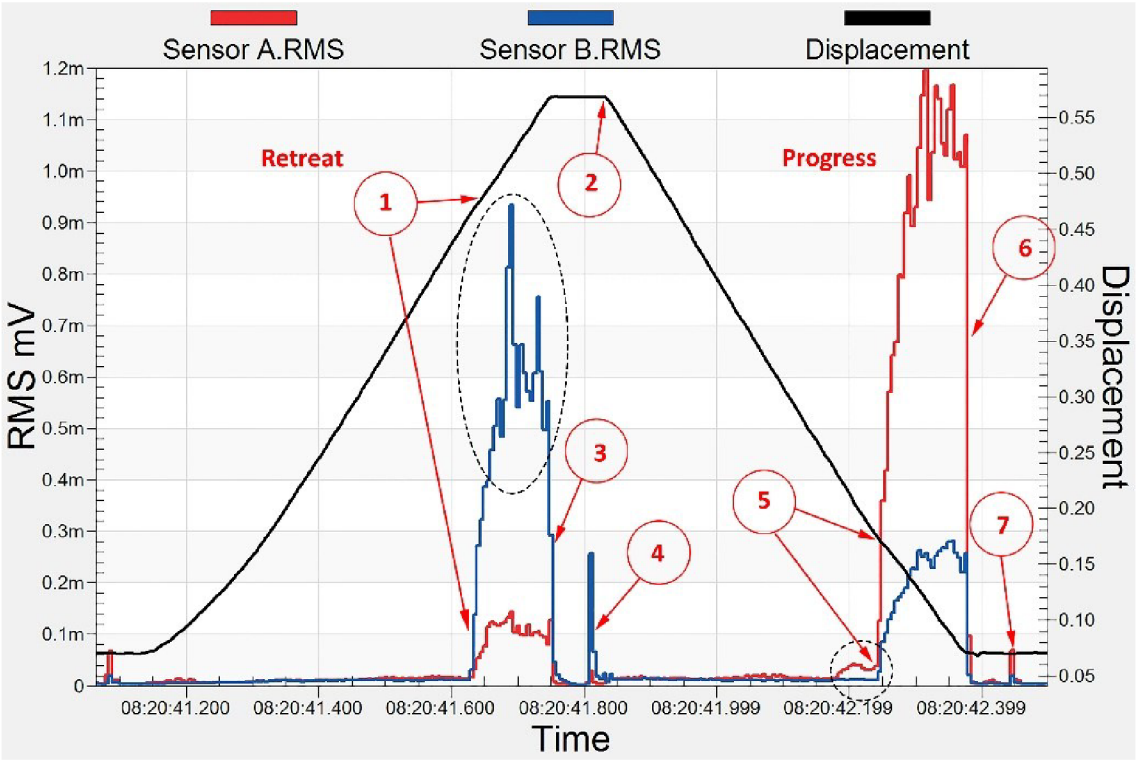

Figure 6.11 Damaged cylinder No.8 after 51100 cycles without damping.

Damaged Cylinder No.8 after 51100 cycles with damping

Piston progress: the signal behaves differently from the initiation of damping which increases and remains constant at the same level until the end of the progress stroke, where the piston then impacts the head cap cushion. The black dotted circles determine the relation between the changes in the signal and possible leakage (PP03). Piston retreat: the signal behaves differently from the initiation of damping which increases to the maximum value then decreases and produce a hit when the piston impacts the rear cap cushion. The black dotted circles determine the relation between the changes in the signal and possible leakage (NP08). See figure 6.12.

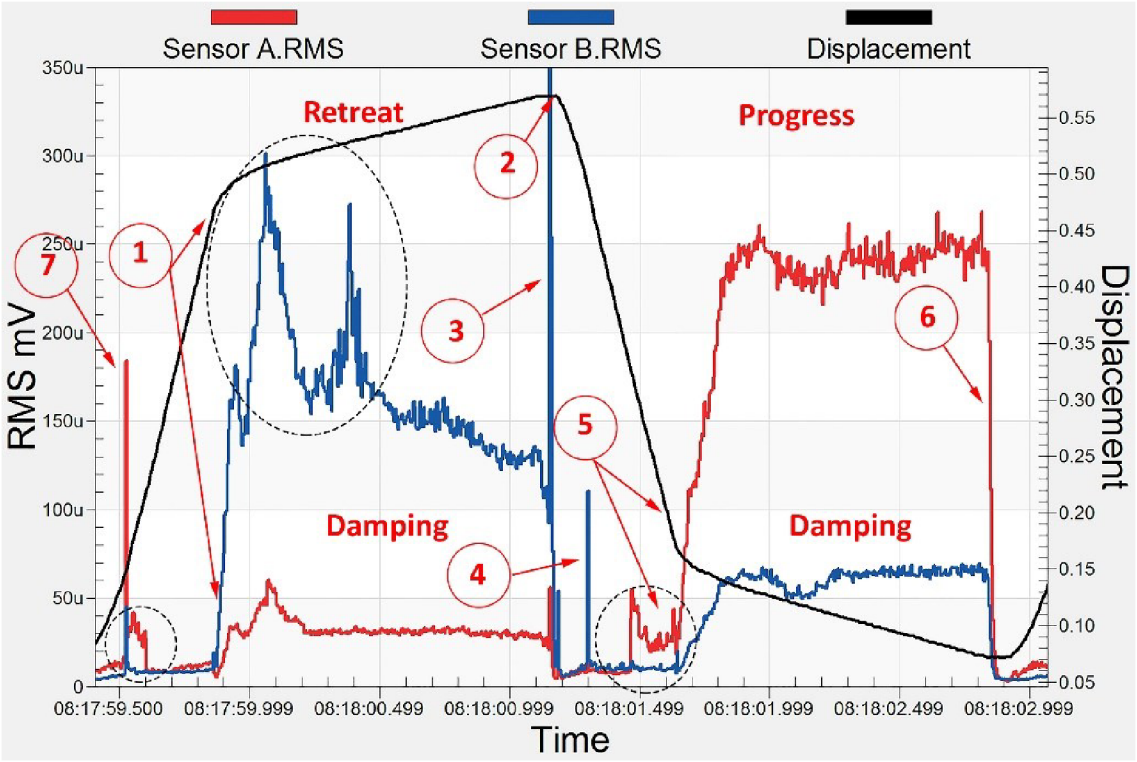

Figure 6.12 Damaged cylinder No.8 after 51100 cycles with damping.

6.3. Mechanical damage detection for pneumatic actuators

The main aim of this research is to find defects in the pneumatic cylinders using acoustic emission method and find a typical acoustic emission signal associated with a particular type of damage in the cylinder. The second aim is to investigate the relation between acoustic emission signal and a coefficient detection, which evaluates the level of damage detection on the basis of the recorded differences between undamaged and damaged cylinders.

Current results show good conformity and repeatability and prove significant sensibility of acoustic emission signal in this application domain of diagnostics, which brings higher quality results than currently used methods. It is evident that the diagnostic of pneumatic cylinder can be a new application domain for acoustic emission method [59].

The conclusions of these measurements are summarized in the value of detection coefficient which determines the ability of the discover defects by acoustic emission. The most serious defects of cylinders are those that have a large degree of severity, which takes into account the worst possible consequences. Undamaged cylinders were tested and compared with damaged. One type of mechanical defect was presented in this study called M04. Moreover, the main parameter is RMS where the left sensor placed on the head cap (A, Red) and the right sensor (B, blue).

6.3.1. Undamaged Cylinders

Undamaged Cylinder No.14 after 101500 cycles without damping

Piston progress: signal behaves smoothly from initiation of throttling until the end of progress stroke then the piston impacts the head cap cushion with a big amplitude of hit in the signal.

Piston retreat: signal behaves smoothly from initiation of throttling until the end of retreat stroke then the piston impacts the rear cap cushion with a small amplitude of hit in the signal Shown in figure 6.13.

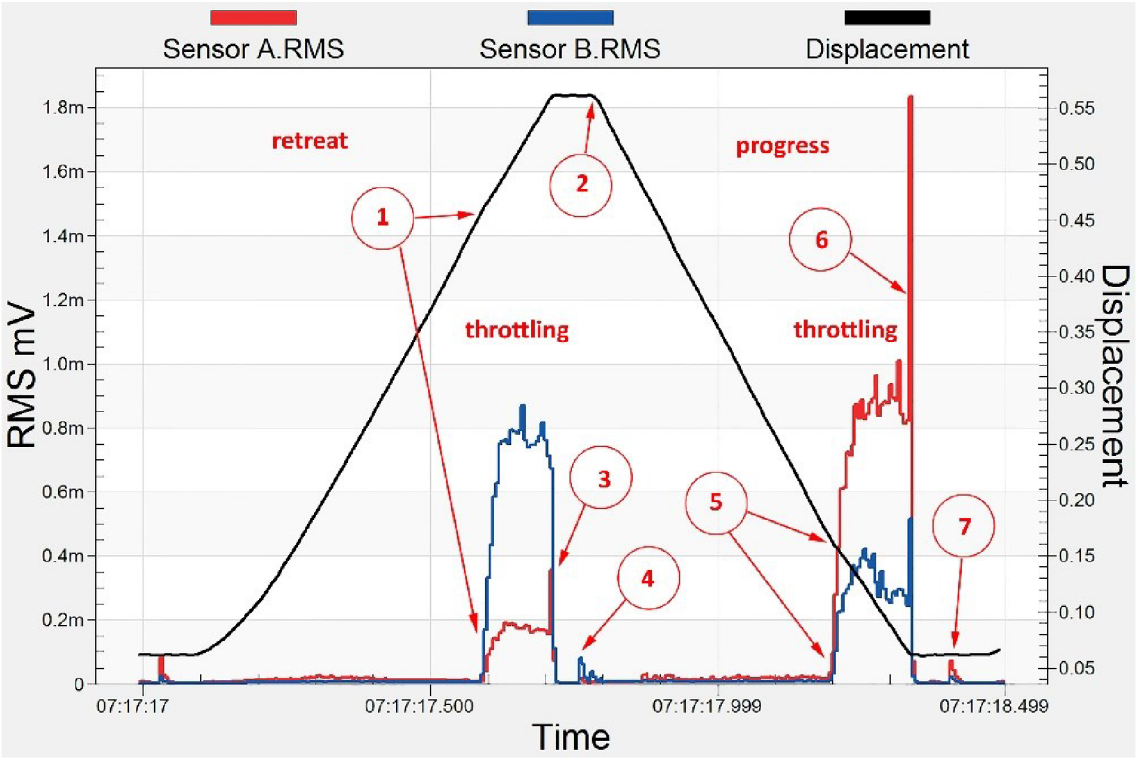

Figure 6.13 Undamaged cylinder No.14 after 101500 cycles without damping.

(1). Initiation of throttling in retreat stroke, (2). Stop time and return to progress stroke, (3). End of retreat stroke, (4). End of throttling in progress stroke, (5). Initiation of throttling in progress stroke, (6). End of progress stroke, (7). End of throttling in r. s.

Undamaged Cylinder No.14 after 101500 cycles with damping

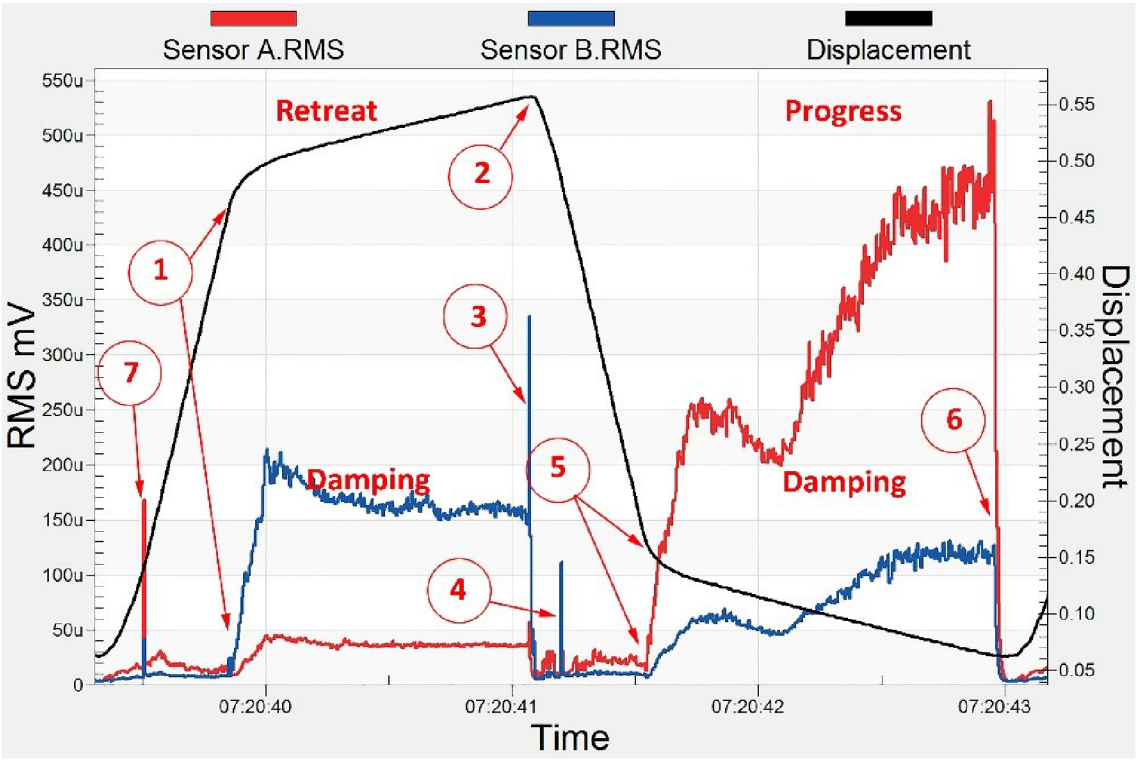

Figure 6.14 Undamaged cylinder No.14 after 101500 cycles with damping.

Piston progress: signal behaves from initiation of damping with constant level and it increases until the end of progress stroke, then piston impacts head cap cushion with a high amplitude of hit in the signal. Shown in figure 6.14.
Piston retreat: signal behaves from the initiation of damping with constant level until the end of retreat stroke then piston impacts rear cap cushion with a high amplitude of hit in the signal. Number of cycles of undamaged cylinder is 101500 cycles that take place without damping. In the progress stroke, it does not exhibit significant signal fluctuations throughout the movement of piston from the initiation of progress stroke until the piston cushion portion contacts the cushion seal. From that, moment there is an increase in the amplitude of the signal until it stops (piston impacts head cap cushion) ended with significant hit. A similar situation occurs during the retreat stoke, the signal behaves similarly when the piston impacts rear cap cushion.

6.3.2. Damaged Cylinders

Damaged Cylinder No.3 after 51100 cycles without damping

Piston progress: signal behaves differently from initiation of throttling which increases and vibrates until the end of the progress stroke and it ends when the piston impacts the head cap cushion. Piston retreat: signal behaves differently from initiation of throttling which increases to maximum value then it decreases, vibrates and ends when the piston impacts the rear cap cushion Shown in figure 6.15.

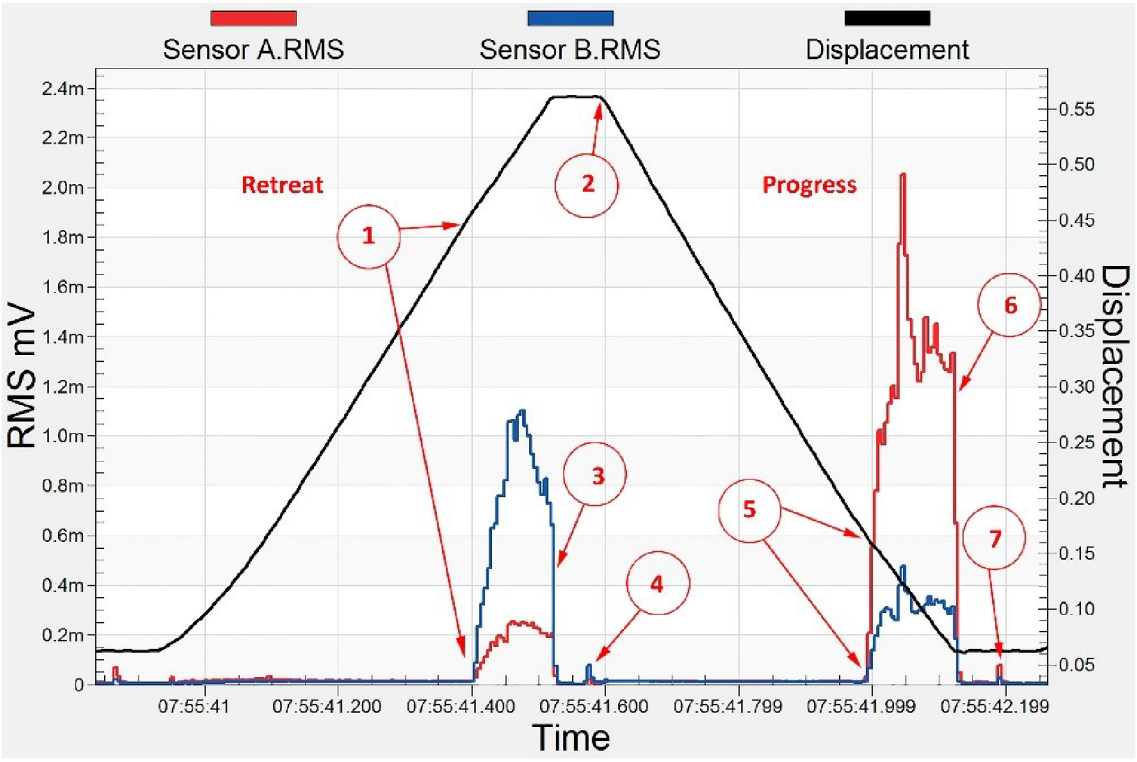

Figure 6.15 Damaged cylinder No.3 after 51100 cycles without damping.

Damaged Cylinder No.3 after 51100 cycles with damping

Piston progress: signal behaves differently from initiation of damping which increases and decreases stays constant at the same level until the end of the progress stroke, then the piston impacts the head cap cushion. Piston retreat: signal behaves differently from initiation of damping which increases to the maximum value then it decreases then it increases and stays constant until the piston impacts the rear cap cushion. The comparison between damaged cylinders without damping shows a significant higher signal level in the area of throttling process, including higher hit at the start of the retreat stroke. In this case, it recorded leaks Shown in figure 6.16.

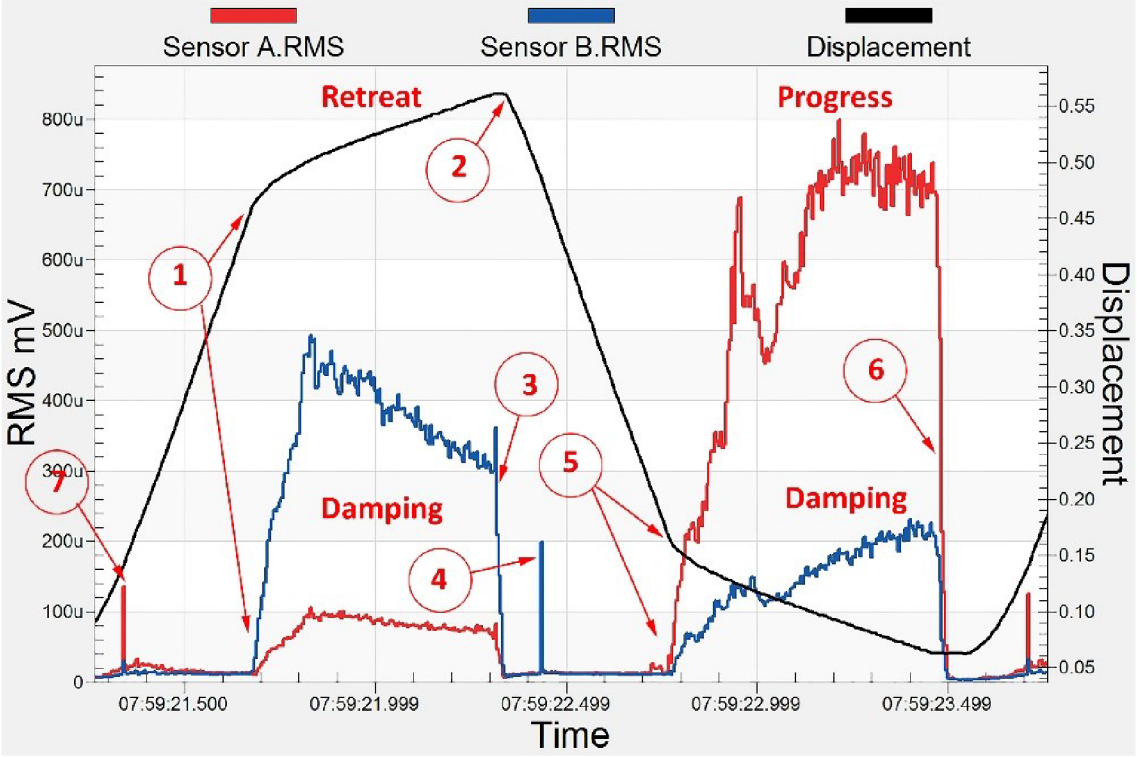

Figure 6.16 Damaged cylinder No.3 after 51100 cycles with damping.

6.4. The criteria of acoustic emission testing for leakage

6.4

Undamaged and damaged cylinders were compared to find distinctive differences that determine whether the cylinder is damaged or undamaged. In this study, several undamaged cylinders were tested by acoustic emission, before artificial defects were created in each one. The signals from the progress and retreat strokes were recorded and analysed into many parameters. The RMS was normalized, and the different responses between damaged and undamaged pneumatic cylinders were recognized by the time delay of the strokes. The differences were identified by comparing the max RMS from sensor A and the max RMS from sensor B for one cycle in the retreat stroke. The damaged and undamaged cylinders were distinguished using the difference in energy values present in the signals of the two sensors in the retreat stroke. And the final evaluation of the cylinder was determined by the calculation of the total value of RMS.

The signals were obtained by two sensors, one of them on the right (A) and the other on the left (B). The data was normalized and divided into A and B depending on the sensor. Because of the sensitivity of the sensor and the different responses of sensors and the contact condition between the sensors and the cylinders, the data was normalized to avoid the amplitude errors, in spite of implementing a pen test before each measurement to ensure that the sensors have the same amplitude. However, undamaged and damaged cylinders were compared according to the normalized data to find distinctive differences between them.

All cylinders had the same throttling adjustment before and after creating the artificial defect. When an artificial defect was made in the cylinder, the time of the stroke was extended. The stroke time should be equal but the defect in the cylinder causes this delay as shown in figures 6.17, 6.18.

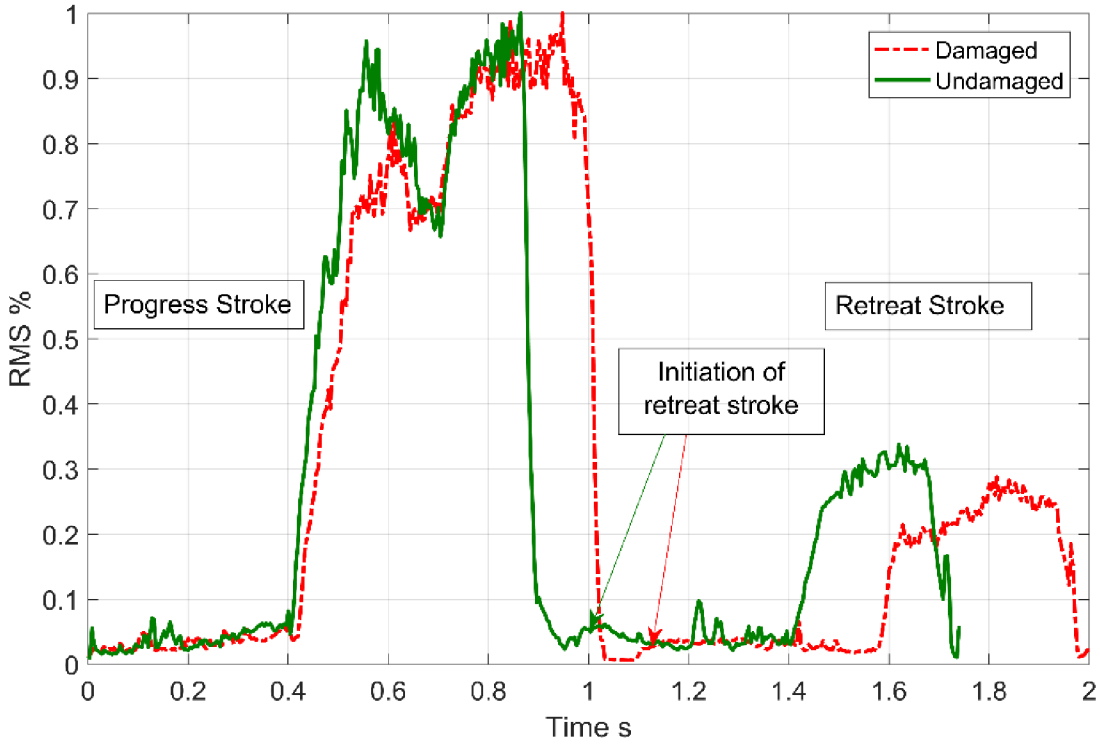

Figure 6.17 Comparing between damaged and undamaged cylinders No. 21, NP08, PP03 derived from the sensor A.

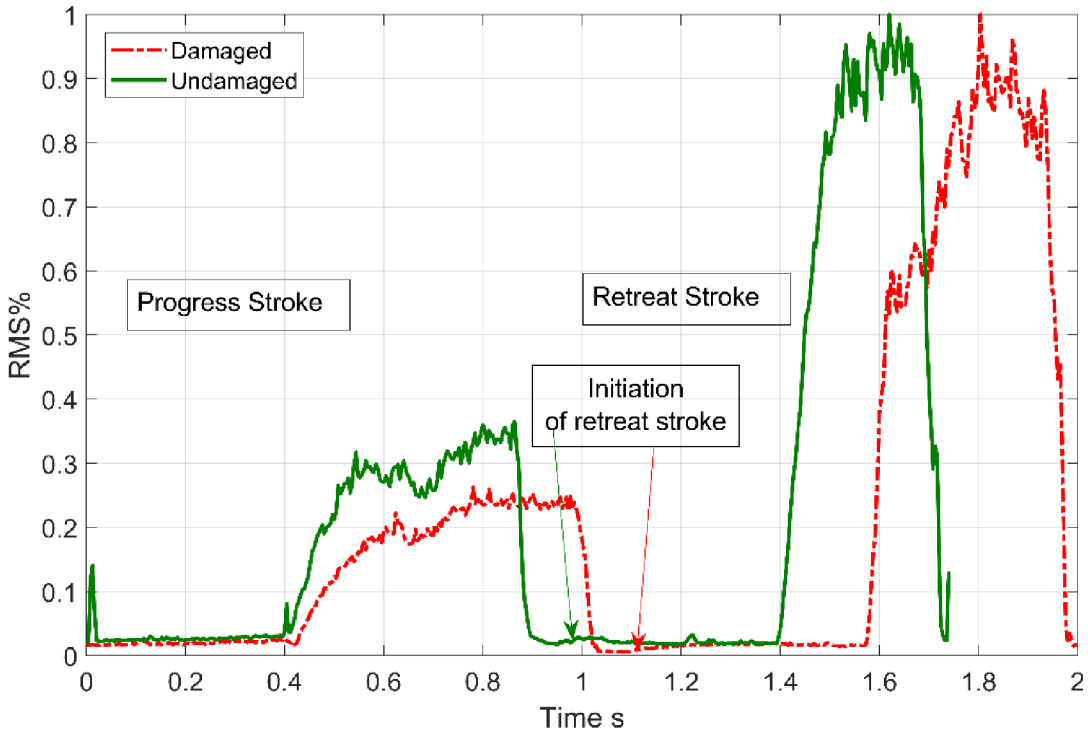

Figure 6.18 Comparing between damaged and undamaged cylinders No. 21, NP08, PP03 derived from the sensor B.

The difference was recognized between an undamaged and damaged cylinder. After these distinctive differences were proved using acoustic emission, the goal of this research is to determine whether newly produced cylinders are acceptable or not.

The ratio between maximum RMS of Acoustic Emission from sensor B and the maximum RMS from sensor A in the retreat stroke, as shown in the figures 6.21, and 6.22, determines whether the cylinder is damaged or undamaged as shown in the table 6.2 and figure 6.19.

Table 6.2 Ratio of RMS A/B undamaged, damaged NP and PP series.

No.	Ratio RMS A/B of damaged dylinder	Ratio RMS A/B of undamaged cylinder
21	1.93	1.48
22	5.89	3.44
23	1.85	1.25
24	1.98	1.39
25	4.61	2.24
26	2.46	1.37
27	2.32	1.22
28	6.18	1.50
29	5.28	2.03
30	1.52	1.29
31	2.93	2.42
32	5.94	2.07
33	6.51	1.05
34	2.50	1.35

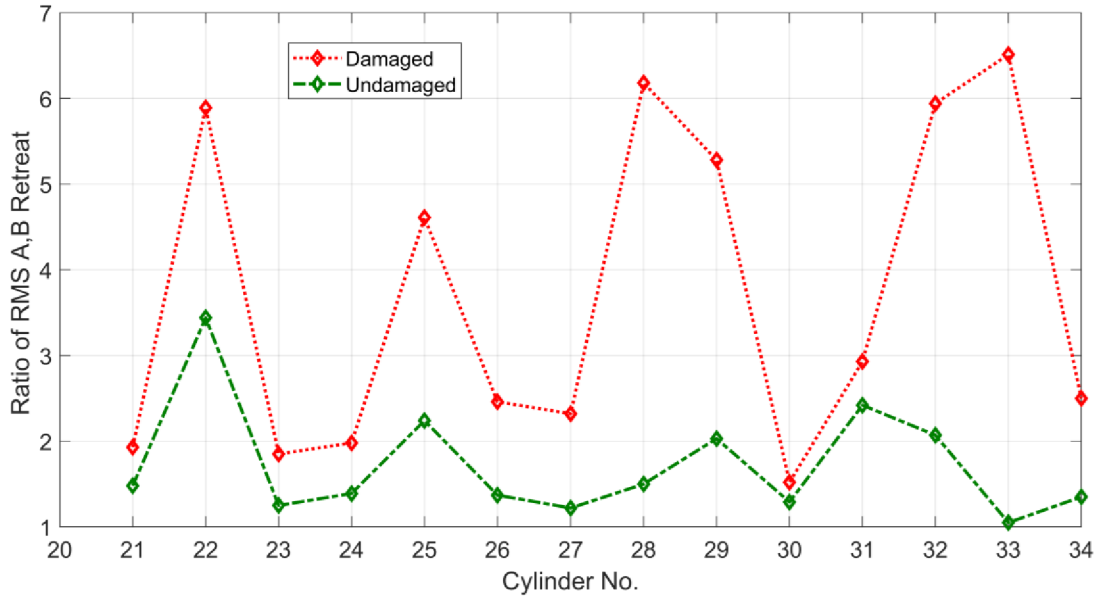

Figure 6.19 Comparing between damaged and undamaged cylinders according to the ratio of RMS values.

In the figure 6.19, there is an area, highlighted in the blue rectangle, where one criterion is not enough to determine the status of the cylinder. This rectangle represents a range of values that do not give a direct indication to whether the cylinder is damaged or undamaged. In this case, a new criterion should be considered.

The first criterion is the difference between curve B and curve A of the signal's energy in the retreat stroke for one cycle, as shown in the figures 6.21, and 6.22, which is given by the following equation 6.3:

$$E_{B-A} = \sum u_{retreat\ B}[i]^2 * \mathrm{dT} - \sum u_{retreat\ A}[i]^2 * \mathrm{dT} \quad [V^2 * s * ohm] \qquad 6.3$$

Where dT is the value of sampling (in our case 0.004s), the area between curve A and curve B demonstrates the value of energy. The value of energy is in inverse proportion to the quality of the cylinder. As shown in figure 6.20 when $E_{B-A} > 0.00000005$ V^2*s*Ohm the cylinder is damaged, and when $E_{B-A} < 0.00000002$ V^2*s*Ohm it is undamaged.

Table 6.3 Total Energy of undamaged, damaged NP and PP series.

No.	E_{B-A} (V^2*s*ohm) Damaged Cylinder	E_{B-A} (V^2*s*ohm) Undamaged Cylinder
21	0.0000000513	0.0000000075
22	0.0000000976	0.0000000268
23	0.0000000892	0.0000000010
24	0.0000000837	0.0000000084
25	0.0000001708	0.0000000041
26	0.0000001038	0.0000000037
27	0.0000001074	0.0000000010
28	0.0000001044	0.0000000084
29	0.0000000480	0.0000000217
30	0.0000000269	0.0000000067
31	0.0000001701	0.0000000075
32	0.0000002325	0.0000000055
33	0.0000001537	0.0000000050
34	0.0000000265	0.0000000083

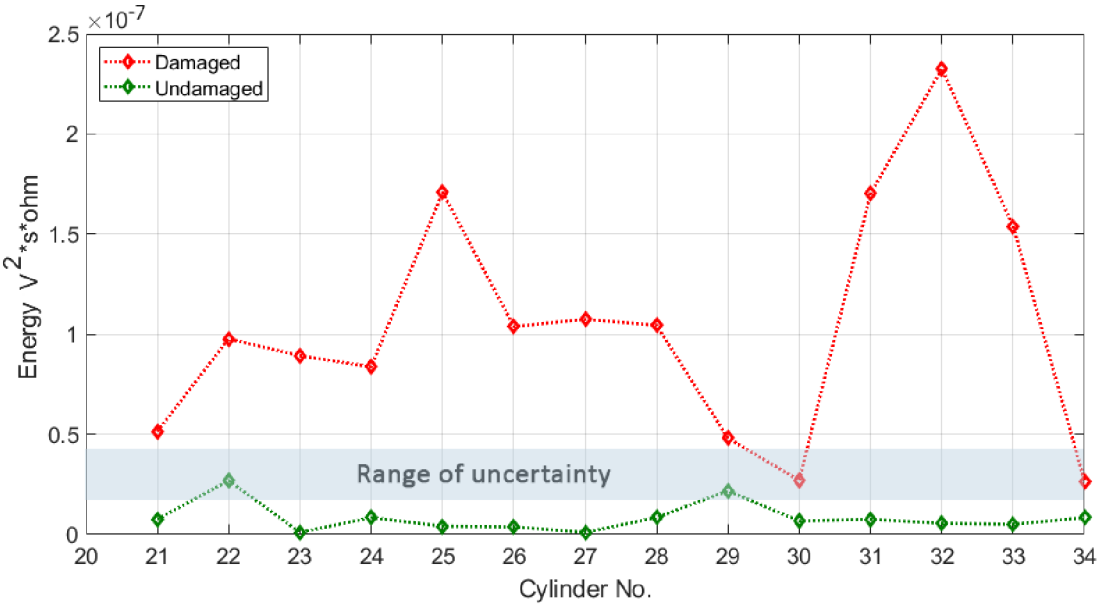

Figure 6.20 Comparing between damaged and undamaged cylinders according to the energy values.

Undamaged cylinders No. 22, 29 and damaged cylinders No. 30, 34, are in the blue rectangle in figure 6.20.

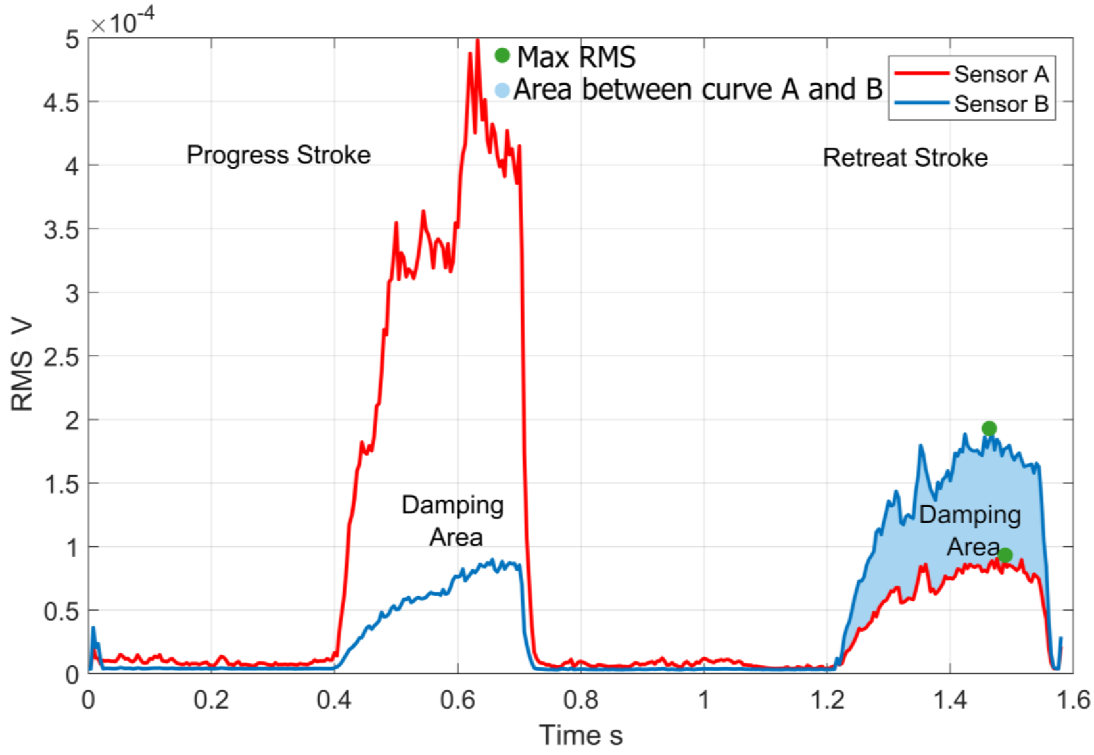

Figure 6.21 RMS dependency on time for undamaged cylinder No.32 with damping.

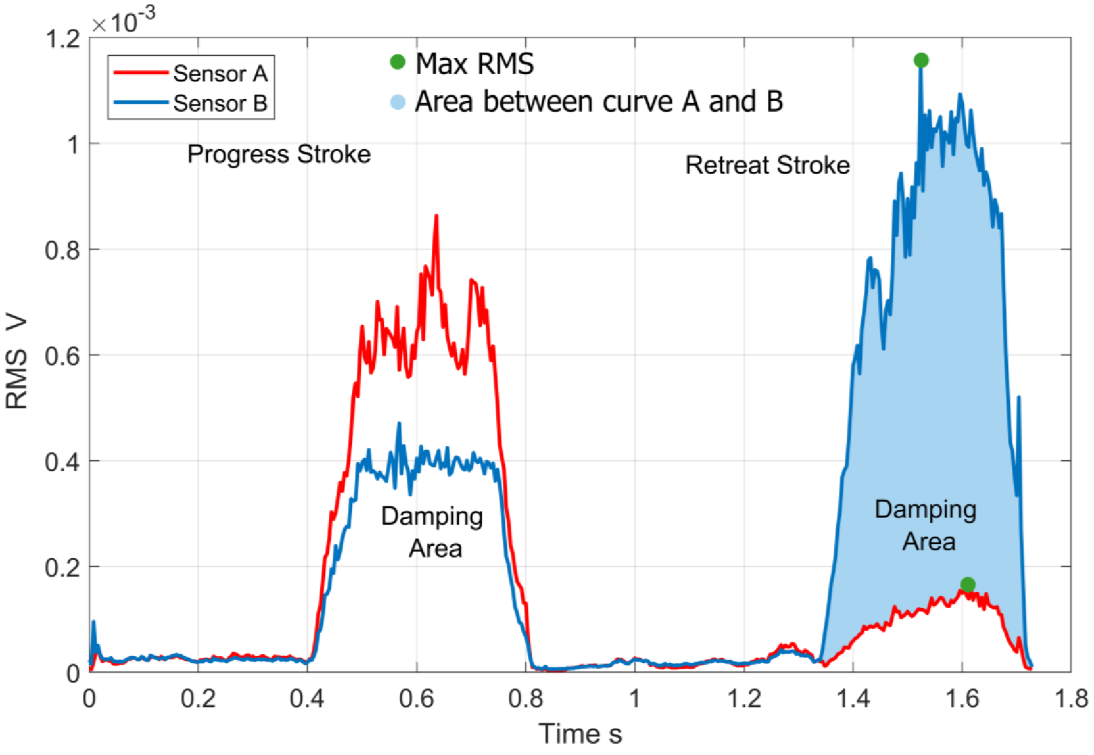

Figure 6.22 RMS dependency on time for damaged cylinder No.32 with damping.

The second criterion is applied as follows: The total value of RMS was calculated for each cylinder from the sensor B at one cycle according to the time. The results were demonstrated in table 6.4. As shown in figure 6.23 when $\sum RMS > 0.18$ mV the cylinder is damaged, and when $\sum RMS < 0.14$ mV it is undamaged.

$$\text{RMS} = \sqrt{\sum(U[i]^2)/N} \qquad 6.4$$

Table 6.4 the total sum of RMS for undamaged, damaged NP and PP series.

No.	RMS mV Damaged Cylinder	RMS mV Undamaged Cylinder
21	0.20399026	0.06381114
22	0.26766794	0.13312215
23	0.26758626	0.04344217
24	0.27923112	0.07665541
25	0.33832573	0.09231223
26	0.28376115	0.06386531
27	0.28637894	0.06279574
28	0.20399026	0.10889962
29	0.18967130	0.11321014
30	0.26022269	0.17795030
31	0.32940824	0.03470239
32	0.33832573	0.13976290
33	0.34906962	0.13976186
34	0.14118696	0.11026634

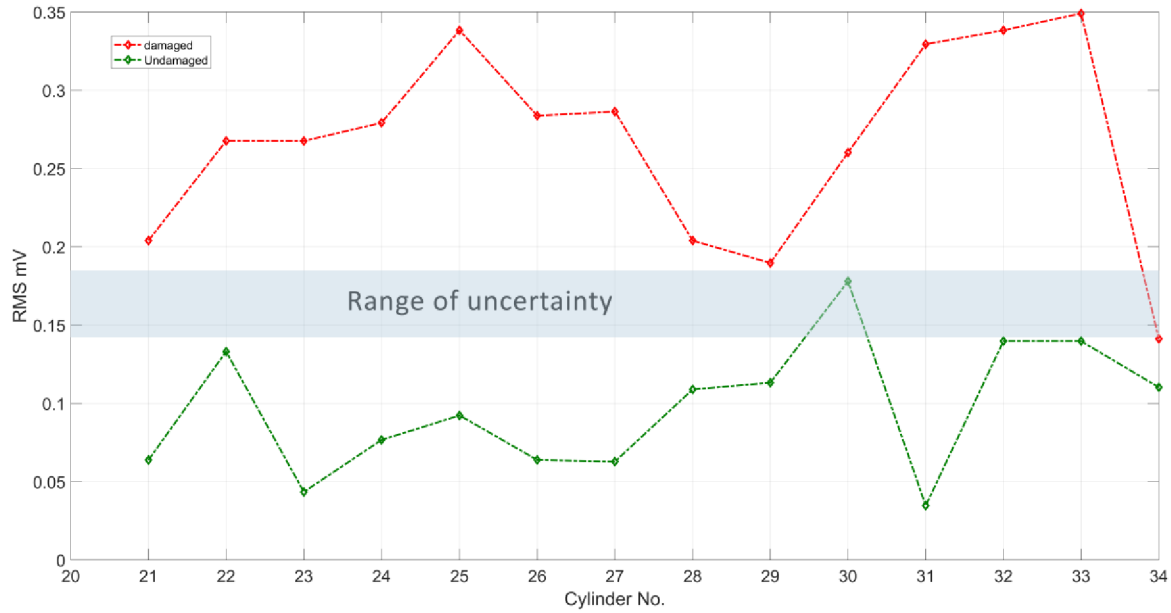

Figure 6.23 Comparing between damaged and undamaged cylinders NP08, PP03, NP07 according to the RMS values

The value of $\sum RMS$ from sensor B at one cycle can evaluate the quality of the cylinder, as observed; the smaller the value the better the quality.

6.5. Relationship between acoustic emission signal and loads on pneumatic cylinders

The cylinders in our experiment were loaded gradually by different weights in a vertical direction. The effect of the defect occurs when the cylinder is loaded at the retreat and progress strokes. This defect affects the relationship between the applied load and the recorded signal of the sensors. The signals of the acoustic emission were recorded from the progress and retreat strokes and then analysed. The time delay is calculated between the digital input and the initiation of movement, and the time of the stroke. The energy and root mean square of the acoustic emission compare between the distinctive different responses in damaged and undamaged pneumatic cylinders, with and without loading. The energy and AE_{rms} were calculated for each cylinder with gradual loading. The results of the test showed a linear relationship between the AE_{rms} curve and loading.

Loads were applied to the cylinders during the test. The aim was to enlarge the amount of leakage. Two sensors were fixed on the head and rear cap of the cylinder. The cylinder was fixed under the table while the load was applied above the cylinder; the signal was recorded from the progress and retreat strokes. In another assembly, the cylinder was fixed above the table while the loads were applied below the rod of the piston. The signals were recorded from the progress and retreat strokes as shown in figure 6.24.

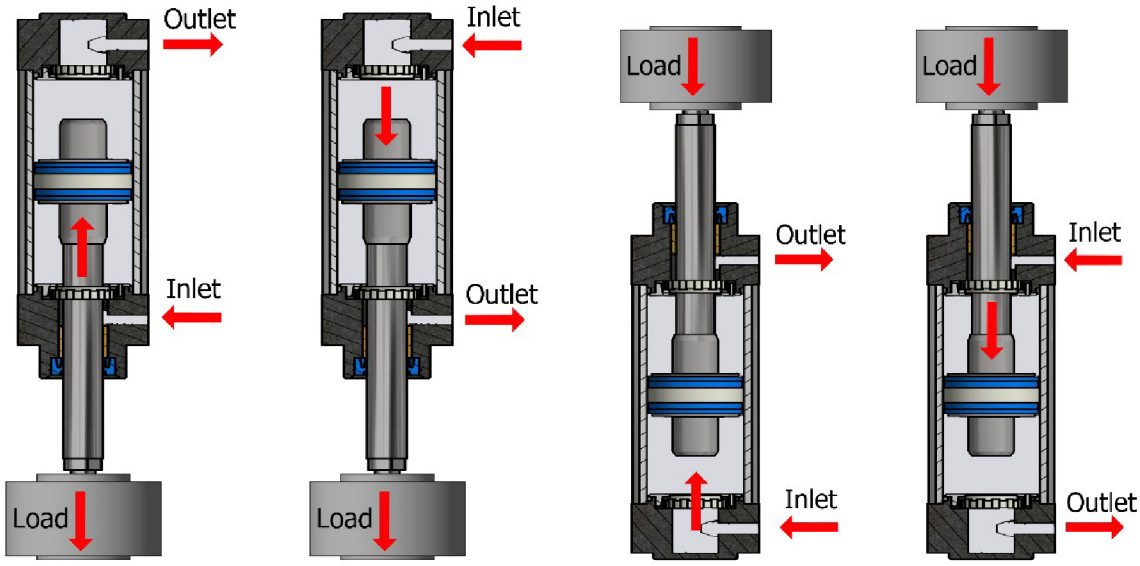

a) Retreat stroke b) Progress stroke c) Progress stroke d) Retreat stroke
Load is below piston Load is above piston

Figure 6.24 Position of load related to the cylinder.

5.5.1. The load is below the piston of the undamaged cylinder

When a 1kg load is applied below the cylinder.

In the progress stroke, the load and the pressure are in the same direction. After the valve is opened by the digital input, the air hits the piston and makes a peak in the signal. The time between the digital signal and the initiation of movement is 0.069 s. There are some effects on the signal at the beginning due to the air passing through the throttle nozzle; the piston vibrates at the beginning of its movement then the speed of its movement becomes steady until the initiation of the damping phase.

The high amplitude of AE near sensor A is a result of the damping that happened in the head cap of the cylinder. When the head cushion piston impacts the head cushion cap, a small peak in the signal appears, and after that, the air is expelled. The time of the stroke is 1.067s.
In the retreat stroke, the load and the pressure are in different directions. After the valve is opened by digital input, the air impacts the piston and makes a peak in the signal. There is a delay in the movement and the signal at the beginning because it needs enough pressure to move the piston. This delay is 0.246 s. Following that, the speed of its movement becomes steady until the initiation of the damping phase.
The high amplitude of AE near sensor B is a result of the damping that happens in the rear cap of the cylinder. When the rear cushion piston impacts the rear cushion cap, a small peak in the signal appears. After that air is expelled. The time of the stroke is 1.149s.

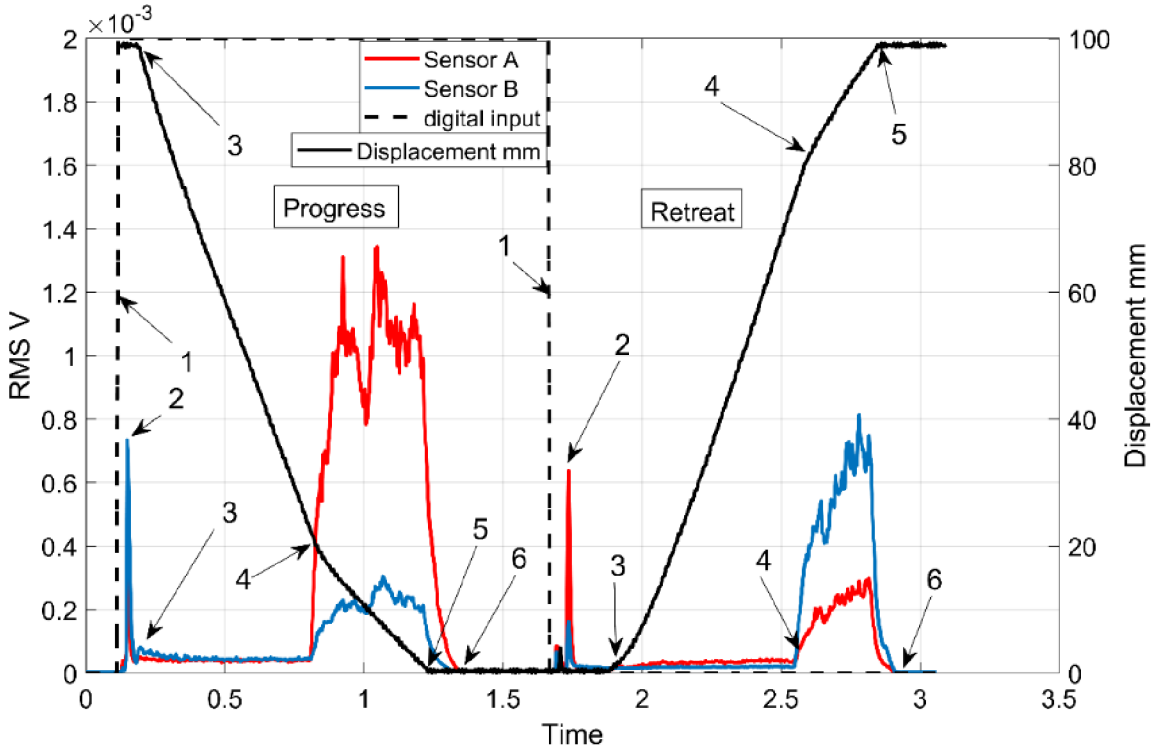

Figure 6.25 Load of 1 kg was applied below the undamaged cylinder.

(1) the valve is opened by the digital input to let the air pass through the port, (2) the impact of the air at the cushion piston, (3) the initiation of movement, (4) the initiation of the damping phase 21.7mm before the TDC, (5) when the cushion piston impacts the cushion cap, and stops, (6) the end of venting air and relaxing and the end of the stroke.

When a 21kg load is applied below the cylinder.
In the progress stroke, the load and the pressure are in the same direction. After the valve is opened by the digital input the air hits the piston and makes a peak in the signal. The time between the digital signal and the initiation of movement is 0.069 s. There are big effects on the signal at the beginning because of the air passing through the throttle nozzle and the load pushes the pressure forward. The piston vibrates at the beginning of its movement, and then the speed of its movement becomes steady until the initiation of the damping phase.
The high amplitude of AE near sensor A is a result of the damping that happens in the head cap of the cylinder. When the head cushion piston impacts the head cushion cap, a small peak in the signal appears, after that air is expelled. The time of the stroke is 0.952s.

In the retreat stroke, the load and the pressure are in different directions. After the valve is opened by the digital input, the air impacts the piston and makes a peak in the signal. There is

a delay in the movement and the signal at the beginning because it needs enough pressure to move the piston. This delay is 0.49s, and then the speed of its movement becomes steady until the initiation of the damping phase.

The high amplitude of AE near sensor B is a result of the damping that happens in the rear cap of the cylinder. When the rear cushion piston impacts the rear cushion cap, a small peak in the signal appears, and after that air is expelled. The time of the stroke is 1.532s.

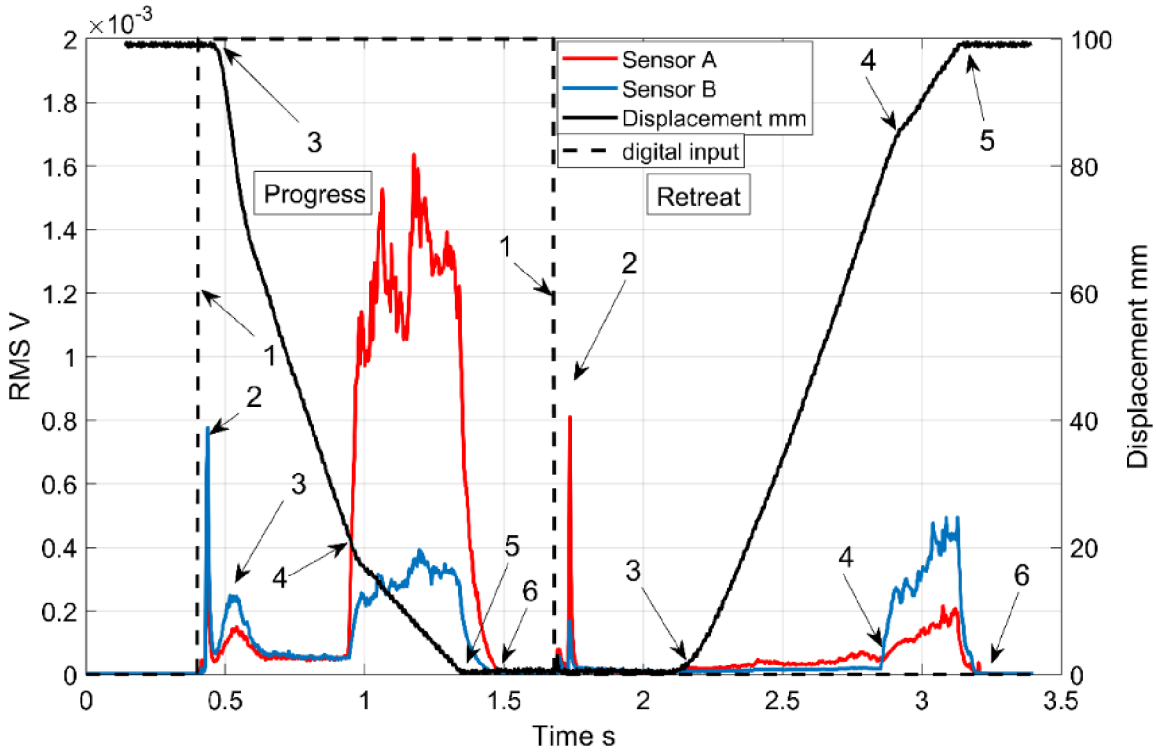

Figure 6.26 Load 21 kg was applied below the undamaged cylinder.

6.5.2. The load is above the piston of the undamaged cylinder

When a 1kg load was applied above the cylinder.

In the progress stroke, the load and the pressure are in different directions, it acts in the same way as in the previous example. The time between the digital signal and the initiation of movement is 0.07s, and the time of the stroke is 1.101s.

In the retreat stroke, the load and the pressure are in the same direction, and it acts in the same way as the previous example. The time between the digital signal and the initiation of movement is 0.195 s, and the time of the stroke is 1.098s.

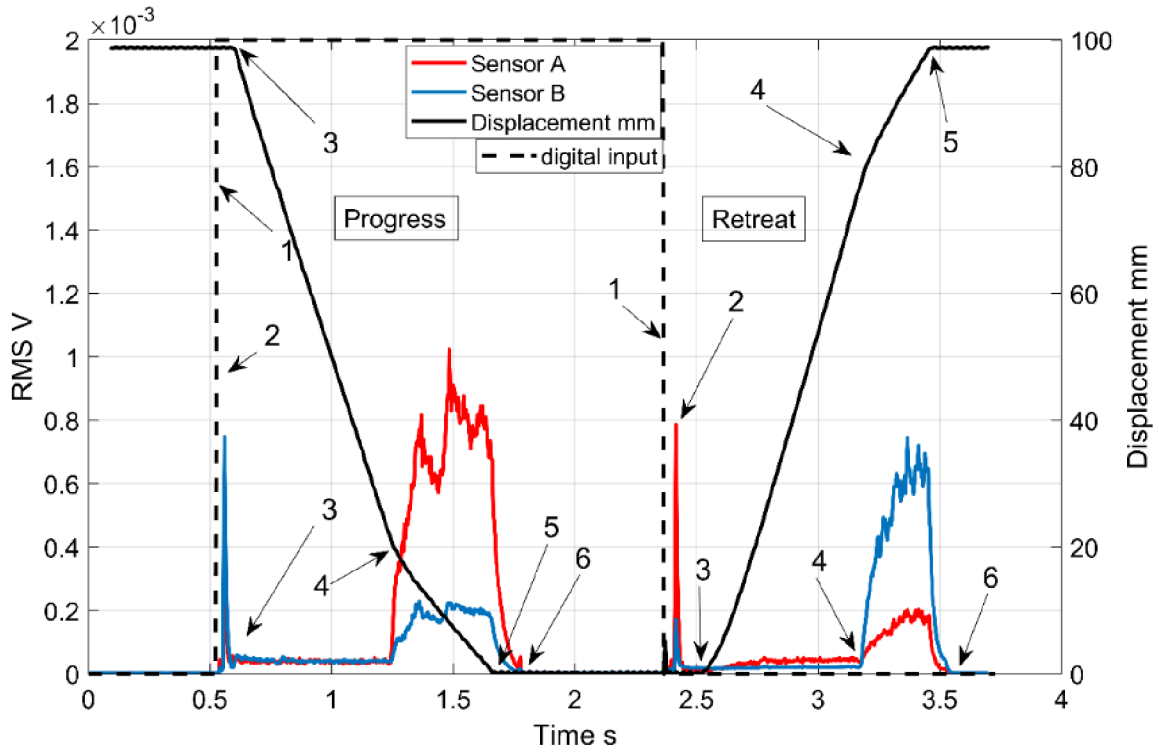

Figure 6.27 Load 1 kg was applied above the undamaged cylinder.

When a 21kg load was applied above the cylinder.

In the progress stroke, the load and the pressure are in different directions, and it acts in the same way as seen previously. The time between the digital signal and the initiation of the movement is 0.227 s, and the time of the stroke is 1.386s.

In the retreat stroke, the load and the pressure are in the same direction, and gain it acts in the same way as seen previously. The time between the digital signal and the initiation of the movement is 0.138 s, and the time of the stroke is 0.906s.

Table 6.5 Calculation of strokes time for undamaged cylinder the load is above and below.

Loads	Time	Time between digital input and initiation of movement		the time of the stroke	
	stroke	Progress	Retreat	Progress	Retreat
Loads below	1kg	0.069	0.246	1.067	1.149
	21kg	0.069	0.49	0.952	1.532
Loads above	1kg	0.07	0.195	1.101	1.098
	21kg	0.227	0.138	1.386	0.906

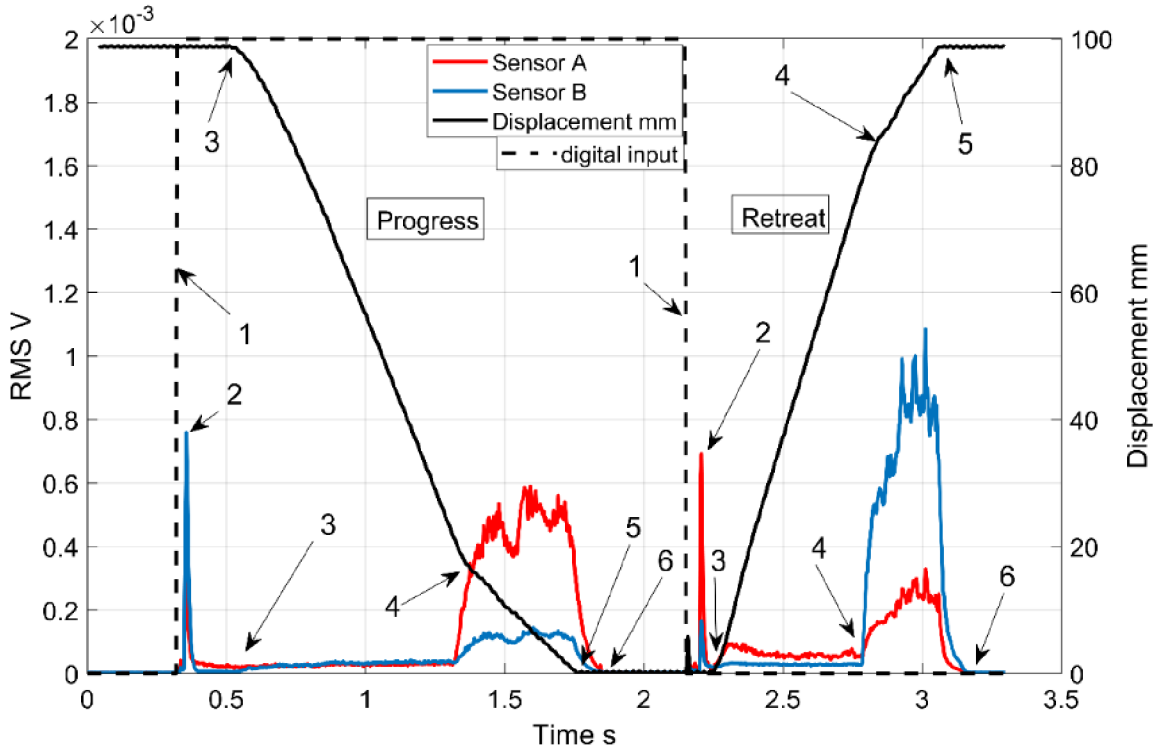

Figure 6.28 Load 21 kg was applied above the undamaged cylinder.

When the load is below the cylinder, the RMS amplitude from sensor A in the progress stroke for 21kg is higher than the RMS amplitude from sensor B for 1 kg, whereas, the RMS amplitude from sensor A in the retreat stroke for 21kg is lower than the RMS amplitude from sensor B for 1 kg.

When the load is above the cylinder, the RMS amplitude from sensor A in the progress stroke for 21kg is lower than the RMS amplitude from sensor B for 1 kg, whereas, the RMS from sensor A in the retreat stroke for 21kg is higher than the RMS amplitude from sensor B for 1 kg.

The total RMS was calculated for each loading and with different positions: the progress and retreat strokes with above and below loading, as shown in the following table 6.6:

Table 6.6 Value of RMS from sensor A and B according to load.

Load kg	Load is below				Load is above			
	Progress stroke		Retreat stroke		Progress stroke		Retreat stroke	
	RMS of A (mV)	RMS of B (mV)	RMS of A(mV)	RMS of B(mV)	RMS of A(mV)	RMS of B(mV)	RMS of A(mV)	RMS of B(mV)
1kg	0.541	0.136	0.107	0.249	0.385	0.119	0.088	0.237
6kg	0.606	0.157	0.102	0.222	0.355	0.111	0.098	0.259
11kg	0.646	0.174	0.097	0.1998	0.304	0.097	0.100	0.278
16kg	0.665	0.179	0.087	0.167	0.353	0.102	0.124	0.328
21kg	0.751	0.202	0.075	0.139	0.234	0.083	0.116	0.328

From the table 6.6 we can draw these four graphs.

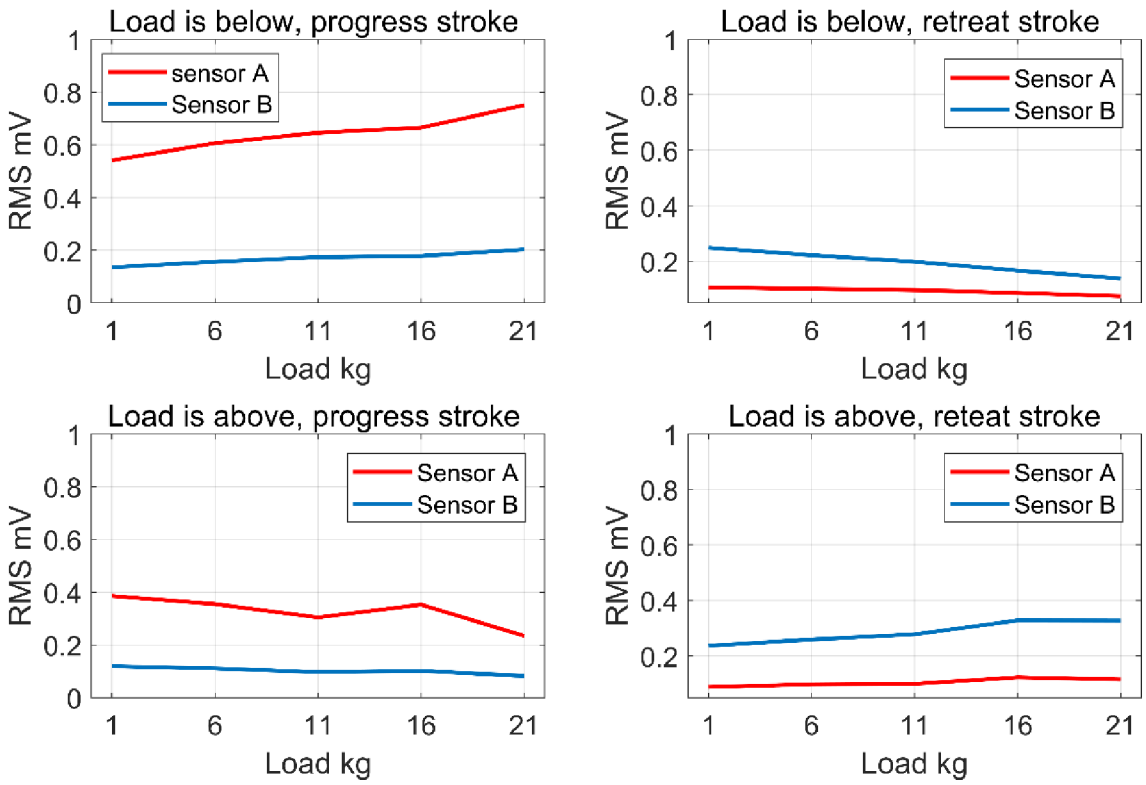

Figure 6.28 Relationship between RMS and loading on undamaged cylinder during one cycle.

a) The relationship between RMS of AE and the loading is linear.
b) In the case of the load being above, when the load increases the RMS decreases in the progress stroke, and when the load increases the RMS increases in the retreat stroke.
c) In the case of the load being below, when the load increases the RMS increases in the progress
d) stroke, and when the load increases the RMS decreases in the retreat stroke.
e) The curve of energy and loading is very similar to that in figure 6.28.

5.5.3. The load is below the piston of the damaged cylinder

When the load is below the cylinder. In the progress stroke, the load and the piston movement are in the same direction; the leak is in port B and the air is expelled through port A, so there is a huge amplitude of RMS from sensor B, and there is a signal from sensor A. The leak continues flowing from port B after the piston stop, so the signal from sensor B is bigger than from sensor A.
In the retreat stroke, the load and the piston movement are in different directions; the leak is from port A and the air is expelled through port B, so there is a huge amplitude of RMS from sensor A, and there is a signal from sensor B. The leak continues flowing from port A after the piston stops, so the signal from sensor A is bigger than from sensor B, as shown in figures 6.29 and 6.30.

5.5.4. The load is above the piston of the damaged cylinder

When the load is above the cylinder. In the progress stroke, the load and the piston movement are in different directions; the leak is in port B and the air is expelled through port A. The RMS from sensor A and the RMS from sensor B are in the same amplitude, and the leak continues flowing from port B after the piston stops, so the signal from sensor B is bigger than from sensor A, as shown in figures 6.31 and 6.32.

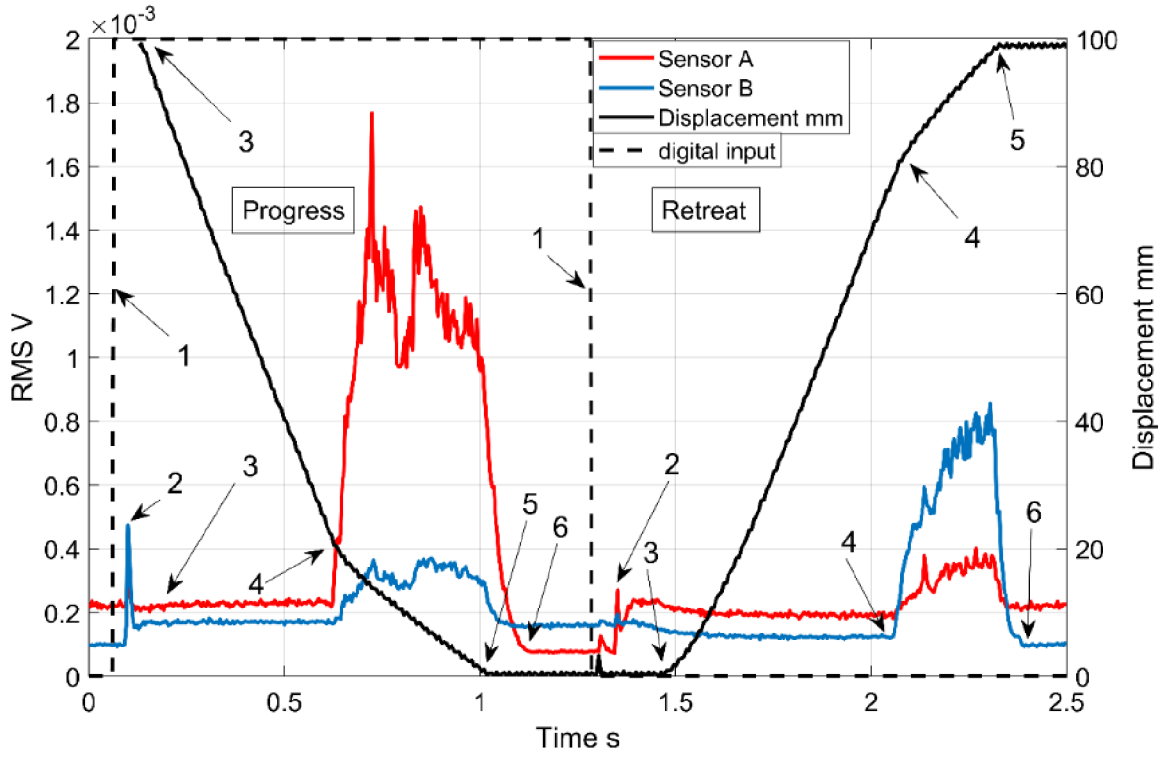

Figure 6.29 Load 1 kg was applied below the damaged cylinder.

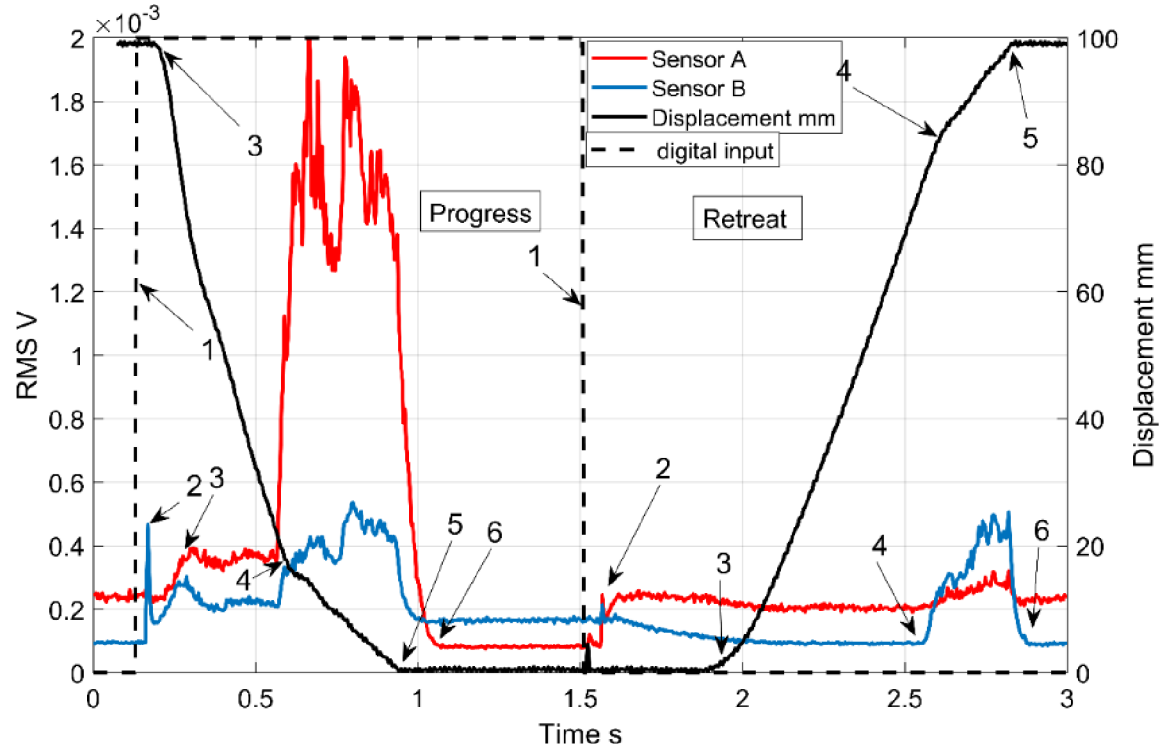

Figure 6.30 Load 21 kg was applied below the damaged cylinder.

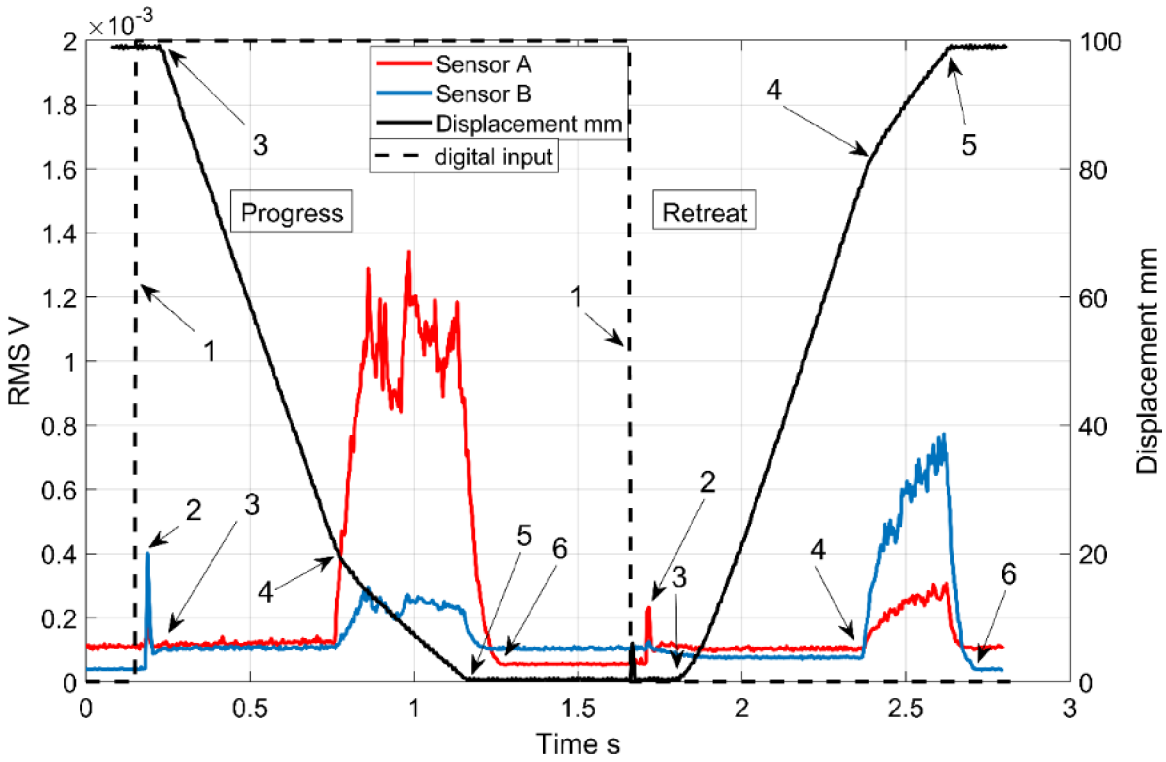

Figure 6.31 Load 1 kg was applied above the damaged cylinder.

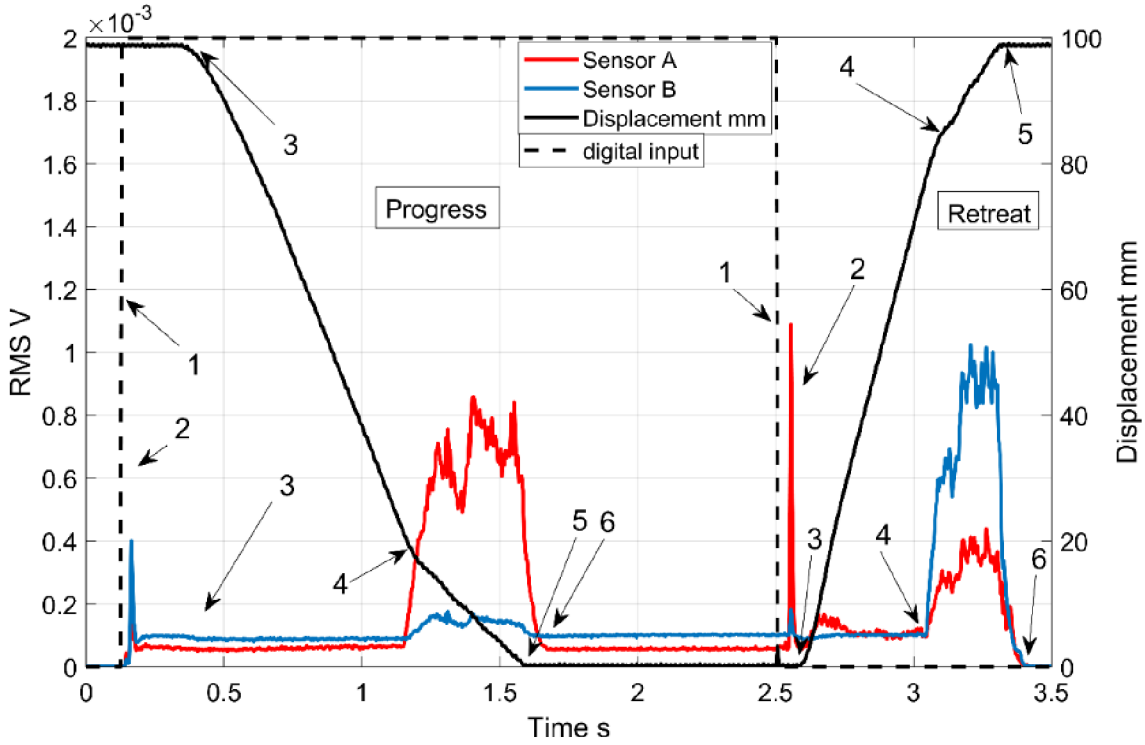

Figure 6.32 Load 21 Kg was applied above the damaged cylinder.

In the retreat stroke, the load and the piston movement are in the same direction, and the leak is from port A and the air is expelled through port B. The RMS from sensor A and the RMS from sensor B are in the same amplitude. The leak continues flowing from port A after the piston stops, so the signal from sensor A is bigger than from sensor B.

The total RMS was calculated for each load for the progress and retreat strokes in two different positions of the cylinder - above and below, as shown in the following table 6.7:

Table 6.7 The value of total RMS from sensor A and B according to load.

Load kg	Load is below				Load is above			
	Progress stroke		Retreat stroke		Progress stroke		Retreat stroke	
	RMS of A (mV)	RMS of B (mV)	RMS of A(mV)	RMS of B(mV)	RMS of A(mV)	RMS of B(mV)	RMS of A(mV)	RMS of B(mV)
1kg	0. 671	0. 223	0. 222	0. 309	0. 582	0. 158	0. 139	0. 265
6kg	0. 756	0. 243	0. 225	0. 287	0. 464	0. 139	0. 12	0. 289
11kg	0. 792	0. 255	0. 209	0. 239	0. 404	0. 136	0. 128	0. 318
16kg	0. 869	0. 266	0. 208	0. 206	0. 382	0. 131	0. 156	0. 352
21kg	0. 957	0. 301	0. 211	0. 183	0. 326	0.0 82	0. 144	0. 361

From the table 6.7 we can draw these four graphs.

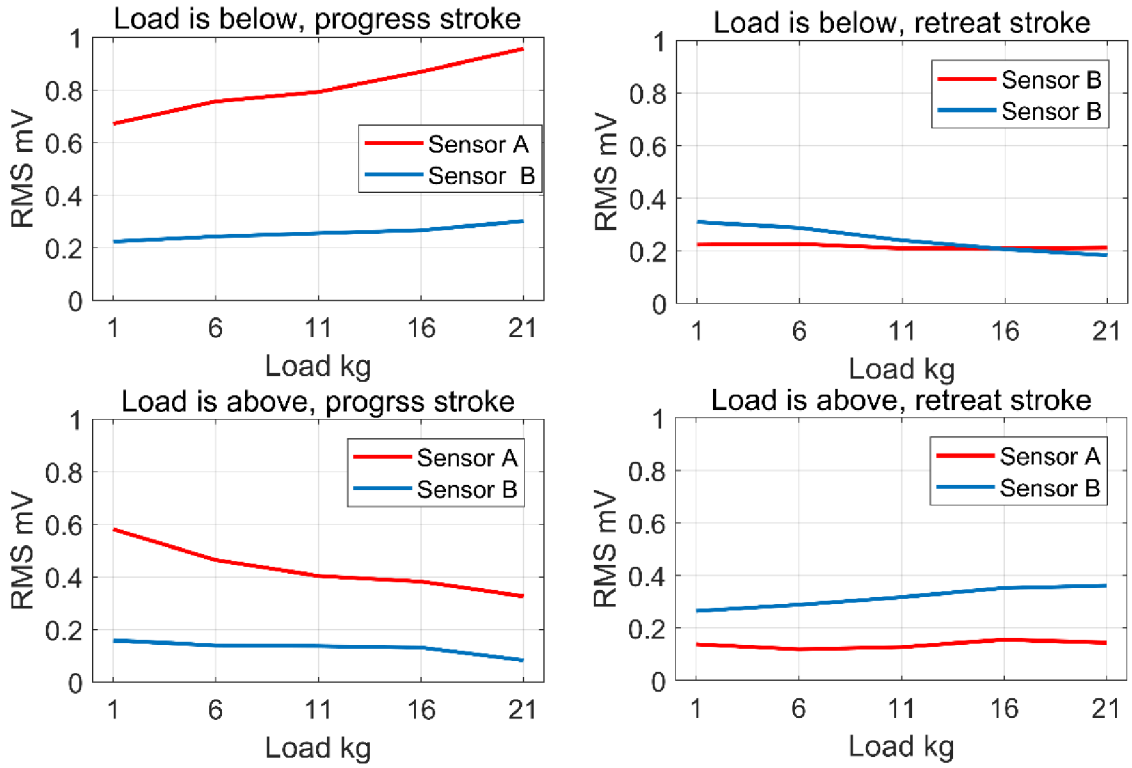

Figure 6.33 Relationship between RMS and loading during one cycle of the damaged cylinder.

When there is a leak in the porting of the cylinder see figure 5.2, the peak of the signal appears during the stroke, not only in the damping phase. The relationship between the RMS of AE and the loading is linear. In the case of the load being above, when the load increases the RMS decreases in the progress stroke, and when the load increases the RMS increases in the retreat stroke. In the case of the load being below, when the load increases the RMS increases in the progress stroke, and when the load increases the RMS decreases in the retreat stroke. The reason for the change in the results between the damaged and undamaged cylinder figures 6.28 and 6.33, in the case where the load is below and the RMS from sensor A increases in the damaged cylinder and decreases in the undamaged cylinder in retreat stroke, is due to the leak near the port.

7. Conclusions

In this study, several undamaged cylinders were tested by acoustic emission, before artificial defects were created in each one. Undamaged and damaged cylinders were compared to find distinctive differences that determine whether the cylinder is damaged or undamaged.

Suitable acoustic emission signal parameters were selected based on the analysis of large data sets. These parameters can be used for more accurate diagnostics of condition monitoring for the development of pneumatic testing devices.

Current results show good conformity and repeatability, acoustic emission application in this domain of diagnostics brings higher quality results than currently used methods.

The frequency spectrum was used as a parameter to compare undamaged and damaged cylinders, which was replaced later by the parameter RMS.

Preliminary results of processed measurements confirm the assumption that the configuration that consists of two sensors located on the head and rear caps provides more detailed results than the configuration that uses only one sensor in the middle of the cylinder body.
The received signals are caused not only by defects, but also by mechanical movements, and inlet and outlet pressurized air.
Acoustic emission detectability of leakage depends on detection sensitivity, detection selectivity, differential pressure, and leak size.

The Acoustic emission can be applied to detect and locate leaks as long as there is enough pressure acting across the leak.

The determination of diagnostic criteria that evaluate the quality of the pneumatic cylinder and detect the defects. There are four criteria to evaluate the cylinder respectively:

- The RMS was normalized; the defect in the cylinder causes a delay in the stroke time, which causes an extension in the damping area. This delay distinguishes between undamaged and damaged cylinder.
- The specific ratio between maximum RMS from the sensor fixed in the head cap A of and the max RMS from the sensor fixed in the rear cap B the cylinder in the retreat stroke can identify whether the cylinder is damaged or undamaged.
  When the ratio is bigger than 3 the cylinder is damaged if the ratio is smaller than 1.7 the cylinder is undamaged.
- The damaged and undamaged cylinders were distinguished using the difference in energy values present in the signals from the two sensors in the retreat stroke. At signal energy $E_{B-A} > 0.000000027$ V2 *s*Ohm the cylinder is damaged, and at $E_{B-A} < 0.000000020$ V2 *s*Ohm it is undamaged.
- The final evaluation of the cylinder was determined by the calculation of the total value of RMS. The value of $\sum RMS$ from sensor B at one cycle can evaluate the quality of the cylinder, the smaller the value the better the quality. At $\sum RMS > 0.18$ mV the cylinder is damaged, and at $\sum RMS < 0.14$ mV it is undamaged.

The cylinders in the experiment were loaded gradually by different weights in a vertical direction. The defect affects the relationship between the applied load and the recorded signal of the sensors. The artificial defects were made in the cylinders and classified according to their severity and detectability.

- The relationship between RMS of AE and the loading is linear.

- Clear explanation of the actuator movement stages, where the certain similarities were found by comparing between the stages of the actuator movement and acoustic emission signals with the potentiometer curve.
- There is a delay in the time of movement and the signal at the beginning because enough pressure is needed to move the piston.
- When the loading and movement of the piston are in opposite directions, the time of the stroke is longer.
- When the loading and movement of the piston are in the same direction, the time of the stroke is shorter.

The load is above	progress stroke	when the load increases the RMS decreases
	retreat stroke	When the load increases the RMS increases
The load is below	progress stroke	when the loading increases the RMS increases
	retreat stroke	When the load increases the RMS decreases

It is confirmed that using acoustic emission method able to diagnose of the defects of pneumatic cylinders, and detect and predict the possible worst defects in the cylinder in practical work and determine the type of defects and its locations.

Future work

It is necessary to make other tests to apply the current criteria on other types of pneumatic cylinders and modify these criteria to be suitable for these cylinders under different conditions. In our laboratory, we test the cylinders in practice, especially when applied in the real-time function and during the loading. Above-mentioned criteria are applied practically on various types of cylinders that help in the opening door system in the buses. Our research continues in this area depending on our experiences during the first stage of this project.

This research will continue to improve a prototype of the newly developed diagnostic apparatus.

8. List of my publications

Conferences

1. MAZAL, P., H. MAHMOUD, V. BUKÁČEK, F., VLAŠIC and M., JANA. Využití Metody Akustické Emise Pro Identifikaci Poškození Pneumatických Válců. *In Defektoskopie 2015 / Nde for Safety.* 2015. Brno: Vysoké Učení Technické V Brně, 2015. S. 81-90. ISBN: 978-80-214-5280- 0.

2. MAHMOUD, H.; F. VLAŠIC and P. MAZAL. Simulation of Operational Loading of Pressure Equipment by Means of Non- Destructive Testing. *by Metal 2015. 2015. Brno: Tanger Ltd., 2015. S. 321-327.* ISBN: 978-80-87294-58- 1.

3. MAHMOUD, H., F. VLAŠIC, P. MAZAL and M. JÁNA. Damage Identification of Pneumatic Components by Acoustic Emission. *In 32nd European Conference on Acoustic Emission Testing.* 1st Edition. Brno: Vutium Brno, Brno University of Technology, 2016. S. 315-322. ISBN: 978-80-214-5386- 9.

4. MAZAL, P., F. VLAŠIC, H. MAHMOUD and M., JANA. The Use of Acoustic Emission Method for Diagnosis of Damage of Pneumatic Cylinders. *In 19th WCNDT 2016 - World Conference on NDT. Munchen, Germany: German Society for NDT*, 2016. S. 1-10. ISBN: 978-3-940283-78- 8.

5. MAZAL, P., F. VLAŠIC and H. MAHMOUD. Use of Acoustic Emission Method for Diagnosis of Damage of Pneumatic Cylinders. *The E- Journal of Non-destructive Testing, 2016*, roč. 2016, č. 1, S. 1-10. ISSN: 1435-4934.

6. JÁNA, M., H. MAHMOUD, P. MAZAL and F. VLAŠIC. Stanovení Koeficientu Odhalení Poškození V Pneumatických Válcích Metodou Akustické Emise. *In Defektoskopie 2016, NDE for Safety.* první. Brno: Vysoké účení technické v Brně, ČNDT, 2016. S. 27-35. ISBN: 978-80-214-5422- 4.

7. MAHMOUD, H., F. VLAŠIC, P. MAZAL, L. NOHÁL and V. KRATOCHVÍLOVÁ. Analysis of Pneumatic Cylinder Damage by Acoustic Emission Method. *In Defektoskopie 2017 (NDE for Safety).* první. Brno: VUT v Brně ve spolupráci s ČNDT, 2017. S. 151-161. ISBN: 978-80-214-5554-2.

8. MAHMOUD, H., F. VLAŠIC and P. MAZAL. Application of Acoustic Emission Method to Diagnose Damage in Pneumatic Cylinders. *In First World Congress on Condition Monitoring. 1st. UK, Northampton: BINDT, 2017.* S. 858-868. ISBN: 9781510844759.

9. MAHMOUD, H., P. MAZAL and F. VLAŠIC. Condition Monitoring of Pneumatic Cylinders by Acoustic Emission. *In Application of Contemporary Non-Destructive Testing in Engineering. Ljubljana, Slovenija: University of Ljubljana, 2017.* S. 231-238. ISBN: 978-961-93537-3-8.

10. MAHMOUD, H., P. MAZAL, F. VLAŠIC and M. JÁNA. Damage Detection for Linear Pneumatic Actuators using Acoustic Emission. *In 33nd European Conference on Acoustic Emission Testing, Senlis, France, 2018.*

11. MAHMOUD, H.; MAZAL, P.; VLAŠIC, F. Метод акустической эмиссии для неразрушающего контроля пневматических цилиндров “Using Acoustic Emission Testing for Pneumatic Actuators Monitoring”. NDT world, 2018, roč. 21, č. 4, s. 64-67. ISSN: 1609-3178.

12. MAHMOUD, H.; MAZAL, P.; VLAŠIC, F.; NOHÁL, L. Leakage Detection for Pneumatic Circle of Bus Door Using Acoustic Emission and other NDT Methods. In Defektoskopie 2018 / NDE for Safety 2018. Brno: Vysoké učení technické v Brně ve spolupráci s Českou společností pro NDT, z.s., 2018. s. 67-77. ISBN: 978-80-214-5684-6.

13. RICHTER, V.; MAHMOUD, H.; MAZAL, P.; SKŘIVÁNKOVÁ, V. The Parameters of Acoustic Emission Signal Proposed to Identification of Damaged and Undamaged Cylinders. European Conference on Acoustic Emission (EWGAE) 2018. Senlis, France: CETIM, 2018. s. 1-13.

Impacted Journals

14. MAHMOUD, H., F. VLAŠIC, P. MAZAL and M. JÁNA. Leakage Analysis of Pneumatic Cylinders Using Acoustic Emission. *Insight BINDT, 2017*, roč. 59, č. 9, s. 500-505. ISSN: 1354-2575 (0.7).

15. MAHMOUD, H., P. MAZAL and F. VLAŠIC. Relationship Between Acoustic Emission Signal and Loads on Pneumatic Cylinders, *Non-destructive Testing and Evaluation, 2019, impacted journal (1.957) in Taylor & Francis under review*.

16. MAHMOUD, H., P. MAZAL, F. VLAŠIC. Detecting the Defects of Pneumatic Actuators Using Acoustic Emission Monitoring. *Insight BINDT, 2019 will be published.*

Certificate of Methodology

TÜV NORD Czech

CERTIFIKÁT

o uznání přezkoušené metodiky
evidenční číslo: 002/17

Zákazník:	**Vysoké učení technické v Brně** **Fakulta strojního inženýrství, Ústav konstruování** **Technická 2896/2, 616 69 Brno** **Česká republika**
IČO:	**00216305**
Metoda:	**Hodnocení provozního stavu přímočarých pneumotorů pomocí metody akustické emise**
Autoři metodiky:	**Ing. František Vlašic, Ph.D.** **doc. Ing. Pavel Mazal, CSc.** **Ing. Houssam Mahmoud** **Ing. Vladimír Bukáček**
Označení:	**TA04011374**
Interní informační označení metodiky:	**Testy pneuválců akustickou emisí**
Místo uložení metodiky:	**Poličské strojírny a.s.,** **Bořiny 1145, Horní Předměstí, 572 01 Polička**

TÜV NORD Czech, s.r.o., certifikační a inspekční společnost, tímto potvrzuje, že přezkoušení výše uvedené metodiky bylo provedeno v souladu s požadavky směrnice S 9.19 „Proces certifikace metodik", viz Certifikační list ke schválení metodiky" ze dne 07.12.2017. Zakázka je vedena pod zakázkovým číslem 5117139/01.

Praha, 07.12.2017
Místo a datum

Certifikační a inspekční společnost TÜV NORD Czech 10 TÜV NORD Czech, s.r.o.

Ing. Daniel Jarchovský
ředitel Divize posuzování shody
TÜV NORD Czech, s.r.o.

TÜV NORD Czech, s.r.o.
Českomoravská 2420/15, CZ-190 00 Praha 9
Telefon: (00420) 296 587 201-9, Telefax: (00420) 296 587 240, E-mail: tuev-nord@tuev-nord.cz
TÜV NORD GROUP

9. Literature

[1] JACKSON, CH., CH. SHERLOCK and P. MOORE, *NDT Handbook: Third Edition: Volume 1, Leak Testing*, American Society for Non-destructive Testing, ISBN: 1-57117-071-5 Year: 1998

[2] MILLER, R.K. and E.VK. HILL: *Acoustic Emission Testing, NDT Handbook, Vol. 6, 3rd edition*, ASNT, Columbus, 2005. ISBN 1-57117-106-1.

[3] *The Pneu Book is produced by SMC Pneumatics (UK) [online]* https://www.smc.eu/portal_ssl/WebContent/local/UK/Pneu_Book/pneubook.pdf

[4] MAZAL, P., F. VLASIC, H. MAHMOUD and M. JANA, The use of Acoustic Emission method for diagnosis of damage of pneumatic cylinders, *WCNDT, vol.19, pp. 2016.*

[5] MAHMOUD, H., F. VLAŠIC, P. MAZAL, L. NOHÁL and V. KRATOCHVÍLOVÁ, Analysis of Pneumatic Cylinder Damage by Acoustic Emission Method. *In Defektoskopie 2017 (NDE for Safety)*. Brno, 2017. s. 151-161. ISBN: 978-80-214-5554-2.

[6] MAHMOUD, H., F. VLASIC, M. JANA, P. MAZAL, condition monitoring of pneumatic cylinders By Acoustic Emission, *14th International Conference of the Slovenian Society for Non-Destructive Testing, 4-6 September 2017.*

[7] GAO, L., F. ZAI, SH. SU, H. WANG, P. CHEN and L. LIU. Study and Application of Acoustic Emission Testing in Fault Diagnosis Of Low -Speed Heavy-Duty Gears Sensors 2011, 11, 599-611; Doi:10.3390/ S110100599.

[8] International Atomic Energy Agency. Training Guidelines in Non-Destructive Testing Techniques: *Leak Testing at Level 2*. VIENNA, 2012.

[9] PLLOCK, A.A., and HSU: Leak Detection Using Acoustic Emission. *Journal of Acoustic Emission. 1982, No. 4, p. 237-243.*

[10] K.A.El-Shorbagy, "An investigation into noise radiation from flow control valves with particular reference to flow rate measurement," Applied Acoustics, vol.16, no.3, pp.169–181, 1983.

[11] M. A. Sharif and R. I. Grosvenor, "Internal valve leakage detection using an acoustic emission measurement system," Transactions of the Institute of Measurement and Control, vol. 20, no.5, pp.233–242,1998.

[12] S.-G. Lee, J.-H. Park, K.-B. Yoo, S.-K. Lee, and S.-Y. Hong, "Evaluation of internal leak in valve using acoustic emission method," Key Engineering Materials, vol.326–328, pp.661–664, 2006.

[13] J.Dickey, J.Dimmick, and P.M.Moore," Acoustic measurement of valve leakage rates," Materials Evaluation, vol. 36, no. 1, pp. 67–77, 1978.

[14] Y. Jiang, Q.-C. Gong, Q. Ye, and C.-L. Liu, "The theoretical analysis and experiments of using ultrasonic to inspect the leak amount," China Academic Journal Electronic Publishing House, no.1, 2005 (Chinese).

[15] Q.-X.Gao, L.-P.Li,H.-D.Rao, J.Yang, and Y.-J.Zhu, "Acoustic emission theory and testing technology for quantitative diagnosis of valve leakages," Journal of Chinese Society of Power Engineering, vol.32, no.1, pp.42–46, 2012 (Chinese).

[16] R.Bayindir and H.Ates, "Low-cost and high sensitively microcontroller based control unit for a friction welding machine," Journal of Materials Processing Technology, vol.189, no.1–3, pp. 126–131, 2007.

[17] J. Yang, L. Li, H. Rao, Y. Zhu, and G. Liu, "Diagnosis of valve leakage fault patterns based on acoustic emission detection," Journal of Chinese Society of Power Engineering, vol. 33, no. 6, pp.455–483,2013.

[18] Y. Wang, C. Xue, X. Jia, and X. Peng, "Fault diagnosis of reciprocating compressor valve with the method integrating acoustic emission signal and simulated valve motion," Mechanical Systems and Signal Processing, vol.56-57, pp.197–212,2015.

[19] A.A. Pollock and S.Y.S. Hsu, "Leak Detection Using Acoustic Emission", Journal of Acoustic Emission, Vol. 1, No. 4, pp. 237-243, 1982.

[20] C.Jomdecha, A.Prateepasen, P.Kaewtrakulpong, and P.Thungsuk, "Corrosion-source location by an FPGA-PC based acoustic emission system," in Proceedings of the IEEE Region 10 Annual International Conference (TENCON '04), vol. 4, pp. 500–601, 2004.

[21] J.G.Dimmick, J.R.NicholasJr., J.W.Dickey, and P.M.Moore, "Acoustical valve leak detector for fluid system maintenance," Naval Engineers Journal, vol.91, no.2, pp.71–83, 1979.

[22] Score (Europe) Limited and Glenugie Engineering Works, "Identifying leaking valves quickly and easily using acoustic emissions measurement technology," Sealing Technology, vol. 2013,no.1,pp.11–12,2013.

[23] T.Nakamura and M.Terada, "Development of leak monitoring system for pressurizer valves," Progress in Nuclear Energy, vol. 15, pp.175–179, 1985.

[24] J. H. Lee, M. R. Lee, J. T. Kim et al., "Condition monitoring of a check valve for nuclear power plants by means of acoustic emission technique," in Proceedings of the 17th International Conference on Structural Mechanics in Reactor Technology, Prague, Czech Republic, August2003.

[25] Q.Gao,L.Li,H.Rao,andJ.Yang, "Research on the relationship between internal fluid leakage through a valve and the acoustic emission features generated from the leakage," Journal of Engineering forThermal Energy and Power, vol.26, no.5, 2011.

[26] W. Kaewwaewnoi, A. Prateepasen, and P. Kaewtrakulpong, " Measurement of valve leakage rate using acoustic emission," in Proceedings of the International Conference on Electrical Engineering/Electronics, Computer, Telecommunications, and Information Technology (ECTI'05), pp.597–600, 2005.

[27] A. Prateepasen, W. Kaewwaewnoi, and P. Kaewtrakulpong, "Smart portable non-invasive instrument for detection of internal air leakage of a valve using acoustic emission signals," Measurement,vol.44,no.2,pp.378–384,2011.

[28] H. Y. Sim, R. Ramli, A. A. Saifizul, and M. A. K. Abdullah, "Empirical investigation of acoustic emission signals for valve failure identification by using statistical method," Measurement, vol.58, pp.165–174, 2014.

[29] YAN JIN, Y. HENG-HU, Y. HONG, Z. FENG, L. ZHEN, W. PING and Y. YAN. *Non-destructive Detection of Valves Using Acoustic Emission Technique*. DOI:10.1155/2015/749371. ISBN 10.1155/2015/749371. http://www.hindawi.com/journals/amse/2015/749371/

[30] S.-H.Seong,S.Hur, J.-S.Kimetal., "Development of diagnosis algorithm for the check valve with spectral estimations and neural network models using acoustic signals," Annals of Nuclear Energy,vol.32, no.5, pp.479–492, 2005.

[31] The American Society for Testing and Materials, Annual Book of ASTM Standards; Volume 03.03, Standard E750-88 Standard Practice for Charac- terizing Acoustic emission Instrument, Philadelphia, PA, 1993.

[32] KAEWWAEWNOI, W., A. PRATEEPASEN and A. KAEWTRAKULPONG. *Study on Correlation of AE Signals from Different AE Sensors in Valve Leakage Rate Detection.* January 2007. http://www.ecti-thailand.org/assets/papers/195_pub_16.pdf

[33] Kupperman, D.S., Claytor, T.N. an Groenwald R. "Acoustic Leak Detection for Reactor Coolant Systems," Nuclear Engineering and Design, Vol. 86, pp. 13-20, 1985.

[34] Miller, R.K., Pollock, A.A., Watts, D.J., Carlyle, J.M., Tafure, A.N. and Yezzi, J.J. "A Reference Standard for the Development of Acoustic Emission Pipeline Leak Detection Technique," NDT&E International, Vol. 32, pp. 1-8, 1999.

[35] Grabec, I. "Application of Cross Correlation Techniques for Localization of Acoustic Emission Sources," Ultrasonics, Vol. 41, pp. 111-115, 1978.

[36] Gao, Y., Brennan, M.J., Joseph, P.F., Muggleton, J.M. and Hunaidi, O. "A Model of the Correlation Function of Leak Noise in Buried Plastic Pipes," Journal of Sound and Vibration, Vol. 277, pp. 133-148, 2004.

[37] Fukuda, T. And Mitsuoka, T. "Applications of Computer Data Processing and Robotic Technology," Computers in Industry, Vol. 7, pp. 5-13, 1986.

[38] Ahadi, M. And Bakhtiar, M.S. "Leak Detection in Water-Filled Plastic Pipes through the Application of Tuned Wavelet Transforms to Acoustic Emission Signals," Applied Acoustics, Vol. 71, pp. 634-639, 2010.

[39] Jiao, J., He, C., Wu, B. And Fei, R. "A New Technique for Modal Acoustic Emission Pipeline Leak Location with One Sensor," Insight, Vol. 46, No. 7, pp. 392-395, 2004.

[40] Muggleton, J.M., Brennan, M.J., Linford, P.W. "Axisymmetric Wave Propagation in Fluid-Filled Pipes: Wavenumber Measurements in in Vacuo and Buried Pipes," Journal of Sound and Vibration, Vol. 270, pp. 171-190, 2004.

[41] Yang, J., Qingxin, Y. and Guanghai, L. "Leak Identification Method for Buried Gas Pipeline Based on Spatial-Temporal Data Fusion," IEEE International Conference on Control and Automation, Guangzhou, China, pp. 774-777, 2007.

[42] Laodeno, R.N., Nishino, H. And Yoshida, K. "Characterization of AE Signals Generated by Gas Leak on Pipe with Artificial Defect at Different Wall Thickness," Materials Transactions, Vol. 49, No. 10, pp. 23412346, 2008.

[43] Ozevin, D. and Harding J. "Novel Leak Localization in Pressurized Pipeline Networks using Acoustic Emission and Geometric Connectivity," International Journal of Pressure Vessels and Piping, Vol. 92, pp. 6369, 2012

[44] Farova Z., Prevorovsk Z., Kus V., Serge Dos Santos. Experimental signal deconvolution in acoustic emission identification set. International Workshop of NDT Experts, Prague, 10–12 October 2011.

[45] Shama,A.;El-Shaib,M.; Sharara,A.; Nasser, D.Y. Experimental study for leakage detection in subsea pipeline by applying acoustic emission technique. In Proceedings of the International Congress of the International Maritime Association of the Mediterranean, Lisbon, Portugal, 9–11 October 2017.

[46] Xu, C.; Gong, P.; Xie, J.; Shi, H.; Chen, G.; Song, G. An acoustic emission based multi-level approach to buried gas pipeline leakage localization. J. Loss Prev. Process Ind. 2016, 44, 397–404. [CrossRef]

[47] Mostafapour, A.; Davoodi, S. Leakage locating in underground high pressure gas pipe by acoustic emission method. J. Nondestruct. Eval. 2013, 32, 113–123. [CrossRef]

[48] DAVOODI, S. and A. MOSTAFAPOUR, Modeling Acoustic Emission Signals Caused by Leakage in Pressurized Gas Pipe, Published online: 9 November 2012 © Springer Science Business Media New York 2012, *J Non-destructive Eval (2013)* 32:67–80 DOI 10.1007/s10921-012-0160-x

[49] ANASTASOPOULOS, A., D. KOUROUSIS and K BOLLAS. Acoustic Emission Leak Detection of Liquid Filled Buried Pipeline. *Envirocoustics ABEE, El. Venizelou 7 & Delfon, 14452 Metamorphosis, Athens, Greece J. Acoustic Emission, 2009.*

[50] LEE, S., S. PARK and Y. KIM. Field Application Study for Leak Detection Using Acoustic Emission Technology. *Transactions of the Korean Nuclear Society Spring Meeting. Jeju, Korea, May 10-11, 2007.*

[51] AUGUTIS AND SAUNORIS. *Investigation of High Frequency Vibrations of Pneumatic Cylinders.* ISSN 1392-2114 ULTRAGARSAS, Nr.2 (51). 2004. http://citeseerx.ist.psu.edu/viewdoc/download?doi=10.1.1.561.8728&rep=rep1&type=pdf

[52] FUJITA, T., J. JANG, T. KAGAWA and M. TAKEUCHI, Dynamics of Pneumatic Cylinder Systems, *Japan*Department of Control & Systems Engineering, Faculty of Engineering Tohin University of Yokohama 1999.*

[53] DOLL, M., R. NEUMANN and O. SAWODNY, Dimensioning of pneumatic cylinders for motion tasks, *Germany*; *Institute for System Dynamics, University of Stuttgart, Stuttgart, International Journal of Fluid Power, 2015, Vol. 16, No. 1, 11–24,* http://dx.doi.org/10.1080/14399776.2015.1012437

[54] JÁNA, M., Defects of linear pneumatic actuator PS. TA04011374 - A new non-destructive diagnostics system of pneumatic and hydraulic components. Enterprise standard Polička 5. 5. 2015.

[55] *Standard Guide for Mounting Piezoelectric Acoustic Emission Sensors Designation*: E650– 97. This standard is copyrighted by ASTM, 100 Barr Harbor Drive, West Conshohocken, PA 19428-2959, United States. I

[56] *DAKEL*, http://www.dakel.cz/index.php?pg=prod/sens/idk09_en

[57] MAHMOUD, H., F VLASIC, P MAZAL and M JANA; Damage identification of pneumatic components by Acoustic Emission, *Czech Society for Non-destructive Testing, EWGAE, Vol. 32, pp. 315-322, September 07-09, 2016,* ISBN: 978-80-214-5386- 9.

[58] MAHMOUD, H., F. VLAŠIC, P. MAZAL and M. JÁNA, Leakage Analysis of Pneumatic Cylinders Using Acoustic Emission. *INSIGHT, 2017,* roč. 59, č. 9, s.500-505.ISSN:1354-2575.

[59] MAHMOUD, H., F. VLAŠIC and P. MAZAL, Application of Acoustic Emission Method to Diagnose Damage in Pneumatic Cylinders. *In First World Congress on Condition Monitoring. 1st. UK, Northampton: BINDT, 2017*. s. 858-868. ISBN: 9781510844759.

LIST OF SYMBOLS AND ABBREVIATIONS

#	Symbol	Name
1	NDT	Non-destructive testing
2	AE	Acoustic emission
3	D	Detection - coefficient
4	S	Severity - coefficient
5	NP01,02	Leaks above the piston
6	PP01,02	Leaks below the piston
7	VP01,02	Leaks in motion
8	ZP01,02	Leaks shock when inserting the rod
9	Z01,02	Deterioration in the friction conditions
10	M01,02	Mechanical defects
11	T	On-load time (minutes),
12	P	Pressure (psi)
13	t	Off-load time (minutes)
14	V	Volume (cubic feet)
15	ATEQ	Automatic measurement of quality
16	UT	Ultrasonic
17	ASL	Average signal level
18	ΔT	The time span of the testing
19	PZT	Piezoelectric transducer
20	WD	Wide band
21	RMS	Root mean square
22	LT	Leak testing
23	Q	Leakage rate in ml/sec
24	P	Inlet pressure in bars
25	S	Valve size in inches.
26	Re	Reynolds number
27	HFV	High frequency vibrations
28	FFT	Fast Fourier transform
29	HHT	Hilbert-Huang transform
30	v	Voltage signal from an AE sensor
31	T	The integration time of the signal
32	N	The number of discrete AE data within the interval T
33	DAE	Coefficient of detection for AE
34	E	Energy ($V^2 * s * ohm$)
35	U	Voltage V
36	dT	The value of sampling
37	AE_{rms}	Root mean square of AE
38	ρ	The density
39	v_f	Flow velocity
40	r	Radius of flow path
41	η	The viscosity
42	L	Length
43	$R_{y_1y_2}(\tau)$	Cross correlation coefficient
44	y1 and y2	Signals
45	τ	Time delay
46	x	Linear localization

LIST OF FIGURES

LIST OF TABLES

The code of the MATLAB program

The code of the MATLAB program that opens TEXT file that received from ZEDEMON and calculate the parameters of AE to find the differences between damaged and undamaged cylinder by mathematical operations, and plot a figure of RMS was taken from sensor A and Sensor B, and determine the maximum of RMS and the energy.

Open EXCEL file

```
% --------------------------------------------------------------------
function Untitled_11_Callback(hObject, eventdata, handles)
[filename pathname]=uigetfile('C:\Users\Houssam\Desktop\all\21.xlsx');
handles.fullname=strcat(pathname, filename);
set(handles.text2,'string',filename);
guidata(hObject,handles);
fullname=handles.fullname;
[TimeRelativesec,TimedmyHMS,RMSV,RMSdBAE,ASLV,ASLdBAE,MAX_sigV,MAX_sigdBAE,
MAX_absV,MAX_absdBAE,UCount1logNsec,UCount2logNsec,UCount1ThresholdV] =
importfilexls(fullname);
handles.TimeRelativesec=TimeRelativesec;
handles.RMSV=RMSV;
handles.TimedmyHMS=TimedmyHMS;
handles.RMSdBAE=RMSdBAE;
handles.ASLV =ASLV;
handles.ASLdBAE =ASLdBAE;
handles.MAX_sigV =MAX_sigV;
handles.MAX_sigdBAE =MAX_sigdBAE;
handles.MAX_absV =MAX_absV;
handles.MAX_absdBAE =MAX_absdBAE;
handles.UCount1logNsec =UCount1logNsec;
handles.UCount2logNsec =UCount2logNsec;
handles.UCount1ThresholdV =UCount1ThresholdV;
guidata(hObject,handles);
[filename1 pathname1]=uigetfile(fullname,'*.xlsx');
handles.fullname1=strcat(pathname1, filename1);
set(handles.text3,'string',filename1);
guidata(hObject,handles);
fullname1=handles.fullname1;
[TimeRelativesec1,TimedmyHMS1,RMSV1,RMSdBAE1,ASLV1,ASLdBAE1,MAX_sigV1,MAX_s
igdBAE1,MAX_absV1,MAX_absdBAE1,UCount1logNsec1,UCount2logNsec1,UCount1Thres
holdV1] = importfilexls(fullname1);
handles.TimeRelativesec1=TimeRelativesec1;
handles.RMSV1=RMSV1;
handles.TimedmyHMS1=TimedmyHMS1;
handles.RMSdBAE1=RMSdBAE1;
handles.ASLV1 =ASLV1;
handles.ASLdBAE1 =ASLdBAE1;
handles.MAX_sigV1 =MAX_sigV1;
handles.MAX_sigdBAE1 =MAX_sigdBAE1;
handles.MAX_absV1 =MAX_absV1;
handles.MAX_absdBAE1 =MAX_absdBAE1;
handles.UCount1logNsec1 =UCount1logNsec1;
handles.UCount2logNsec1 =UCount2logNsec1;
handles.UCount1ThresholdV1 =UCount1ThresholdV1;
guidata(hObject,handles);
setpopup(handles.pop,eventdata, handles);
% --------------------------------------------------------------------
function[TimeRelativesec,TimedmyHMS,RMSV,RMSdBAE,ASLV,ASLdBAE,MAX_sigV,MAX_
sigdBAE,MAX_absV,MAX_absdBAE,UCount1logNsec,UCount2logNsec,UCount1Threshold
V] = importfilexls(workbookFile)
%% Import the data
data = xlsread(workbookFile);
TimeRelativesec = data(:,1);
```

```
TimedmyHMS = data(:,2);
RMSV = data(:,3);
RMSdBAE = data(:,4);
ASLV = data(:,5);
ASLdBAE = data(:,6);
MAX_sigV = data(:,7);
MAX_sigdBAE = data(:,8);
MAX_absV = data(:,9);
MAX_absdBAE = data(:,10);
UCount1logNsec = data(:,11);
UCount2logNsec = data(:,12);
UCount1ThresholdV = data(:,13);

% ------------------------------------------------------------------
Print the figure and calculate all the parameter
% ------------------------------------------------------------------

function print_ClickedCallback(hObject, eventdata, handles)
cla;
time=handles.TimeRelativesec; %obtain the Time from the memory
time1=handles.TimeRelativesec1;
RMS=handles.RMSV;
RMS1=handles.RMSV1;
Time=time-min(time);% To make the time starting from zero, min:
returns the minimum of Time.
Time1=time1-min(time1);

% divide the one cycle to progress and retreat strokesfrom
sensor A
N=numel(t);    %returns the number of elements
N1=numel(t1);
if rem(N,2)==0; %Remainder after division on 2
   xx=N/2;
  else
   xx=(N+1)/2;
end
 rr1 =RMS(1:xx, 1); %the value of RMS for Progress stroke A
 rr2=RMS(xx:end , 1); %the value of RMS for retreat stroke A
% divide the one cycle to progress and retreat strokesfrom
sensor B
if rem(N1,2)==0; %Remainder after division on 2
   xx1=N1/2;
  else
   xx1=(N1+1)/2;
end
 rr3 =RMS1(1:xx, 1); %the value of RMS for Progress stroke B
 rr4=RMS1(xx:end , 1); %the value of RMS for retreat stroke B
 dd=t(xx); %returns the value of time in the middle
%Print the figure between RMS and Time
hold on
  plot(handles.axes1,t, RMS, 'r');
  plot(handles.axes1,t1, RMS1, 'b');
  plot(handles.axes1,[1 1]*dd, ylim,'g');
  axes(handles.axes1);
  xlabel('Time s', 'FontSize', v2);
  ylabel('RMS', 'FontSize', v2);
hold off
```

```
%Calculate the difference between Max RMS of sensor A and
sensor B.
MaxA1=max(rr1); % Max RMS of progress stroke of sensor A
MaxA2=max(rr2); % Max RMS of retreat stroke of sensor A
MaxB1=max(rr3); % Max RMS of progress stroke of sensor B
MaxB2=max(rr4); % Max RMS of retreat stroke of sensor B
BA22=( MaxB2- MaxA2);
BA11=( MaxB1- MaxA1);
BA21=( MaxB2/ MaxA1);
AA21=( MaxA2/ MaxA1);
BB21=( MaxB2- MaxB1);
if MaxB2> MaxA2
ttta B2onA2= MaxB2/ MaxA2;
else
    ttta B2onA2= MaxA2/ MaxB2;
end
B2onA2= MaxB2/ MaxB1;
set(handles.edit14,'string',ttta);
if(B2onA2<1.8&& B2onA2>1)
    set(handles.text9,'string','Undamaged','foregroundColor','[0,0.5,0]')
     set(handles.text10,'string','Undamaged','foregroundColor','[0,0.5,0]')
elseif (B2onA2<2.3&& B2onA2>1.8)
    set(handles.text9,'string','Acceptable','foregroundColor','[1,0.84,0]')
         if(BA21>1&& AA21>1)
          set(handles.text10,'string','Mechanical Defect')
         else
         set(handles.text10,'string','Leak Defect ')
        end
elseif(B2onA2<2.7 && B2onA2>2.3)

set(handles.text9,'string','Dangerous','foregroundColor','[1,0.6,0.78]')
    if(BA11>0&& AA21>1)
     set(handles.text10,'string','Mechanical Defect')
    else
     set(handles.text10,'string','Leak Defect ')
   end
else
    set(handles.text9,'string','Damaged ','foregroundColor','r')
    if(BA21>1&& AA21>1)
    set(handles.text10,'string','Mechanical Defect')
     else
    set(handles.text10,'string','Leak Defect ')
     end
end
%calculate the total of RMS
rmsA1=RMS.^2; %square of RMS of sensor A
rmsA2=sum(rms1); %total of RMS
rmsA3=rms2/numel(RMS); %average of RMS
rmsA4=(rms3^0.5)*1000; %root of average of RMS
rmsB1=RMS1.^2; %square of RMS of sensor B
rmsB2=sum(rmsi1); %total of RMS
rmsB3=rmsi2/numel(RMS1); %average of RMS
rmsB4=(rmsi3^0.5)*1000; %root of average of RMS
E1=rms2*0.004-rmsi2*0.004; % difference of energy of RMS
rrr1=rr1.^2; %the square value of RMS for Progress stroke A
rrr2=rr2.^2; %the square value of RMS for retreat stroke A
rrr3=rr3.^2; %the square value of RMS for Progress stroke B
rrr4=rr4.^2; %the square value of RMS for retreat stroke B
```

```
rrrr1=sum(rrr1); %total of RMS
rrrr2=sum(rrr2); %total of RMS
rrrr3=sum(rrr3); %total of RMS
rrrr4=sum(rrr4); %total of RMS
rr5=rrrr1*0.004-rrrr3*0.004; %difference of energy of RMS
rr6=rrrr2*0.004-rrrr4*0.004; %difference of energy of RMS
set(handles.edit15,'string',E1*1000) ;
set(handles.edit16,'string',rr5*1000);
set(handles.edit17,'string',rr6*1000);
set(handles.edit2,'string',rmsB4);
if(rmsB4<0.1)
    set(handles.text5,'string','Undamaged','foregroundColor','[0,0.5,0]')
    elseif(rmsB4<0.15&&rmsB4>0.1)
    set(handles.text5,'string','Acceptable','foregroundColor','[1,0.84,0]')
    elseif(rmsB4<0.2&&rmsB4>0.15)

set(handles.text5,'string','Dangerous','foregroundColor','[1,0.6,0.78]')
else
    set(handles.text5,'string','Damaged','foregroundColor','r')
end
% --------------------------------------------------------------------
% Delete all
function Delete_ClickedCallback(hObject, eventdata, handles)
cla;
set(handles.edit2,'string','');
set(handles.edit14,'string','');
set(handles.text5,'string','');
set(handles.text9,'string','');
set(handles.text10,'string','');
set(handles.text21,'string','');
set(handles.text5,'Backgroundcolor','white');
set(handles.text9,'Backgroundcolor','white');
set(handles.text9,'Backgroundcolor','white');
set(handles.text21,'Backgroundcolor','white');
clc;
clear;
cla;
% --------------------------------------------------------------------
% TO SAVE THE FIGURE WITH ALL CALCULATION
function save1_ClickedCallback(hObject, eventdata, handles)
set(handles.uipanel1,'visible','off');
axes(handles.axes1);
NoCylinder=get(handles.edit13,'string');
Case=get(handles.text9,'string');
pathname='C:\Users\Houssam\Desktop\photo\';
newfile=strcat(pathname, NoCylinder, Case);
[filename, pathname, filterindex] =
uiputfile({'*.jpg;*.tif;*.png'},'figure1',newfile);
name=fullfile(pathname,filename);
saveas(handles.axes1, name, 'jpg');
guidata(hObject, handles);
set(handles.uipanel1,'visible','on');
```